DISSERTATIONES
BIOLOGICAE
UNIVERSITATIS
TARTUENSIS
**358**

IVAN KISLY

# The pleiotropic functions of ribosomal proteins eL19 and eL24 in the budding yeast ribosome

DISSERTATIONES BIOLOGICAE UNIVERSITATIS TARTUENSIS
**358**

DISSERTATIONES BIOLOGICAE UNIVERSITATIS TARTUENSIS
**358**

**IVAN KISLY**

# The pleiotropic functions of ribosomal proteins eL19 and eL24 in the budding yeast ribosome

UNIVERSITY OF TARTU
Press

Institute of Molecular and Cell Biology, University of Tartu, Estonia

Dissertation is accepted for the commencement of the degree of Doctor of Philosophy in molecular biology on 28.06.2019 by the Council of the Institute of Molecular and Cell Biology, University of Tartu

Supervisors: Prof. Jaanus Remme, PhD
Institute of Molecular and Cell Biology
University of Tartu, Estonia

Dr. Tiina Tamm, PhD
Institute of Molecular and Cell Biology
University of Tartu, Estonia

Opponent: Prof. Denis L.J. Lafontaine, PhD
The Institute of Molecular Biology & Medicine
University of Brussels, Belgium

Commencement: Room No 105, 23B Riia Str., Tartu, on August 27th, 2019, at 10:15

The publication of this thesis is granted by the Institute of Molecular and Cell Biology, University of Tartu

ISSN 1024–6479
ISBN 978-9949-03-134-4 (print)
ISBN 978-9949-03-135-1 (pdf)



University of Tartu Press
www.tyk.ee

# TABLE OF CONTENTS

# LIST OF ORIGINAL PUBLICATIONS

Current thesis is based on the following original publications which will be referred to in the text by their Roman numerals:

**I** **Kisly, I**., Gulay, S.P., Maeorg, U., Dinman, J.D., Remme, J., Tamm, T. (2016). The functional role of eL19 and eB12 intersubunit bridge in the eukaryotic ribosome. Journal of Molecular Biology. 428(10): 2203–2216. doi: 10.1016/j.jmb.2016.03.023.

**II** **Kisly, I.**, Remme, J., Tamm, T. (2019). Ribosomal protein eL24, involved in two intersubunit bridges, stimulates translation initiation and elongation. Nucleic Acids Research. 47(1): 406–420. doi: 10.1093/nar/gky1083.

**III** Piir, K., Tamm, T., **Kisly I.**, Tammsalu, T., Remme, J. (2014). Stepwise splitting of ribosomal proteins from yeast ribosomes by LiCl. PLoS One. 9(7):e101561. doi: 10.1371/journal.pone.0101561.

My contribution to the articles is as follows:

Ref. I Designed and performed experiments, participated in data analysis and writing of manuscript

Ref. II Designed and performed experiments, participated in data analysis and writing of manuscript

Ref. III Designed and performed subunit dissociation assay of 80S ribosomes.

# LIST OF ABBREVIATIONS

aa residues – amino acid residues
ATP – adenosine triphosphate
A-site – acceptor site for transfer RNA
eEF – eukaryotic elongation factor
eIF – eukaryotic initiation factor
eRF – eukaryotic release factor
ES – expansion segment of ribosomal RNA
E-site – exit site for transfer RNA
ETS – external transcribed spacer
FeS – iron-sulfur cluster
GDP – guanosine diphosphate
GTP – guanosine triphosphate
GTPase – guanosine triphosphate hydrolase
ITS – internal transcribed spacer
Met-$tRNA_i^{Met}$ – initiator methionine transfer RNA
MDa – megadalton
mRNA – messenger RNA
MW – molecular weight
nt - nucleotides
Pab1 – polyadenylate-binding protein 1
pre-40S – precursor small ribosomal particle
pre-60S – precursor large ribosomal particle
pre-rRNA – precursor ribosomal RNA
P-site – peptidyl site for transfer RNA
rRNA – ribosomal RNA
RNP – ribonucleoprotein
snoRNP – small nucleolar ribonucleoprotein
tRNA – transfer RNA

# INTRODUCTION

In all three domains of life (*Archaea*, *Bacteria* and *Eukarya*), proteins are synthesized by large ribonucleoprotein particles called ribosomes. These ancient ribozymes are originated in the RNA world as self-replicating pre-cellular complexes and gradually took their modern form by the time of LUCA (last universal common ancestor) (Fox 2010; Noller 2012). All ribosomes consist of two ribosomal subunits: a small and a large one. Structural studies demonstrate that the shape of both subunits is defined by the tertiary structure of ribosomal RNA (rRNA), which is assisted by ribosomal proteins (r-proteins). Yet despite the structural similarity of modern ribosomes, the long evolutionary road has led to the appearance of domain-specific structural elements of ribosomes as well as principles of ribosome assembly and protein synthesis.

Eukaryotic ribosome, the main subject of this thesis, is larger than bacterial or archaeal ribosomes due to the presence of eukaryote-specific expansions of rRNAs, eukaryote-specific r-proteins and protein extensions. These eukaryote-specific moieties form a vast network of intra- and intersubunit interactions that support structure of eukaryotic ribosome and coordinate its function. Integrity of such network contributes to the efficiency of protein synthesis and, therefore, to the normal cellular physiology. The important but largely obscure role in this network is assigned to r-proteins. The globular domains of r-proteins stabilize tertiary structure of rRNA molecules. The long C- and N-terminal extensions connect globular domains with rRNAs and other proteins, providing communication between functional centers of ribosome. Understanding the roles of r-proteins and their domains in the ribosomal machinery is required to shed a light on the principles of protein synthesis.

The theoretical part of the thesis gives a brief literature overview of the budding yeast ribosome and mechanism of protein synthesis in eukaryotes. First, the overall structure of the ribosome is described, with eukaryote-specific features and intersubunit interactions being covered in more detail. Second, assembly pathways of small and large ribosomal subunits are outlined. Finally, the main steps of protein synthesis and roles of intersubunit bridges in these steps are covered.

The experimental part of the thesis focuses on the functions of two r-proteins, eL19 and eL24, at the domain level. The importance of protein domains of eL19 for the assembly of large ribosomal subunit and intersubunit interactions is determined. The roles of eL24 domains in the subunit association and protein synthesis are revealed.

# 1. REVIEW OF LITERATURE

## 1.1. Structure of the budding yeast ribosome

Translation, or protein synthesis, is a universal process carried out by large ribozymes called ribosomes. As ribonucleoprotein molecules budding yeast ribosomes (80S, MW≈3.2 MDa) consist of four rRNA molecules (total MW≈1.9 MDa) and 79 r-protein molecules (total MW≈1.3 MDa). rRNA and r-proteins are unequally divided between a small (40S, MW≈1.2 MDa) and a large (60S, MW≈2.0 MDa) ribosomal subunit (Spahn et al. 2001; Ben-Shem et al. 2011). Small ribosomal subunit ensures recognition of correct start codon during initiation of translation and selection of correct aminoacyl-tRNAs during elongation of translation (reviewed in Dever et al. 2018; Merrick & Pavitt 2018). Large ribosomal subunit catalyzes formation of peptide bond and stimulates hydrolysis of factor-bound GTP molecules (reviewed in Dever et al. 2016; Dever et al. 2018). The interlinked rotation of ribosomal subunits allows translocation of tRNA and mRNA molecules through the ribosome (Frank & Agrawal 2000; Behrmann *et al.* 2015). The three-dimensional shapes of both subunits are mainly defined by folding of rRNAs into tertiary structures. Folding of rRNAs is similar in all domains of life, regardless of extensive phylogenetic variations in the primary sequences and lengths of rRNAs (Spahn et al. 2001; Yusupov et al. 2001; Noller 2005; Ben-Shem et al. 2011; Greber et al. 2012; Anger et al. 2013; Armache et al. 2013; Quast et al. 2013; Cole et al. 2014). High resolution atomic models of ribosomes revealed that rRNA molecules serve as a framework for binding of r-proteins and *vice versa* r-proteins stabilize tertiary structures of rRNAs (Klein et al. 2004; Ben-Shem et al. 2011; Anger et al. 2013; Behrmann et al. 2015; Khatter et al. 2015). R-proteins are among the smallest cellular proteins: in budding yeast ribosome their length varies from 25 aa residues in eL41 up to 387 aa residues in uL3 (Planta & Mager 1998; Warringer & Blomberg 2006). R-proteins possess high isoelectric point and net positive charge compared to non-ribosomal proteins (Kaltschmidt & Wittmann 1970; Kaltschmidt 1971). In addition, r-proteins exhibit charge segregation, where positively charged regions of proteins interact with negatively charged rRNA residues and negatively charged regions of proteins are exposed to the solvent (Klein et al. 2004; Fedyukina et al. 2014). Charge segregation ensures tight binding of r-proteins to rRNA, which supports structure of ribosome (Klein et al. 2004; Fedyukina et al. 2014).

### 1.1.1. Ribosomal subunits of the budding yeast ribosome

Small ribosomal subunit of budding yeast contains 18S rRNA (1800 nt, MW≈0.65 MDa) and 33 r-proteins (total MW≈0.55 MDa) (Planta & Mager 1998; Spahn et al. 2001; Ben-Shem et al. 2011; Ban et al. 2014). The secondary structure of 18S rRNA is sectioned into five domains: 5', central, 3'major,

3'minor and recently defined central domain A (Gulen et al. 2016). These domains, with assistance from r-proteins, fold into nine distinguishable tertiary domains: head, beak, neck, platform, shoulder, body, right foot, left foot and penultimate stem (helix 44) (Figure 1) (Spahn et al. 2001). Such autonomous domain organization allows high degree of movements, exemplified by swiveling of the head domain, which is promoted by the flexible neck domain. During initiation of translation, small ribosomal subunit serves as a binding platform for initiation factors, which drives recruitment of mRNA and delivery of Met-$tRNA_i^{Met}$ to start codon (reviewed in Merrick & Pavitt 2018). mRNA enters the small subunit between the beak and the shoulder domains, mRNA exit site is located between the head and the platform domains (Figure 1). Helices 18 and 34 form the latch that regulates entry of mRNA into the mRNA channel between the head and the body domains (Frank et al. 1995; Schluenzen et al. 2000; Yusupova et al. 2001; Spahn et al. 2004b; Hussain et al. 2014). Although the position of mRNA channel is known, the movement of mRNA through the small subunit is not still well understood. mRNA channel as well as A, P and E tRNA-binding sites are predominated by 18S rRNA helices assisted by r-proteins (Spahn et al. 2001; Ben-Shem et al. 2011). The key function of this subunit during elongation of translation is entrusted to its decoding center at the A site, where helices 18 (G577) and 44 (A1755, A1756) recognize correct interactions between mRNA codon and tRNA anticodon stem loops (Ogle et al. 2001; Loveland et al. 2017). Decoding center is a target for binding of various antibiotics (Garreau de Loubresse *et al.* 2014; Polikanov *et al.* 2018). As an example, aminoglycosides such as neomycin distort spatial orientation of nucleotide residues A1755 and A1756, which leads to decreased accuracy of aminoacyl-tRNA selection (Garreau de Loubresse et al. 2014). However, inhibitory activity of neomycin is lower in eukaryotes compared to prokaryotes, since residues G1645 and A1745 prevent accommodation of aminoglycosides (Fan-Minogue & Bedwell 2008; Garreau de Loubresse et al. 2014).

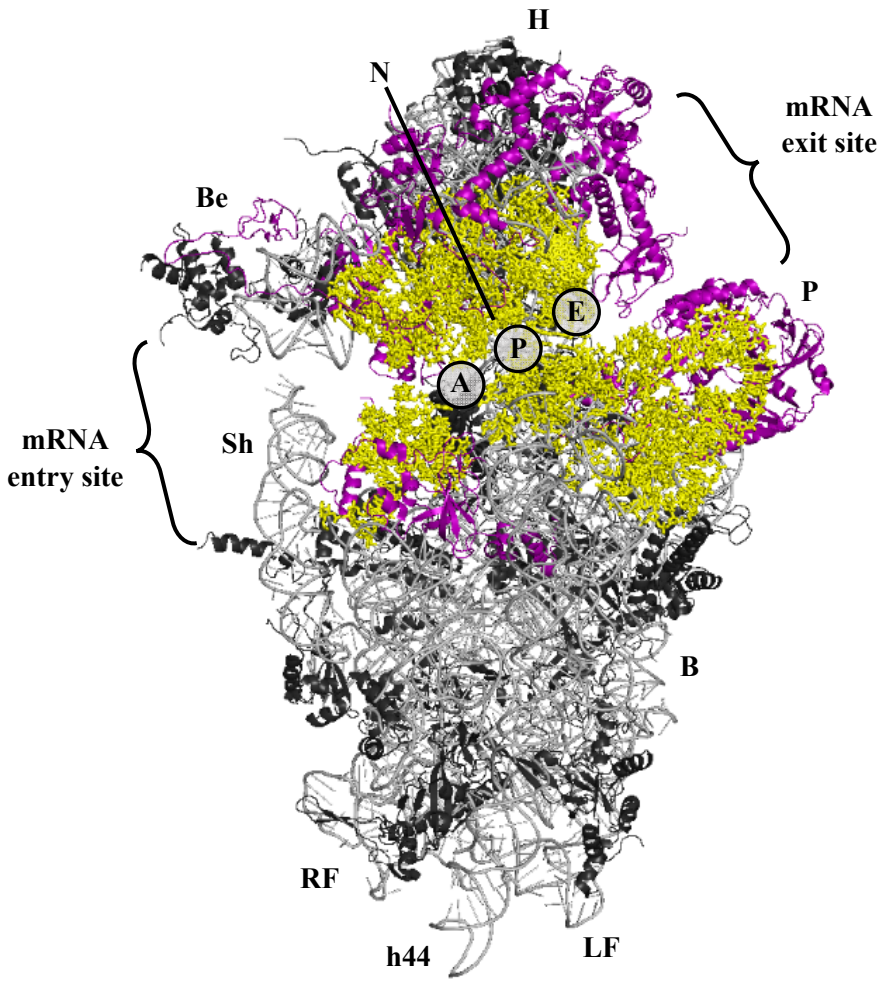


**Figure 1. Intersubunit view at the three-dimensional structure of the small subunit of the budding yeast ribosome.** 18S rRNA and r-proteins are grey and black, respectively. rRNA helices and r-proteins that contribute to the mRNA channel/tRNA-binding sites are yellow and magenta, respectively. Domains of the small subunit, mRNA entry/exit sites and approximate positions of the A, P and E sites are indicated. H, head; Be, beak; N, neck; P, platform; Sh, shoulder; B, body; RF, right foot; LF, left foot; h44, helix 44. PDB coordinates 3U5F and 3U5G (Ben-Shem et al, 2011) were rendered in PyMol.

Large ribosomal subunit of budding yeast contains three rRNA molecules (total MW≈1.26 MDa: 5S rRNA (121 nt), 5.8S rRNA (158 nt) and 25S rRNA (3396 nt)) and 46 r-proteins (total MW≈0.76 MDa) (Planta & Mager 1998; Spahn et al. 2001; Ben-Shem et al. 2011; Ban et al. 2014). The shape of this

subunit is mainly defined by folding of 25S rRNA into seven (0, I-VI) tightly packed and interwoven domains, where recently defined domain 0 serves as a root for other six domains (Petrov et al. 2013; Petrov et al. 2014a). Functional centers and features of the large subunit are distributed between different domains (Figure 2). Domain II is an essential platform for the formation of P-stalk, where r-proteins uL10, uL11, P1 and P2 are bound to helices 42–44 (Spahn et al. 2001; Tchorzewski et al. 2003; Ben-Shem et al. 2011). As an element of GTPase-associated center, P-stalk recruits translation factors and stimulates hydrolysis of factor-bound GTP (Shimizu et al. 2002; Uchiumi et al. 2002; Nomura et al. 2012; Baba et al. 2013). Sarcin-ricin loop, located in the helix 95 of the domain VI, is the second element of the GTPase associated center and has been shown to stabilize the binding of translation factors (Shi et al. 2012). At the opposite side of the large subunit resides L1-stalk, which is a flexible feature formed by r-protein uL1 and helices 75, 76 and 79 of the domain V. It is located near the E site and is involved in the translocation and release of deacylated tRNA (Spahn et al. 2001; Trabuco et al. 2010; Ben-Shem et al. 2011; Reblova et al. 2012; Mohan & Noller 2017). Like in the small subunit, A, P and E tRNA-binding sites of the large subunit are predominated by rRNA helices and additionally assisted by r-proteins. Peptidyl transferase center involves A and P sites, and is formed by helices 73, 74, 80–93 of domain V (Ben-Shem et al. 2011). Although r-proteins stabilize structure of this center, catalysis of the peptide bond formation relies entirely on the rRNA (Nissen et al. 2000). Peptidyl transferase center is targeted by numerous antibiotics that affect proper alignment of the aminoacyl-tRNA and peptidyl-tRNA in the peptidyl transferase center. As an example, anisomycin inhibits peptidyl transferase activity by competing with aminoacyl-tRNA for binding to the A-site cleft (A2820, C2821) (Garreau de Loubresse et al. 2014). Peptide exit tunnel extends from the peptidyl transferase center to the solvent side of the large subunit. Tunnel is formed by 5.8S rRNA and 25S rRNA domains 0, I, III and V, and thus, has an overall electronegative potential. In addition, tunnel wall is supported by r-proteins uL4, uL22, uL23, uL24, uL29 and eL39 (Ben-Shem et al. 2011; Wilson & Beckmann 2011). Peptide exit tunnel participates in regulation of proteins synthesis and folding. The rim around the tunnel exit serves as a site for binding of co-translationally acting chaperones, signal recognition particles and protein conducting channels (reviewed in Wilson & Beckmann 2011). 5.8S rRNA, evolved from the 5' end of prokaryotic 23S rRNA, has been shown to play a role in translocation (Jacq 1981; Abou Elela et al. 1994; Abou Elela & Nazar 1997). Central protuberance, formed by 5S rRNA and r-proteins uL5 and uL18, mediates communication between all described functional centers of the large subunit and also between subunits (Bogdanov et al. 1995; Smith et al. 2001; Dinman 2005).

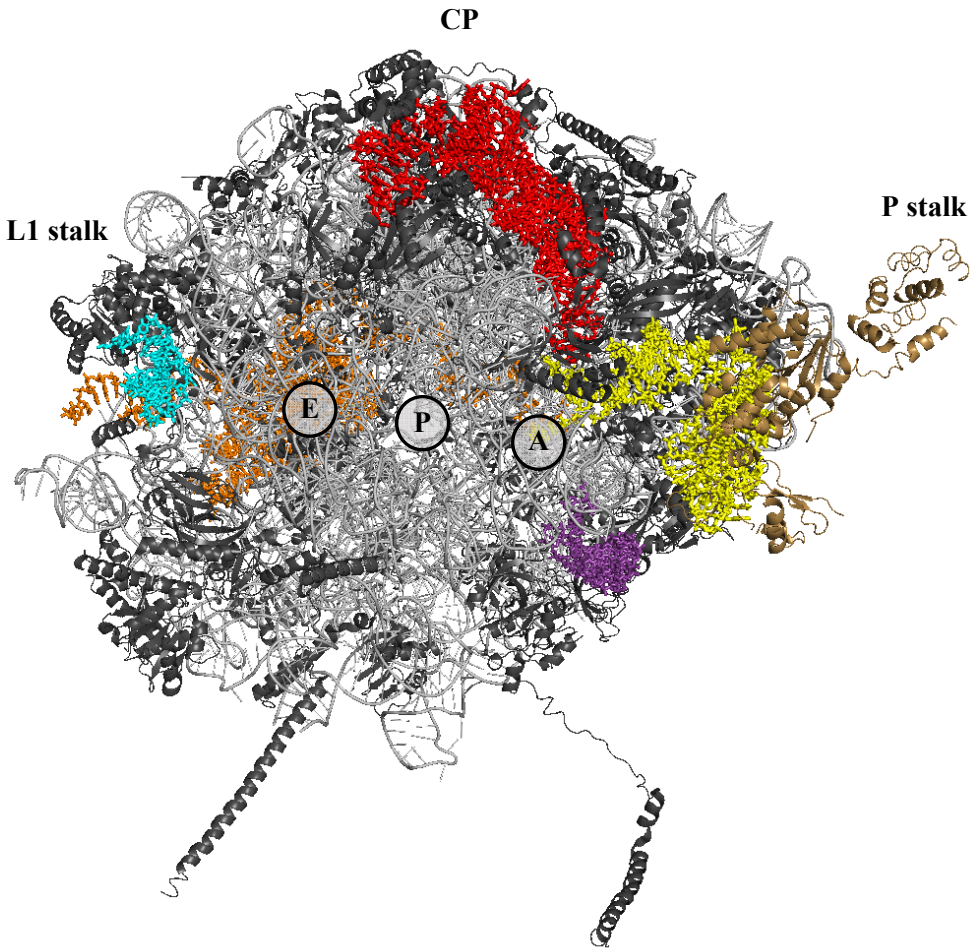


**Figure 2. Intersubunit view at the three-dimensional structure of the large subunit of the budding yeast ribosome.** 5S rRNA is red, 5.8S rRNA is orange, 25S rRNA is grey, r-proteins are black. Landmarks of the large subunit (L1 stalk; P stalk; CP, central protuberance) and approximate positions of the A, P and E sites are indicated. 25S rRNA helices that form L1 stalk are colored cyan. Sarcin-ricin loop is colored purple. 25S rRNA helices and r-proteins that form P stalk are colored yellow and brown, respectively. Peptide exit tunnel is not shown, as it extends from the P site to the solvent side of the subunit. PDB coordinates 3U5H and 3U5I (Ben-Shem et al, 2011) were rendered in PyMol.

### 1.1.2. Eukaryote-specific features of the budding yeast ribosome

Peptidyl transferase center, decoding center and tRNA binding sites are positioned in the common structural core, which is conserved across ribosomes of all life domains. Conserved core comprises ~4400 rRNA bases and ~3000 amino acid residues (Ben-Shem et al. 2011; Melnikov et al. 2012; Melnikov et al. 2018). In addition to the core, eukaryotic ribosomes contain a set of archaea/eukaryote-specific and eukaryote-specific moieties of rRNAs and r-proteins. Differences in mass of eukaryotic ribosomes (3.2 MDa in lower eukaryotes and 4.3 MDa in higher eukaryotes) are attributed solely to the different lengths of eukaryote-specific parts (Armache et al. 2010b, a; Anger et al. 2013; Melnikov et al. 2018). Characteristic structural features of eukaryotic rRNAs are eukaryote-specific rRNA expansion segments – specific rRNA sequences absent in prokaryotic rRNA molecules (Gerbi 1986; Yokoyama & Suzuki 2008; Petrov et al. 2014b). Budding yeast ribosome contains 27 expansion segments (9 in the small and 18 in the large subunit), if compared to *E. coli* ribosome (Ben-Shem et al. 2011; Anger et al. 2013). In the small subunit, the largest cluster of expansion segments resides at the bottom of subunit as a part of the body, helix44, right and left foots. Other segments are located in the head and platform of the small subunit (Figure 3) (Ben-Shem et al. 2011). In the large ribosomal subunit, rRNA expansion segments encircle peptide exit tunnel and can be divided into two clusters (Figure 4) (Ben-Shem et al. 2011). The first cluster is formed at the P-stalk side of the subunit and also connected to the 5S rRNA. The second cluster is located close to the L1-stalk and involves 25S rRNA as well as 5.8S rRNA. Intriguingly, number and complexity of rRNA expansion segments varies between eukaryotic species (Armache et al. 2010a; Anger et al. 2013). As an example, there are 30 expansion segments in the human rRNA. Many of them are longer, if compared to yeast segments, and demonstrate flexible tentacle-like nature (Anger et al. 2013). Increase in the complexity of human rRNAs resulted in the formation of new rRNA-rRNA and rRNA-protein contacts, absent in the budding yeast ribosome (Anger et al. 2013). Several studies have demonstrated/suggested the importance of eukaryote-specific rRNA segments for the ribosome assembly, interactions between subunits and binding of protein factors (Sweeney et al. 1994; Jeeninga et al. 1997; Gomez Ramos et al. 2016; Ramesh & Woolford 2016; Fujii et al. 2018; Knorr et al. 2019).

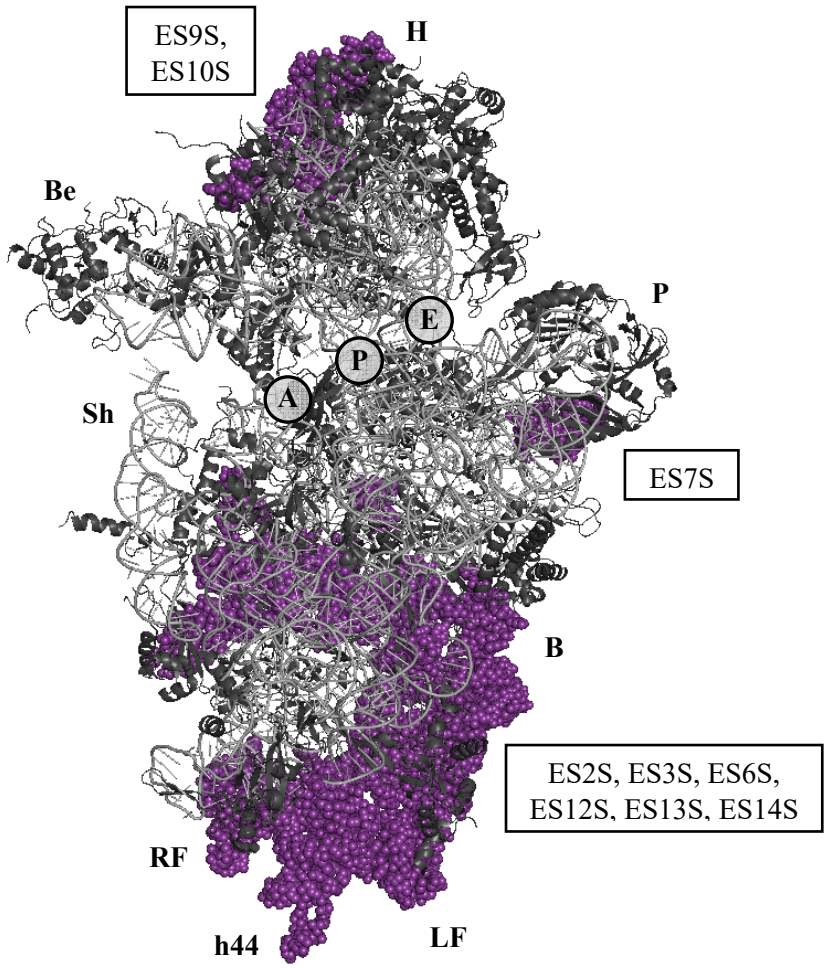


**Figure 3. Intersubunit view at the rRNA expansion segments of the small subunit of the budding yeast ribosome.** 18S rRNA and r-proteins are grey and black, respectively. Domains of the small subunit and approximate positions of the A, P and E sites are indicated. H, head; Be, beak; P, platform; Sh, shoulder; B, body; RF, right foot; LF, left foot; h44, helix 44. rRNA expansion segments are colored purple/red/yellow and indicated. Coordinates and nomenclature of rRNA expansion segments are used as defined in Anger et al, 2013. PDB coordinates 3U5F and 3U5G (Ben-Shem et al, 2011) were rendered in PyMol.

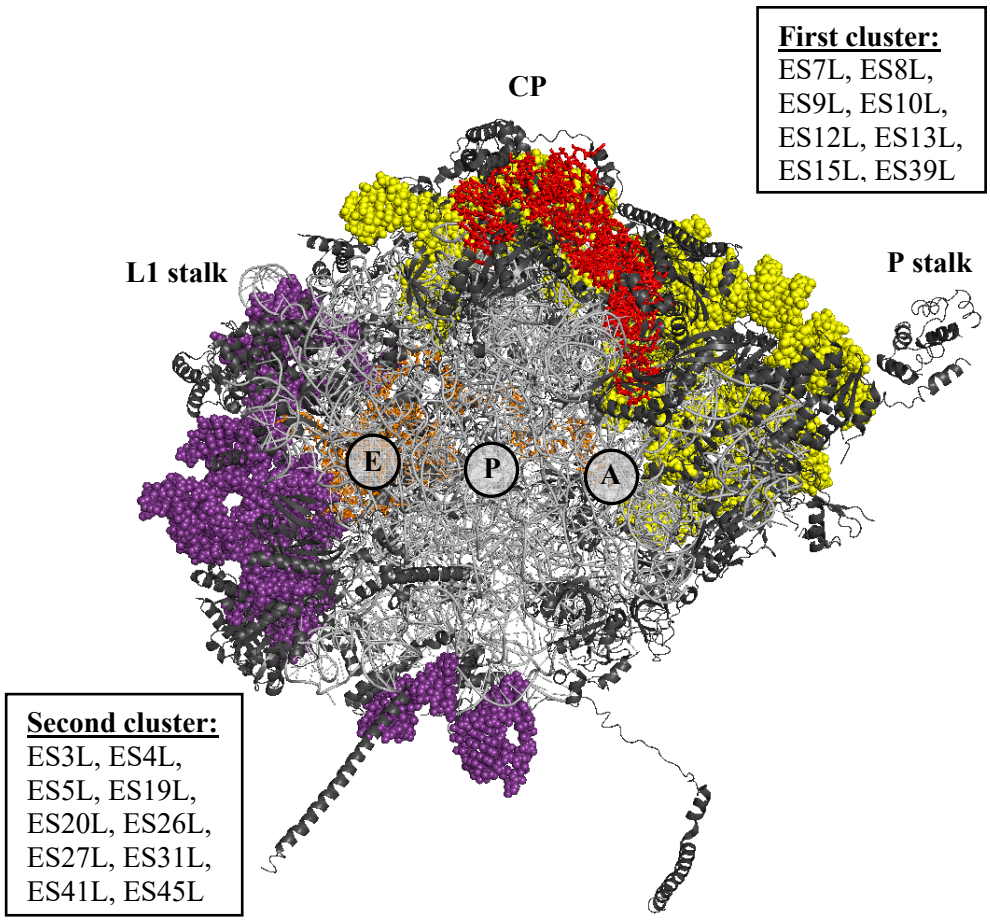


**Figure 4. Intersubunit view at the rRNA expansion segments of the large subunit of the budding yeast ribosome.** 5S rRNA is red, 5.8S rRNA is orange, 25S rRNA is grey, r-proteins are black. Landmarks of the large subunit (L1 stalk; P stalk; CP, central protuberance) and approximate positions of the A, P and E sites are indicated. The first and the second cluster of rRNA expansion segments are indicated and colored yellow and purple, respectively. Coordinates and nomenclature of rRNA expansion segments are used as defined in Anger et al, 2013. PDB coordinates 3U5H and 3U5I (Ben-Shem et al, 2011) were rendered in PyMol.

R-proteins of the budding yeast can be divided into three groups (Figures 5 and 6) (Ban et al. 2014). 33 proteins (15 in the small subunit and 18 in the large subunit) are conserved across all domains of life. 35 proteins (12 in the small and 23 in the large subunit) are conserved between archaeal and eukaryotic ribosomes. Remaining 11 proteins (6 in the small and 5 in the large subunit) are specific only for the eukaryotic ribosomes (Ban et al. 2014). Budding yeast

ribosome misses eukaryote-specific protein eL28 due to possible gene loss (Lecompte et al. 2002). In the small ribosomal subunit, universally conserved proteins are mainly located in the head and body domains, where they contribute to the mRNA channel and tRNA binding sites. Archaea/eukaryote-specific proteins reside at the bottom of the subunit, at the platform domain and at the top of the head. Eukaryote-specific proteins form beak and platform/body domains (Figure 5) (Ben-Shem et al. 2011). In the large ribosomal subunit, universally conserved proteins form central protuberance, tRNA binding sites and GTPase binding site. Archaea/eukaryote-specific and eukaryote-specific proteins follow the cluster organization of rRNA expansion segments (Figure 6) (Ben-Shem et al. 2011).

Despite the small size, many r-proteins have several structural domains. Recent comparison of tertiary structures of universally conserved proteins from different organisms demonstrated that conserved moieties are generally located in globular domains (Melnikov et al. 2018). Eukaryote-specific moieties are found in non-globular N- and C-terminal extensions that frequently reach far from the globular domains (Klinge et al. 2011; Rabl et al. 2011; Melnikov et al. 2018). Such structural organization of r-proteins allows to form the vast neuron-like network of protein-protein interactions, where eukaryote-specific extensions interconnect core functional centers and surface of the ribosome as well as small and large ribosomal subunits (Table 1, Figures 7 and 8) (Klinge et al. 2012; Poirot & Timsit 2016). In the small ribosomal subunit of the budding yeast ribosome, all proteins have at least one protein interaction partner, most proteins interact with 2–3 partners. (Table 1, Figure 7) (Ben-Shem et al. 2011; Poirot & Timsit 2016). In the large ribosomal subunit, only 5 r-proteins do not form any intrasubunit protein-protein interactions, others mostly interact with 2–4 partners (Table 1, Figure 8) (Ben-Shem et al. 2011; Poirot & Timsit 2016). Therefore, eukaryote-specific extensions of r-proteins ensure stability of ribosome structure and provide communication between different ribosomal regions. They contribute to the functional centers, guide tRNAs and mRNAs through the ribosome, provide binding of chaperones and translation factors (reviewed in Ghosh & Komar 2015). In addition, eukaryote-specific extensions play a role in folding of rRNA during ribosome assembly (reviewed in Konikkat & Woolford 2017).

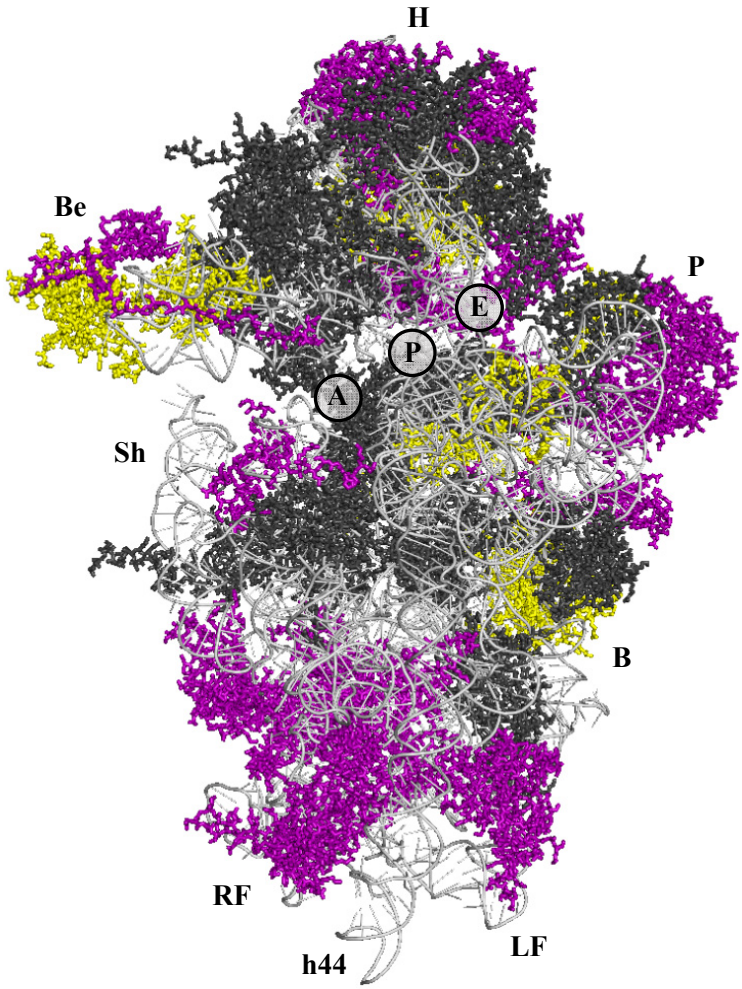


**Figure 5. Position of three groups of r-proteins in the small subunit of the budding yeast ribosome.** rRNA is grey. Universally conserved proteins are black. Archaea/ eukaryote-specific proteins are magenta. Eukaryote-specific proteins are yellow. Domains of the small subunit and approximate positions of the A, P and E sites are indicated. H, head; Be, beak; P, platform; Sh, shoulder; B, body; RF, right foot; LF, left foot; h44, helix 44. Protein groups are according to Ban et al, 2014. PDB coordinates 3U5F and 3U5G (Ben-Shem et al, 2011) were rendered in PyMol.

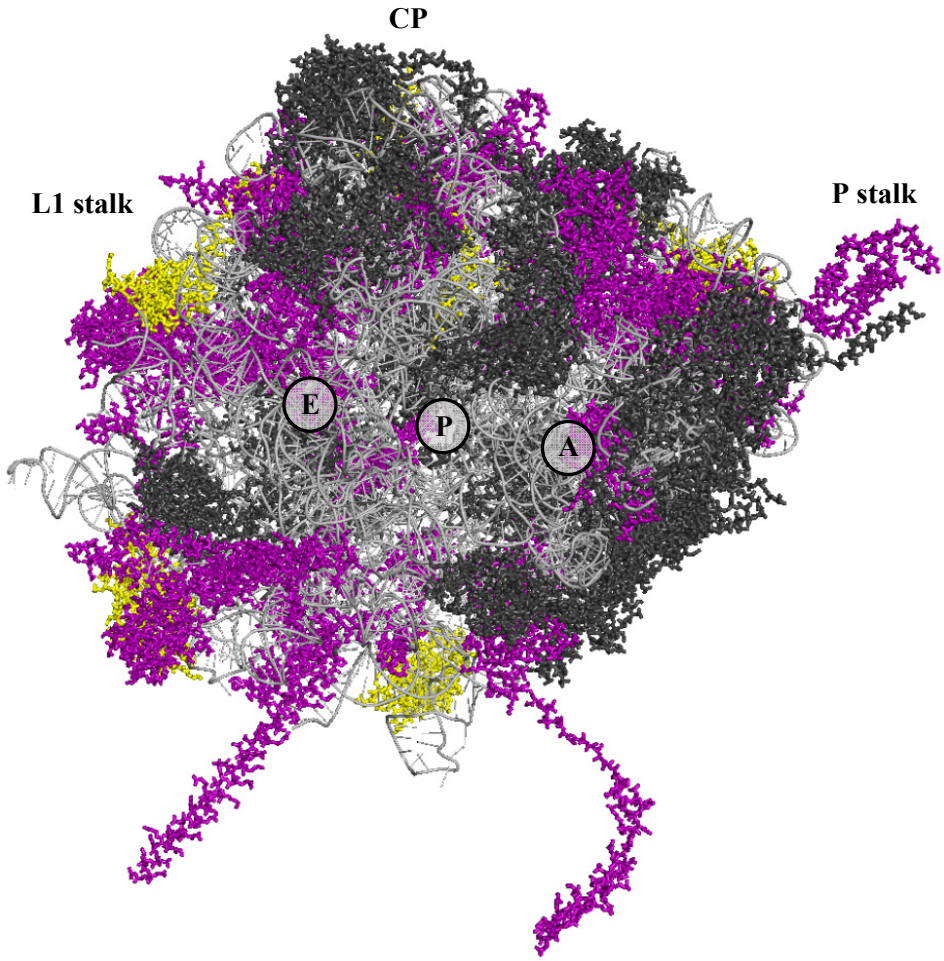


**Figure 6. Position of three groups of r-proteins in the large subunit of the budding yeast ribosome.** rRNA is grey. Conserved proteins are black. Archaea/eukaryote-specific proteins are magenta. Eukaryote-specific proteins are yellow. Landmarks of the large subunit (L1 stalk; P stalk; CP, central protuberance) and approximate positions of the A, P and E sites are indicated. Protein groups are according to Ban et al, 2014. PDB coordinates 3U5H and 3U5I (Ben-Shem et al, 2011) were rendered in PyMol.

**Table 1. Number of intrasubunit protein partners for r-proteins in the budding yeast ribosome.** "Partners" – number of intrasubunit protein partners. "BAE" – universally conserved proteins. "AE" – archaea/eukaryote-specific proteins. "E" – eukaryote-specific proteins. Protein names are according to the new nomenclature from Ban et al, 2014. Proteins that form intersubunit bridges (red) are according to Ben-Shem et al, 2011. Table is adapted with modifications from Poirot and Timsit, 2016.

| Subunit | Partners | BAE | AE | E |
|---|---|---|---|---|
| **40S** | 1 | **uS19** | **eS8**, eS28, eS31 | |
| | 2 | uS11 | **eS1**, **eS6**, eS17, eS19, eS30 | **eS7**, eS12, eS26 |
| | 3 | uS2, uS7, uS9, uS10, uS12, **uS13**, uS14 | eS10, eS24, eS25, eS27 | eS10 |
| | 4 | **uS15** | eS4 | eS21 |
| | 5 | uS3, uS4, uS5, **uS17** | | |
| | 8 | uS8 | | |
| **60S** | 0 | | **eL19**, eL31, eL38, **eL41** | eL22 |
| | 1 | uL22 | eL40 | eL29 |
| | 2 | **uL5**, **uL14**, uL24, | **eL24**, **eL43** | |
| | 3 | **uL2**, **uL3**, uL16, uL18, uL23, | **eL30**, eL32, eL34, eL37, eL42 | eL6, eL27 |
| | 4 | uL6, uL29, uL30, | eL14, eL18, eL33, eL39 | eL36 |
| | 5 | uL13, uL15 | eL8 | |
| | 6 | | eL13, eL20, eL21 | |
| | 7 | | eL15 | |
| | 8 | uL4 | | |

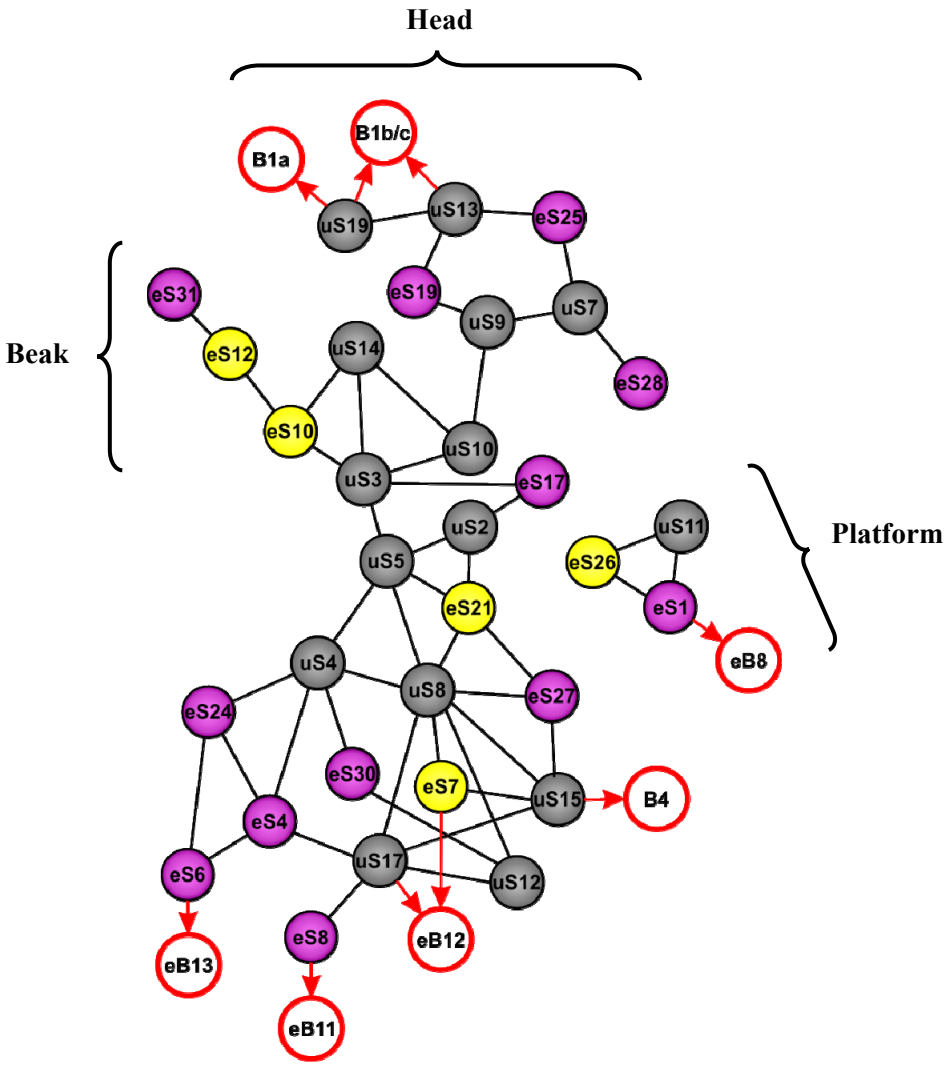


**Figure 7. Network of intrasubunit protein-protein interactions in the small subunit of the budding yeast ribosome.** Universally conserved proteins are grey, archaea/ eukaryote-specific proteins are purple, eukaryote-specific proteins are yellow. Approximate positions of the small subunit domains are indicated. Intersubunit bridges are incorporated into network as a red circles. Protein names are according to the new nomenclature from Ban et al, 2014. Proteins that form intersubunit bridges are according to Ben-Shem et al, 2011. Figure is adapted with modifications from Poirot and Timsit, 2016.

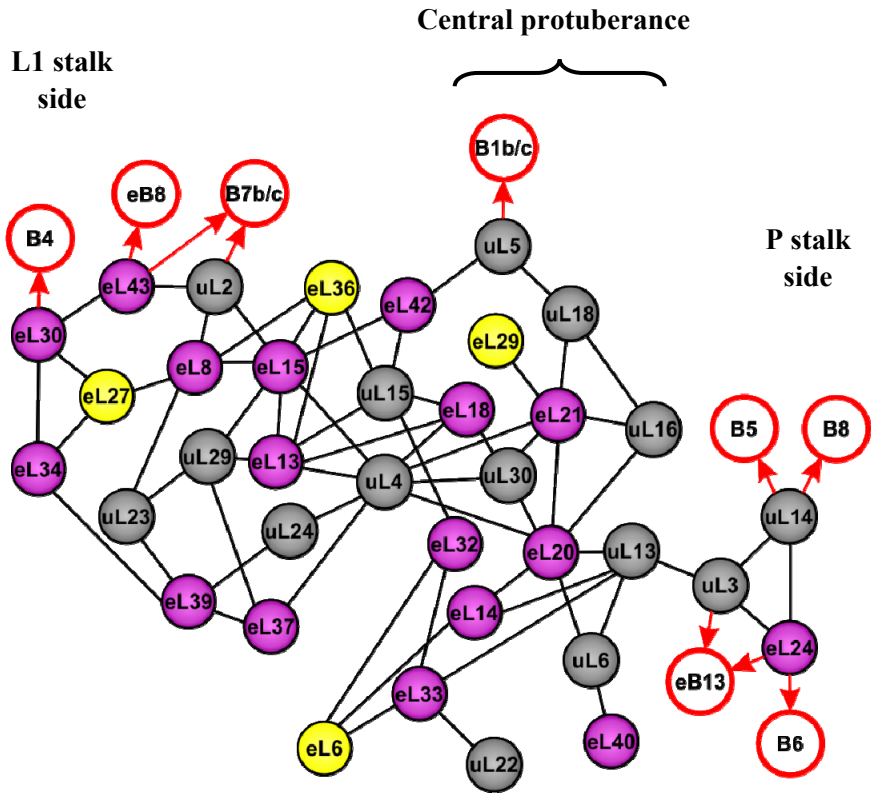


**Figure 8. Network of intrasubunit protein-protein interactions in the large subunit of the budding yeast ribosome.** Universally conserved proteins are grey, archaea/ eukaryote-specific proteins are magenta and eukaryote-specific proteins are yellow. Approximate positions of the large subunit landmarks are indicated. Intersubunit bridges are incorporated into network as a red circles. Protein names are according to the new nomenclature from Ban et al, 2014. Proteins that form intersubunit bridges are according to Ben-Shem et al, 2011. Figure is adapted with modifications from Poirot and Timsit, 2016.

### 1.1.3. Intersubunit bridges of the budding yeast ribosome

The overall conformation and functionality of ribosome depends not only on the intrasubunit interactions, but also on the communication between ribosomal subunits provided by intersubunit contacts called bridges. High-resolution atomic model of the budding yeast ribosome describes 17 intersubunit bridges, comprising three types of interactions: rRNA-rRNA, protein-rRNA and protein-protein (Tables 2, 3 and 4, Figures 9 and 10) (Ben-Shem et al. 2011). rRNA-rRNA type interactions are suggested to be the most stable and unchanged during protein synthesis. These are located in the relatively static regions at the functional core of ribosome (Figures 9 and 10) (Gao et al. 2003; Ben-Shem et al. 2011). Protein-rRNA and especially protein-protein interactions are more

dynamic than rRNA-rRNA interactions. Consequently, these interactions are found peripherally, where extensive relative movements of ribosomal subunits occur (Figures 9 and 10) (Gao et al. 2003; Ben-Shem et al. 2011).

Comparison of available structural models of bacterial and eukaryotic ribosomes resulted in division of intersubunit bridges into two groups. Twelve intersubunit bridges are conserved, as they have very similar composition and location in ribosomes of both *Bacteria* and *Eukarya* (Spahn et al. 2001; Yusupov et al. 2001; Ben-Shem et al. 2011). Conserved bridges are positioned in the conserved structural core (Tables 2 and 3, Figures 9 and 10). At the date, the roles of conserved intersubunit bridges were extensively studied in the bacterial ribosome and to lesser extent in the budding yeast ribosome (described below). Six conserved bridges (B2a, B2b, B2c, B3 and B7a) are solely formed by rRNA-rRNA interactions between domain IV of 25S rRNA (helices 62, 64, 66, 67, 68, 69, 70 and 71) and 18S rRNA (helices 23, 24, 44 and 45) (Table 2, Figures 9 and 10). These bridges do not act independently, but overlap and form an extensive area of rRNA-rRNA interactions that follows the pathway of tRNAs and mRNA through the ribosome (Figures 9 and 10) (Ben-Shem et al. 2011). Structural studies of bacterial ribosomes suggest rRNA-rRNA bridges ensure association of ribosomal subunits, but also allow their rotation (Gao et al. 2003). Importance of these bridges for the ribosome processivity (B2a), fidelity of decoding (B3) and translocation (B7a) has been shown (Kipper et al. 2009; Sun et al. 2011; Liu & Fredrick 2013).

**Table 2. Components of the rRNA-rRNA intersubunit bridges in the budding yeast ribosome.** Helices of 18S and 25S rRNAs that form intersubunit bridges in pre- and post-translocational conformations of ribosome are shown. "№" – number of intersubnit rRNA-rRNA contacts. Bridge nomenclature and interactions are from Ben-Shem et al, 2011.

| Bridge | Pre-translocational | | | Post-translocational | | |
|---|---|---|---|---|---|---|
| | 18S rRNA | 25S rRNA | № | 18S rRNA | 25S rRNA | № |
| **B2a** | h24 | H69 | 2 | h24 | H69 | 2 |
| | h44 | H69 | 11 | h44 | H69 | 11 |
| | h45 | H69 | 2 | h45 | H69 | 2 |
| **B2b** | h24 | H68 | 1 | h24 | H68 | 2 |
| | h24 | H70 | 2 | h45 | H70 | 1 |
| | h45 | H71 | 3 | h45 | H71 | 2 |
| **B2c** | h24 | H66 | 1 | h24 | H67 | 2 |
| | h24 | H67 | 3 | | | |
| **B3** | h44 | H62 | 1 | h44 | H62 | 1 |
| | h44 | H64 | 2 | h44 | H64 | 3 |
| | h44 | H70 | 14 | h44 | H70 | 14 |
| **B7a** | h23 | H68 | 3 | h23 | H68 | 2 |

Six conserved bridges (B1a, B4, B5, B6, B7b/c and B8) are formed by protein-rRNA interactions that are assisted by several rRNA-rRNA and protein-protein contacts (Table 3, Figures 9 and 10). Conserved bridge B1b/c is the one and only solely protein-protein bridge (Ben-Shem et al. 2011). Bridges B1a and B1b/c are distinctive as they form a cluster of interactions between the central protuberance of the large subunit and the head domain of the small subunit (Table 3, Figures 9 and 10). Bridge B1a connects a highly flexible A-site finger (25S rRNA helix 38) of the large subunit with helix 33 and protein uS19 of the small subunit. B1b/c is a protein-protein type intersubunit bridge formed between protein uL5 of the large subunit and proteins uS13 and uS19 of the small subunit. Position of the B1a bridge allows large conformational changes in this bridges during swivel of the head domain. As a result, bridge B1a is present in the pre-translocational, but not in the post-translocational conformation (Ben-Shem et al. 2011). In addition, components of B1a and B1b/c are directly connected to the tRNA binding sites and mRNA channel. In the small ribosomal subunit, C-terminal extension of uS13 interacts with P-site tRNA, while C-terminal extension of uS19 interacts with A-site tRNA and mRNA (Bulygin et al. 2005; Armache et al. 2010b; Khairulina et al. 2010; Budkevich et al. 2011). In the large ribosomal subunit, protein uL5 interacts with P-site tRNA and factor eEF3 (Triana-Alonso et al. 1995; Spahn et al. 2001; Andersen et al. 2006; Svidritskiy et al. 2014). A-site finger interacts with A-site tRNA (Spahn et al. 2001; Budkevich et al. 2011; Behrmann et al. 2015). Such position of bridges B1a and B1b/c allows them to transmit information from the decoding center of the small subunit to the large subunit and to be involved in translocation (Sergiev et al. 2005; Komoda et al. 2006; Rakauskaite & Dinman 2006; Rhodin & Dinman 2011; Liu & Fredrick 2013; Bowen et al. 2015).

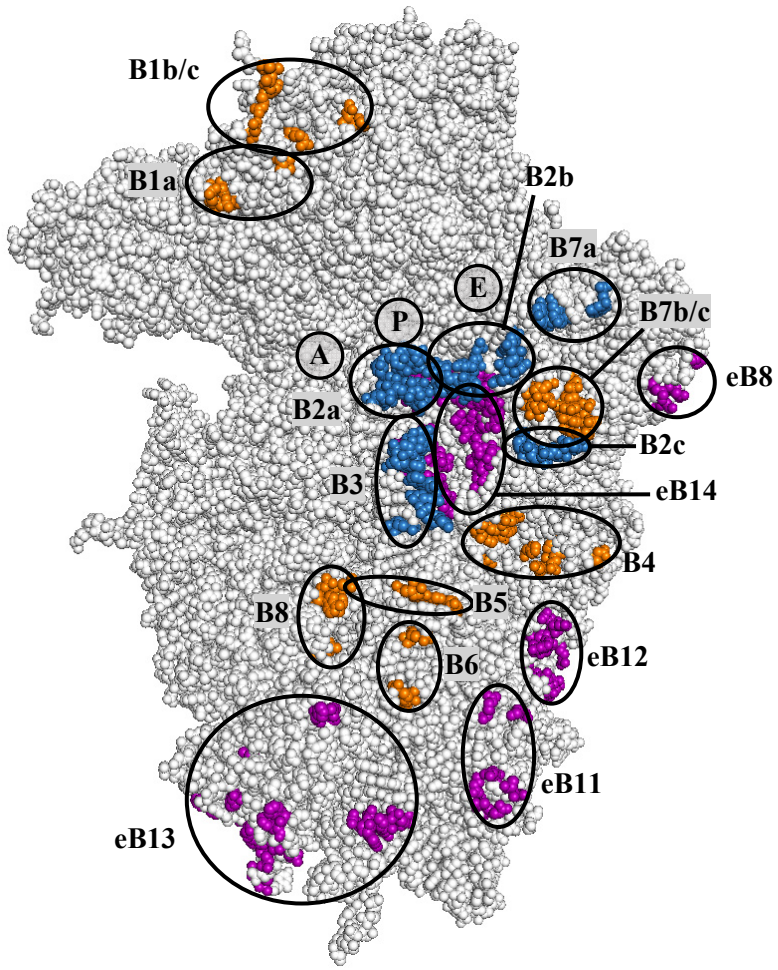


**Figure 9. Position of the intersubunit bridges in the small subunit of the budding yeast ribosome.** rRNA and r-proteins are white spheres. Conserved bridges that contain only rRNA-rRNA contacts are blue. Conserved bridges that comprise protein component are orange. Eukaryote-specific bridges are magenta. Approximate positions of the A, P and E sites are indicated. Bridge nomenclature and coordinates are from Ben-Shem et al, 2011. PDB coordinates 3U5F and 3U5G (Ben-Shem et al, 2011) were rendered in PyMol.

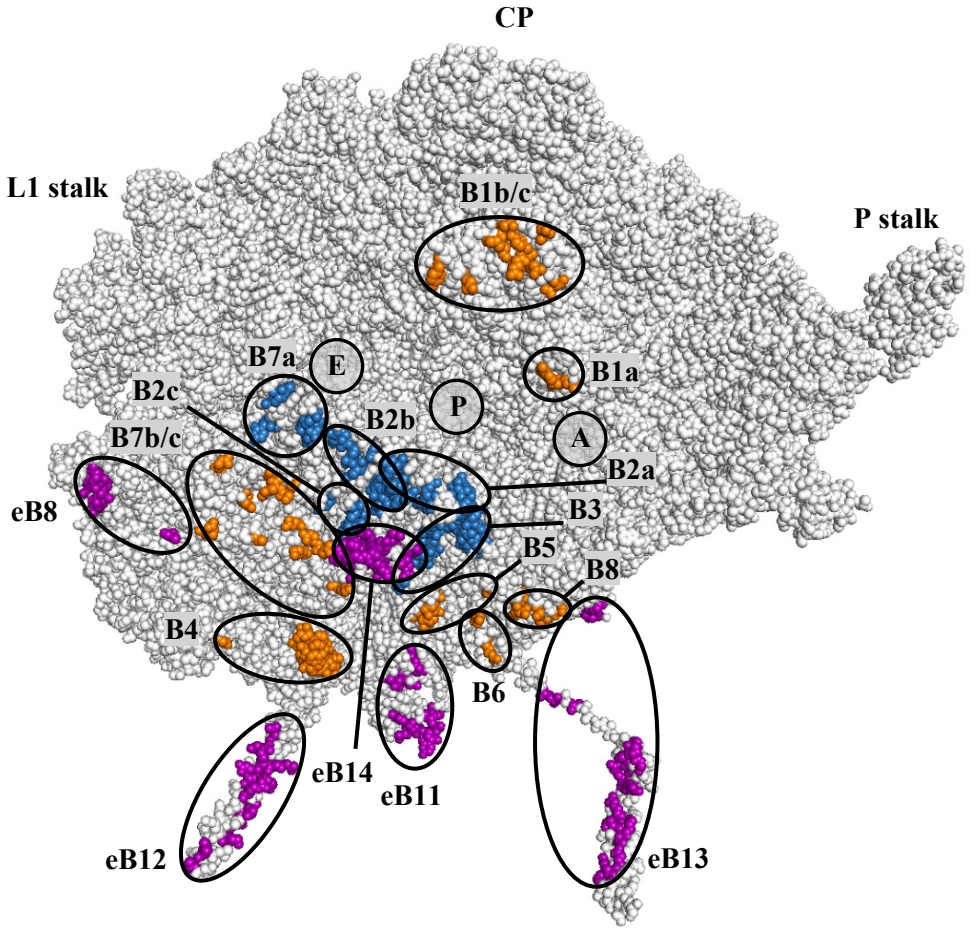


**Figure 10. Position of the intersubunit bridges in the large subunit of the budding yeast ribosome.** rRNA and r-proteins are grey spheres. Conserved bridges that contain only rRNA-rRNA contacts are blue. Conserved bridges that comprise protein component are orange. Eukaryote-specific bridges are magenta. Landmarks of the large subunit (L1 stalk; P stalk; CP, central protuberance) and approximate positions of the A, P and E sites are indicated. Bridge nomenclature and coordinates are from Ben-Shem et al, 2011. PDB coordinates 3U5H and 3U5I (Ben-Shem et al, 2011) were rendered in PyMol.

**Table 3. Components of the protein-containing conserved intersubunit bridges in the budding yeast ribosome.** Components of intersubunit bridges in small (40S) and large (60S) subunits in pre- and post-translocational conformations of ribosome are shown. "№" – number of intersubunit contacts. Protein names are according to the new nomenclature from Ban et al, 2014. Bridge nomenclature and interactions are from Ben-Shem et al, 2011.

| | Pre-translocational | | | Post-translocational | | |
|---|---|---|---|---|---|---|
| **Bridge** | **40S** | **60S** | **№** | **40S** | **60S** | **№** |
| **B1a** | h33 | H38 | 1 | - | - | - |
| | uS19 | H38 | 2 | | | |
| **B1b/c** | uS13 | uL5 | 2 | uS13 | uL5 | 2 |
| | uS19 | uL5 | 6 | uS19 | uL5 | 5 |
| **B4** | h20 | H34 | 6 | h20 | H34 | 7 |
| | uS15 | H34 | 1 | uS15 | H34 | 5 |
| | uS15 | eL30 | 1 | | | |
| **B5** | h44 | H62 | 1 | h44 | H62 | 2 |
| | h14 | uL14 | 1 | h14 | uL14 | 1 |
| | h44 | uL14 | 4 | h44 | uL14 | 4 |
| **B6** | h44 | eL24 | 2 | h44 | eL24 | 2 |
| **B7b/c** | h24 | uL2 | 6 | h24 | uL2 | 4 |
| | h24 | eL43 | 1 | h24 | eL43 | 4 |
| | | | | h27 | eL43 | 1 |
| **B8** | h14 | uL14 | 4 | h14 | uL14 | 5 |

**Table 4. Components of the eukaryote-specific intersubunit bridges in the budding yeast ribosome.** Components of intersubunit bridges in small (40S) and large (60S) subunits in pre- and post-translocational conformation of ribosome are shown. "№" – number of intersubunit contacts. Protein names are according to the new nomenclature from Ban et al, 2014. Bridge nomenclature and interactions are from Ben-Shem et al, 2011.

| | Pre-translocational | | | Post-translocational | | |
|---|---|---|---|---|---|---|
| **Bridge** | **40S** | **60S** | **№** | **40S** | **60S** | **№** |
| **eB8** | eS1 | ES31L | 2 | eS1 | ES31L | 2 |
| | | | | eS1 | eL43 | 2 |
| **eB11** | eS8 | H63 | 1 | eS8 | ES41L | 5 |
| | eS8 | ES41L | 6 | | | |
| **eB12** | ES6S | eL19 | 13 | ES6S | eL19 | 14 |
| | uS17 | eL19 | 3 | eS7 | eL19 | 2 |
| **eB13** | eS6 | uL3 | 3 | h6 | uL3 | 1 |
| | eS6 | eL24 | 8 | ES3S | eL24 | 6 |
| | | | | ES12S | eL24 | 3 |
| | | | | eS6 | uL3 | 2 |
| | | | | eS6 | eL24 | 11 |
| **eB14** | h27 | eL41 | 10 | h27 | eL41 | 10 |
| | h44 | eL41 | 4 | h44 | eL41 | 5 |
| | h45 | eL41 | 14 | h45 | eL41 | 14 |

Bridges B5, B6 and B8 form a cluster of intersubunit bridges near the binding sites for translational GTPases (Table 3, Figures 9 and 10) (Ben-Shem et al. 2011). In both pre- and post-translocational states, bridges B5 and B8 are formed by interactions between protein uL14 of the large subunit and helices 44 and/or 14 of the small subunit. Third bridge of this cluster, B6, is formed between protein eL24 of the large subunit and helix 44 of the small subunit (Table 3) Therefore, helix 44 links all three bridges of this cluster with rRNA-rRNA bridges B2a and B3 (Tables 2 and 3). Protein uL14 locates closely to the binding sites of eEF2 and eIF5B and directly interacts with eRF1, eRF3, eIF6 and ABCE1/Rli1 (Gartmann et al. 2010; Klinge et al. 2011; Becker et al. 2012; Taylor et al. 2012; Fernandez et al. 2013; Preis et al. 2014; Kiosze-Becker et al. 2016; Pellegrino et al. 2018). Protein eL24 forms eukaryote-specific bridge eB13, which is discussed below (Ben-Shem et al. 2011). In the bacterial ribosome, bridges B5, B6 and B8 has been shown to regulate fidelity of decoding (Sun et al. 2011). Additionally, B8 bridge regulates the rate of translocation (McClory et al. 2010; Fagan et al. 2013; Liu & Fredrick 2013).

Bridges B4 and B7b/c connect body/platform of the small subunit with L1 stalk side of the large subunit (Table 3, Figures 9 and 10) (Ben-Shem et al. 2011). B4 is formed by interactions between helix 34 and protein eL30 of the large subunit and helix 20 and protein uS15 of the small subunit. Bridge B7b/c is formed by interactions of proteins uL2 and eL43 of the large ribosomal subunit with helix 24 of the small ribosomal subunit (Table 3). Interestingly, components of bridges B4 and B7b/c are tightly connected to other intersubunit bridges (Figures 7 and 8). Protein eL43 is also involved in the formation of bridge eB8 (Figure 8). Helix 24 of the 18S rRNA links bridge B7b/c with rRNA-rRNA bridges B2a, B2b and B2c (Tables 2 and 3). Protein uS15 interacts with protein eS7, which is a component of the eB12 bridge (Figure 7). As a part of such extensively interconnected intersubunit contacts, bridges B4 and B7b/c regulate rotational state of ribosome (Liu & Fredrick 2013; Musalgaonkar et al. 2014; Bock et al. 2015).

Five out of seventeen intersubunit bridges in the budding yeast ribosome are specific for eukaryotic ribosomes (Figures 9 and 10, Table 4). These bridges are predominated by eukaryote-specific moieties of rRNAs and r-proteins. Only one of the eukaryote-specific bridges, eB14, locates in the core of the ribosome (Figures 9 and 10). The rest four bridges (eB8, eB11, eB12 and eB13) are positioned at the peripheral regions, where relative motion of ribosomal subunits is most pronounced (Figures 9 and 10) (Ben-Shem et al. 2011). Peripheral eukaryote-specific bridges are mainly formed by protein-rRNA interactions, and to a lesser extent by protein-protein interactions. Therefore, these bridges probably support the movement of ribosomal subunits (Ben-Shem et al. 2011; Behrmann et al. 2015). The functional importance of eukaryote-specific bridges remains largely obscure due to limited number of studies, if compare to knowledge about conserved bridges. The role of eB8 and eB11 or their components in the protein synthesis is solely derived from structural studies of eukaryotic ribosomes, as no functional studies were yet conducted.

The role of eB14 was assessed in two published studies utilizing deletion of protein eL41 (Dresios et al. 2003; Meskauskas et al. 2003). In this thesis, the importance of bridge eB12 and eB13 for different aspects of ribosome functionality is demonstrated (chapters 2.1.1. and 2.2.1.) (References I and II).

Bridge eB8 is a small bridge at the E site side of the ribosome (Figures 9 and 10) (Ben-Shem et al. 2011). In both translocational states this bridge comprises two contacts between eukaryote-specific rRNA segment ES31L of the large subunit and protein eS1 of the small subunit. In the post-translocational conformation, these contacts are assisted by two additional interactions between proteins eL43 and eS1 (Table 4). Both large subunit components of this bridge, protein eL43 and 25S rRNA segment ES31L, interact with each other and are also interconnected with the L1 stalk through the protein eL8. Protein eL43 also links bridge eB8 with bridges B4 and B7b/c (Figure 8). Small subunit component of the eB8 bridge, protein eS1, locates on the edge of the platform domain, but its extension reaches the E-site of the small subunit. This protein interacts with components of the mRNA channel – 18S rRNA helix 26 and proteins eS26 and uS11 (Figure 7) (Ben-Shem et al. 2011). Crosslink studies of the mammalian ribosomes showed that helix 26, as well as both eS26 and uS11, interact with mRNA molecules in the mRNA channel (Demeshkina et al. 2003; Graifer et al. 2004; Pisarev et al. 2008). It is possible that such position of eB8 allows this bridge to regulate translocation events at the E site side of the ribosome (Figure 9 and 10).

Bridge eB11 is formed by interactions between 25S rRNA expansion segment ES41L of the large subunit and protein eS8 of the small subunit. In the pre-translocational conformation, this bridge has one additional contact of helix 63 of 25S rRNA with protein eS8 (Table 4, Figure 9 and 10). Segment ES41L is a part of the second cluster of eukaryote-specific segments that extend to L1 stalk (Figure 4). Protein eS8 locates at the left foot of the small subunit, where it interacts with expansion segment ES3S of the 18S rRNA (Figure 3). This makes eS8 a part of the eukaryote-specific cluster at the bottom of the small subunit. Protein eS8 also interacts with protein uS17, which is the component of the eukaryote-specific bridge eB12 (Figure 7). Helix 63 of 25S rRNA interacts with other component of the eB12 bridge - protein eL19 (Ben-Shem et al. 2011). Therefore, eB11 bridge is interconnected with bridge eB12.

Bridge eB12 is distinctive by the long C-terminal α-helix of protein eL19 that extends from the E site side of the large subunit (Figure 10). Helix interacts with 18S rRNA expansion segment ES6S of the small ribosomal subunit (Table 4, Figure 9). Interestingly, the N-terminal domain and the middle region of eL19 do not interact with any r-protein of the large ribosomal subunit, but are buried within the 25S rRNA. Segment ES6S belongs to the largest cluster of eukaryote-specific expansion segments of the 18S rRNA (Figure 3). Structural studies have shown that eB12 bridge is dynamical. In the pre-translocational state, additional interactions between C-terminal α-helix of eL19 and uS17 occur. In the post-translocational state, interactions with uS17 are replaced by interactions with eS7 (Table 4) (Ben-Shem et al. 2011) Proteins uS17 and eS7

interact with uS8, which has a largest number of contacts with other small subunit proteins (Figure 7). Therefore, all three small subunit components of the eB12 bridge are parts of protein-protein interaction network that may transduce information from the periphery of the small subunit to its central part. This network also interconnects eB12 with bridges eB11 (interaction of uS17 with eS8) and B4 (interaction of uS17 with uS15) (Figure 7). Functions of the eB12 bridge and its main component, protein eL19, are further discussed in chapter 2.1.

By analogy to eB12, bridge eB13 is recognizable by the long C-terminal α-helix and the linker region of protein eL24 that extend from the A-site side of large subunit (Figure 10). Bulk of the eB13 bridge is formed by interactions of α-helix and linker of eL19 with protein eS6 of the small ribosomal subunit. These contacts are assisted by interactions between uL3 and eS6 (Table 4, Figures 9 and 10). In the post-translocational state additional contacts of eL24 with 18S rRNA (h6, ES3S and ES12S) occur (Table 4). Unfortunately, possible interactions of eL24 with 18S rRNA are not visible in the pre-translocational state due to incomplete structure of the eL24 (Ben-Shem et al. 2011). The N-terminal domain of the eL24 resides on the surface of the large subunit and interacts with proteins uL3 and uL14 (Figure 8). Collectively, interconnected proteins uL3, uL14 and eL24 form a structural cluster that gives rise to the interconnected intersubunit bridges B5, B6, B8 and eB13 (Figure 8). Functions of the eB13 bridge and its main component, protein eL24, are discussed in chapter 2.2.

Bridge eB14 is an exceptional eukaryote-specific bridge, as it is located at the core of the ribosome (Table 4, Figures 9 and 10) (Ben-Shem et al. 2011). This bridge is formed by extensive interactions of the smallest r-protein eL41 of the large ribosomal subunit with conserved 18S rRNA helices 27, 44 and 45 (Table 4). Interestingly, while only two aa residues of the eL41 interact with large ribosomal subunit, 18 aa residues out of 25 aa residues in the eL41 interact with small subunit. Due to its position at the core of the ribosome near the helix 69, bridge eB14 may cooperate with rRNA-rRNA bridges B2a, B2b and B3 (Tables 2 and 4, Figures 9 and 10). This bridge may participate in fine-tuning of ribosome functionality, as deletion of eL41 results in mildly decreased peptidyl transferase activity and fidelity of translation (Dresios et al. 2003; Meskauskas et al. 2003).

Altogether, structural studies indicate that all bridges are interconnected through the network of interactions, which involves not only r-proteins and rRNAs, but also tRNAs, mRNA and translation factors. Functional studies demonstrate that integrity of intersubunit bridges is important for the functionality of ribosomes.

## 1.2. Assembly of the budding yeast ribosome

Assembly of the yeast ribosome is a nontrivial task, as it requires coordinate expression of ~150 rRNA genes and 137 genes encoding for r-proteins, accompanied by action of ~76 small nucleolar ribonucleoproteins (snoRNP) and ~200 assembly factors (reviewed in Konikkat & Woolford 2017; Chaker-Margot 2018; Klinge & Woolford 2019). It is estimated that exponentially growing budding yeast cell produces 2000 ribosomes per minute, which makes ribosome assembly an extremely fast, energy consuming and thereby critical for cellular homeostasis process (Kief & Warner 1981; Warner 1999; Strunk & Karbstein 2009). Assembly starts in the nucleolus, where transcription of 35S precursor rRNA (pre-rRNA) by polymerase I occurs (Miller & Beatty 1969; Neyer et al. 2016). 35S pre-rRNA contains two external transcribed spacers (5'ETS and 3'ETS), two internal transcribed spacers (ITS1 and ITS2) and sequences for 18S rRNA, 5.8S rRNA and 25S rRNA (Figure 11) (reviewed in Konikkat & Woolford 2017; Klinge & Woolford 2019). In parallel, polymerase III transcribes 5S rRNA (Dieci et al. 2007; Han et al. 2018). During assembly, pre-rRNAs undergo hierarchical processing, folding, chemical modification and assembly with r-proteins and assembly factors (reviewed in Fernandez-Pevida et al. 2015; Henras et al. 2015). Assembly machinery proceeds through the subsequent nucleolar, nucleoplasmic and cytoplasmic steps to result in mature small and large ribosomal subunits (Figure 11). R-proteins that form intersubunit bridges are also involved in assembly of ribosomal subunits, as they coordinate folding of rRNAs and binding of numerous assembly factors and other r-proteins.

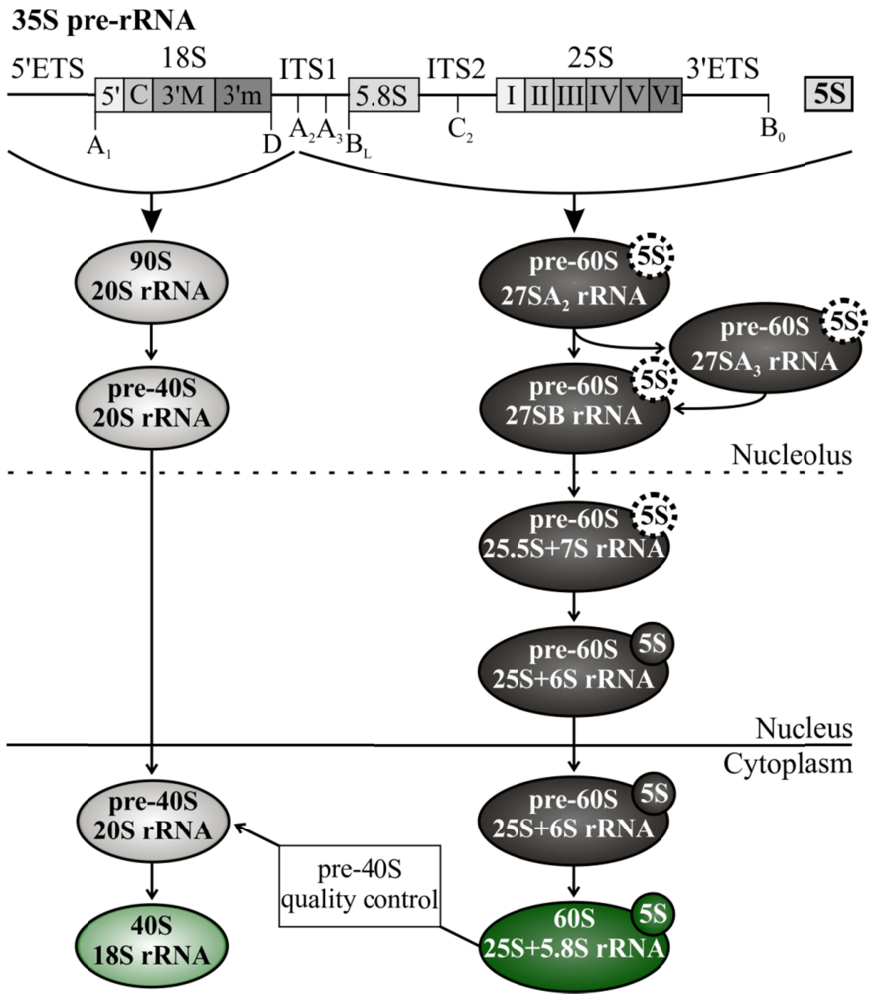


**Figure 11. The assembly pathways of small and large subunits of the budding yeast ribosome.** Regions and cleavage sites of 35S pre-rRNA are shown. Domains of 18S rRNA (5'; C, central; 3'M, 3' major; 3'm, 3' minor) and 25S rRNA (I-VI) are indicated. Domain A of the 18S rRNA and domain 0 of the 25S rRNA are not shown as they are specific for the secondary and tertiary structures of rRNAs. Pre-ribosomal particles and their rRNA content are shown. Pre-40S and pre-60S particles are light and dark grey, respectively. Mature 40S and 60S subunits are light and dark green, respectively. Dotted 5S ring indicates not fully assembled 5S RNP. Filled 5S ring indicates stably associated 5S RNP.

### 1.2.1. Assembly of the small ribosomal subunit

Initial assembly of the small ribosomal subunit occurs co-transcriptionally in the nucleolus while 5'ETS, 18S rRNA and ITS1 of 35S pre-rRNA are transcribed. These regions are progressively packed into the 90S pre-ribosomal particle with a molecular weight of ~5 MDa (Figure 11) (Dragon et al. 2002; Osheim et al. 2004; Perez-Fernandez et al. 2007; Perez-Fernandez et al. 2011; Chaker-Margot et al. 2015; Zhang et al. 2016). About 40 % of this mass is attributed to the 5'ETS particle, which is generated by the large subcomplexes UtpA, UtpB and U3 snoRNP along with multiple factors that are bound to the 5'ETS region (Chaker-Margot et al. 2015; Sun et al. 2017). Structural studies have demonstrated that domains of 18S rRNA in the 90S pre-ribosomal particles are already folded into native-like structures (Kornprobst et al. 2016; Cheng et al. 2017; Sun et al. 2017). Domains are associated with 19 r-proteins that predominantly adopt mature conformations: 8 proteins are in the 5' domain, 6 proteins are in the central domain, 5 proteins are in the 3' major domain (Figure 12) (Sun et al. 2017). Six r-proteins that form intersubunit bridges (eS1, eS6, eS7, eS8, uS15 and uS17) are already associated at this stage (Sun et al. 2017). Nonetheless, 18S rRNA is not yet fully packed as rRNA domains are still organized into independent structures covered by assembly factors (Kornprobst et al. 2016; Barandun et al. 2017; Cheng et al. 2017; Sun et al. 2017).

To form pre-40S ribosomal particles, 35S pre-rRNA is cleaved at the $A_2$, which in rapidly growing yeast cells occurs co-transcriptionally once RNA polymerase I has reached ~1.2–1.5 kb downstream of that site (Osheim et al. 2004; Kos & Tollervey 2010; Axt et al. 2014). Cleavage results in the formation of 20S and $27SA_2$ pre- rRNAs and thereby separates pathways of small and large ribosomal subunit assembly (Figure 11). Other critical steps at this point include cleavage at the $A_1$ site, removal and degradation of 5'ETS particle, formation of central pseudoknot, further folding of 18S rRNA domains, incorporation of r-proteins and assembly/export factors. During this processes, pre-40S ribosomal particle is transited from the nucleolus to the nucleoplasm and then subsequently exported to the cytoplasm, where domains of 18S rRNA are finally folded (reviewed in Chaker-Margot 2018). Assembly of the head domain includes incorporation of two r-proteins, uS13 and uS19, that eventually form intersubunit bridges B1a and B1b/c (Figure 12) (Sun et al. 2017). Interestingly, the latest steps of cytoplasmic maturation of pre-40S particles involve association with mature large ribosomal subunits, which is particularly promoted by eIF5B (Lebaron et al. 2012). Formation of such 80S-like complexes allows to quality control the translation competence of the pre-40S ribosomal particles (Lebaron et al. 2012; Strunk et al. 2012). Dissociation of 80S-like complexes triggers cleavage of the 20S pre-rRNA at the D site and dissociation of last assembly factors (Vanrobays et al. 2004; Lamanna & Karbstein 2009; Granneman et al. 2010; Lamanna & Karbstein 2011; Heuer et al. 2017b; Scaiola et al. 2018). Following that, newly made mature 40S subunits are ready to enter the translation pool.

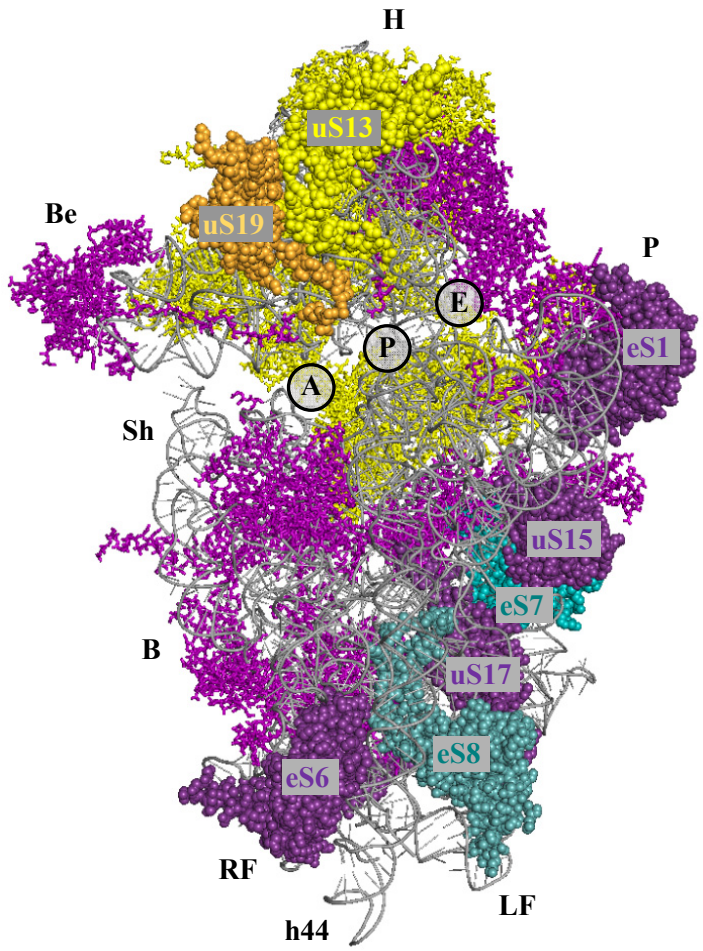


**Figure 12. Hierarchical assembly of r-proteins in the small subunit of the budding yeast ribosome.** rRNA is colored grey. Landmarks of the small subunit and approximate positions of the A, P and E sites are indicated. H, head; Be, beak; P, platform; Sh, shoulder; B, body; RF, right foot; LF, left foot; h44. R-proteins associated with 90S particles are colored purple/teal. R-proteins assembled during pre-40S maturation are colored yellow/orange. R-proteins involved in the formation of intersubunit bridges are shown as spheres and indicated. PDB coordinates 3U5F and 3U5G (Ben-Shem et al, 2011) were rendered in PyMol.

### 1.2.2. Assembly of the large ribosomal subunit

Assembly of the large ribosomal subunit is more complex than that of the small subunit (Figure 11). Initial folding of 5.8S rRNA and domains I and II of 25S rRNA occurs co-transcriptionally while $A_2$ is not yet cleaved (Kater et al. 2017; Sanghai et al. 2018). To form $27SA_2$ pre-rRNA, nascent transcript is cleaved at the $A_2$ and $B_0$ sites. Following that, 3'ETS and ITS1 are removed, which yields 27SB pre-rRNAs (Allmang & Tollervey 1998; Konikkat & Woolford 2017). To remove 3'ETS, $27SA_2$ pre-rRNA is processed by exonuclease Rex1 to give mature 3'end (Henras et al. 2015). ITS1 is removed in two alternative pathways (Figure 11). In the major pathway, 85-90 % of $27SA_2$ pre-rRNA is cleaved at the $A_3$ site ($27SA_3$ pre-rRNA) and then processed by exonucleases to form $27SB_S$ pre-rRNA (Chu et al. 1994; Henry et al. 1994; Lygerou et al. 1996; Johnson 1997; Oeffinger et al. 2009). In the minor pathway, 15–10 % of $27SA_2$ pre-rRNA is cleaved at the $B_L$ site, yielding $27SB_L$ pre-rRNA (Henry et al. 1994; Konikkat & Woolford 2017). Recent cryo-EM studies of the earliest pre-60S particles revealed that 27SB pre-rRNAs are already associated with 18 r-proteins (Figure 13) (Kater et al. 2017). Eleven of these proteins, along with 13 assembly factors, have been shown to be required for the removal of ITS1 (Lebreton et al. 2008; Poll et al. 2009; Gamalinda et al. 2014; Chen et al. 2017; Kater et al. 2017). Removal of ITS1 also depends on the presence of r-protein uL3, which later forms intersubunit bridge eB13 (Poll et al. 2009; Gamalinda et al. 2014). All these proteins assist in the initial folding of domains I and II and 5.8S rRNA region of pre-rRNA at the solvent side of pre-60S subunit (Kater et al. 2017; Sanghai et al. 2018). Pre-rRNA is subsequently circularized by interactions between domains I, II and VI (Kater et al. 2017; Sanghai et al. 2018; Zhou et al. 2019). Initially flexible domains III, IV and V fold towards the intersubunit side of the pre-60S subunit, giving rise to peptide exit tunnel and peptidyl transferase center (Kater et al. 2017; Sanghai et al. 2018). Final nucleolar step of assembly, cleavage of ITS2 at the C2 site, results in the formation of 7S and 25.5S pre-rRNAs (Schillewaert et al. 2012; Castle et al. 2013; Gasse et al. 2015). At this step, pre-60S particles contain 30 r-proteins, including bridge-forming proteins uL14, eL19 and eL30 (Figure 13) (Kater et al. 2017). Eleven of these r-proteins, including uL14 and eL19, are important for the cleavage of 27SB pre-rRNA at the C2 site (Poll et al. 2009; Gamalinda et al. 2014). Cleavage triggers transit of pre-60S particles from the nucleolus to the nucleoplasm, where 7S and 25.5S pre-rRNAs are processed to 6S pre-rRNA and 25S rRNA (Mitchell et al. 1997; Geerlings et al. 2000; Gadal et al. 2002; Schillewaert et al. 2012; Gasse et al. 2015; Fromm et al. 2017). Processing of the 7S rRNA depends on the presence of two bridge-forming proteins, uL2 and eL43 (Poll et al. 2009; Gamalinda et al. 2014). At the nucleoplasmic step, formation of the mature central protuberance occurs - 5S RNP (r-proteins uL18 and uL5 bound to 5S rRNA) rotates ~180$^{o}$ to its mature position (Leidig et al. 2014; Madru et al. 2015; Wu et al. 2016). Although 5S RNP may be associated with the earliest nucleolar pre-60S particles, it becomes structurally stable only

in the nucleoplasm (Zhang et al. 2007; Calvino et al. 2015; Kater et al. 2017). Stabilization of the 5S RNP allows further assembly of peptidyl transferase center. At this point, pre-60S particles comprise in total 37 r-proteins (Figure 13) (Kater et al. 2017) Final nuclear step of the assembly involves structural proofreading of peptide exit tunnel and peptidyl transferase center as well as maturation of P stalk (Bradatsch et al. 2012; Matsuo et al. 2014; Sarkar et al. 2016; Wu et al. 2016; Klinge & Woolford 2019). Correct folding of functional centers ensures binding of export factors that shield negative charges of pre-60S particle while guiding it through the nuclear pore complexes (Stage-Zimmermann et al. 2000; Oeffinger et al. 2004; Hackmann et al. 2011; Bradatsch et al. 2012; Konikkat & Woolford 2017). Upon export to the cytoplasm, 6S pre-rRNA is processed into mature 5.8S rRNA, which has been proposed to be a signal that export has completed (Thomson & Tollervey 2010). Processing of the 6S pre-rRNA and cytoplasmic release of assembly factors particularly depends on the presence of the bridge-forming protein uL5 (Gamalinda et al. 2014). Cytoplasmic step involves assembly of the last 9 r-proteins, including bridge-forming eL24 and eL41, and final folding of P stalk (Figure 13) (Saveanu et al. 2003; Lo et al. 2009; Lo et al. 2010; Konikkat & Woolford 2017; Ma et al. 2017). Cytoplasmic pre-60S particles progress into mature active 60S subunits once assembly factors complete quality control and dissociate from all functional centers (Panse & Johnson 2010; Karbstein 2013).

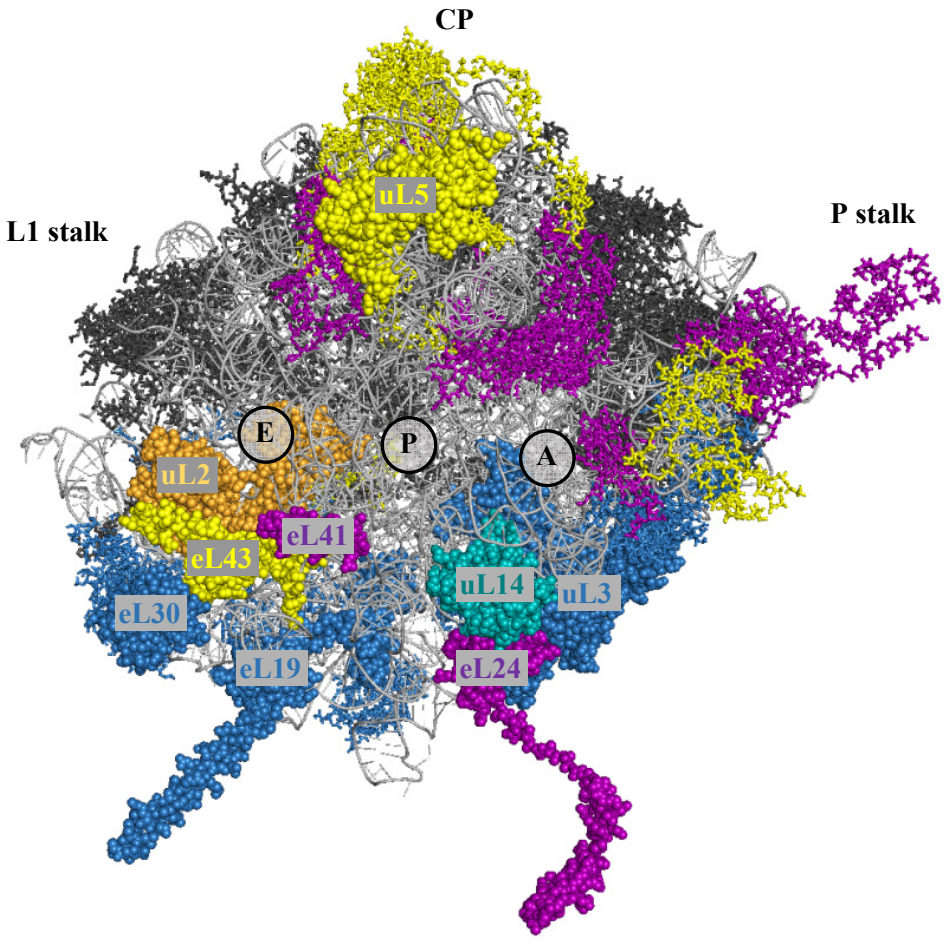


**Figure 13. Hierarchical assembly of r-proteins in the large subunit of the budding yeast ribosome.** rRNA molecules are colored grey. Landmarks of the large subunit (L1 stalk; P stalk; CP, central protuberance) and approximate positions of the A, P and E sites are indicated. R-proteins associated with earliest determined pre-60S particles are colored black. R-proteins further assembled before transit from the nucleolus to the nucleoplasm are colored blue/teal. R-proteins assembled in the nucleoplasm are colored yellow/orange. R-proteins assembled in the cytoplasm are colored magenta. R-proteins involved in the formation of intersubunit bridges are shown as spheres and indicated. PDB coordinates 3U5H and 3U5I (Ben-Shem et al, 2011) were rendered in PyMol.

## 1.3. Eukaryotic translation

Translation of mRNA, or protein synthesis, is a decoding of mRNA nucleotide sequence into protein amino acid sequence. Translation can be divided into four steps: initiation, elongation, termination and ribosome recycling. Interplay of these steps determines efficiency/quality of protein synthesis and protein folding. It has been estimated that exponentially growing yeast cell synthesizes about 13000 proteins per second (von der Haar 2008). Rapidity and accuracy of translation is provided, among other things, by proper binding of translation factors and communication between ribosomal subunits. All these, in turn, depend on the functionality of ribosomal intersubunit bridges.

### 1.3.1. Translation initiation

Canonical translation initiation depends on the presence of cap structure at the 5'end and poly(A) tail at the 3'end of mRNA molecule. Cap-dependent initiation of translation occurs through a scanning mechanism: where preinitiation complex moves along mRNA in a 3' direction and selects for a start codon (reviewed in Kozak 1978; Merrick & Pavitt 2018).

Initiation begins with the formation of ternary complex, where GTP-bound eIF2 is associated with Met-tRNA$_i^{Met}$ (Kapp & Lorsch 2004; Kapp et al. 2006). Ternary complex, additionally stabilized by eIF5, is subsequently docked to the small subunit, resulting in the formation of 43S preinitiation complex (Figure 14 step 2) (Algire et al. 2002; Majumdar et al. 2003; Olsen et al. 2003; Jennings et al. 2017). Docking of ternary complex is allowed by the rotation of the head domain of small subunit, which is induced by the cooperative binding of factors eIF1 and eIF1A near the P and A sites, respectively (Figure 14 step 1). In addition, head rotation opens a latch in the mRNA entry channel required for the recruitment of mRNA (Passmore et al. 2007; Hussain et al. 2014; Llacer et al. 2015). Factors eIF1 and eIF1A keep Met-tRNA$_i^{Met}$ in the preferable for mRNA scanning incompletely bound P$_{out}$ state (Saini et al. 2010; Hashem et al. 2013; Zhang et al. 2015). Formation of the 43S preinitiation complex is also promoted by eIF3, the largest initiation factor. eIF3 embraces the solvent side of the small subunit near the mRNA entry and exit channels, and interacts with other initiation factors (Aylett et al. 2015; Llacer et al. 2015; Aitken et al. 2016; Simonetti et al. 2016).

mRNA is loaded into the opened mRNA channel of the small subunit through the activation by eIF4F complex, which consists of four factors: eIF4A, eIF4B, eIF4E and eIF4G (Figure 14 step 3) (Gingras et al. 1999). Loading starts with recognition of the 5' cap structure containing mRNAs by the cap-binding eIF4E (Sonenberg et al. 1978; O'Leary et al. 2013). Factor eIF4G interacts with eIF4E and poly(A) tail-bound Pab1. This interactions circularize mRNA to give a cap-to-tail closed loop (Kessler & Sachs 1998; Wells et al. 1998; Gross et al. 2003; Archer et al. 2015). ATP-dependent RNA helicase eIF4A, stimulated by

eIF4B, unwinds mRNA secondary structures and eliminates mRNA-bound proteins at the 5' end of mRNA (Grifo et al. 1984; Abramson et al. 1987; Rozen et al. 1990). 48S preinitiation complex is formed through attachment of circularized mRNA to the 43S preinitiation complex, which is mediated by factors eIF3, eIF5, eIF4B and eIF4G (Figure 14 step 4) (Dever et al. 2016).

Preinitiation complex scans 5' untranslated region of mRNA for the correct codon-anticodon interactions between mRNA and Met-tRNA$_i^{Met}$ (Figure 14 step 5) (Cigan et al. 1988). Recognition of start codon by the Met-tRNA$_i^{Met}$ anticodon leads to an extensive rearrangements in the preinitiation complex, resulting if the fully engaged $P_{in}$ state of Met-tRNA$_i^{Met}$. Back-rotation of the head to the closed conformation fixates preinitiation complex at the start codon and prevents further scanning (Hussain et al. 2014; Llacer et al. 2015). Factors eIF1, GDP-bound eIF2 and eIF5 are released (Figure 14 step 6) (Kapp & Lorsch 2004; Unbehaun et al. 2004; Cheung et al. 2007; Jennings & Pavitt 2010; Jennings et al. 2017).

Joining of ribosomal subunits is promoted by the GTP-bound eIF5B, which is recruited after the release of eEF2 (Figure 14 step 7) (Olsen et al. 2003; Acker et al. 2009; Fernandez et al. 2013; Zheng et al. 2014; Yamamoto et al. 2014). Cryo-EM reconstructions of the mammalian 80S initiation complexes suggest that eIF5B-promoted subunit joining occurs with rolling of the small subunit (Yamamoto et al. 2014). Hydrolysis of the eIF5B-bound GTP is followed by back-rolling of the small subunit. This results in the unique P/pa tRNA position, where the anticodon of tRNA is in the P site and the 3'CCA end of tRNA is in the A site. Upon the dissociation of GDP-bound eIF5B, the 3'CCA end of tRNA is relocated to the elongation-competent P/P position (Yamamoto et al. 2014). Following that, GDP-bound eIF5B and eEF1A dissociate from the ribosome (Figure 14 step 8) (Fringer et al. 2007; Acker et al. 2009). Interestingly, it has been proposed that factor eIF3 remains associated with 80S ribosome during the joining of ribosomal subunits and few elongation cycles after (reviewed in Valasek et al. 2017). Initiation of translation leads to the formation of 80S ribosome, where the anticodon of Met-tRNA$_i^{Met}$ in the P site is base-pared with the start codon of mRNA. At the same time, vacant A site is ready to accept aminoacyl-tRNA.

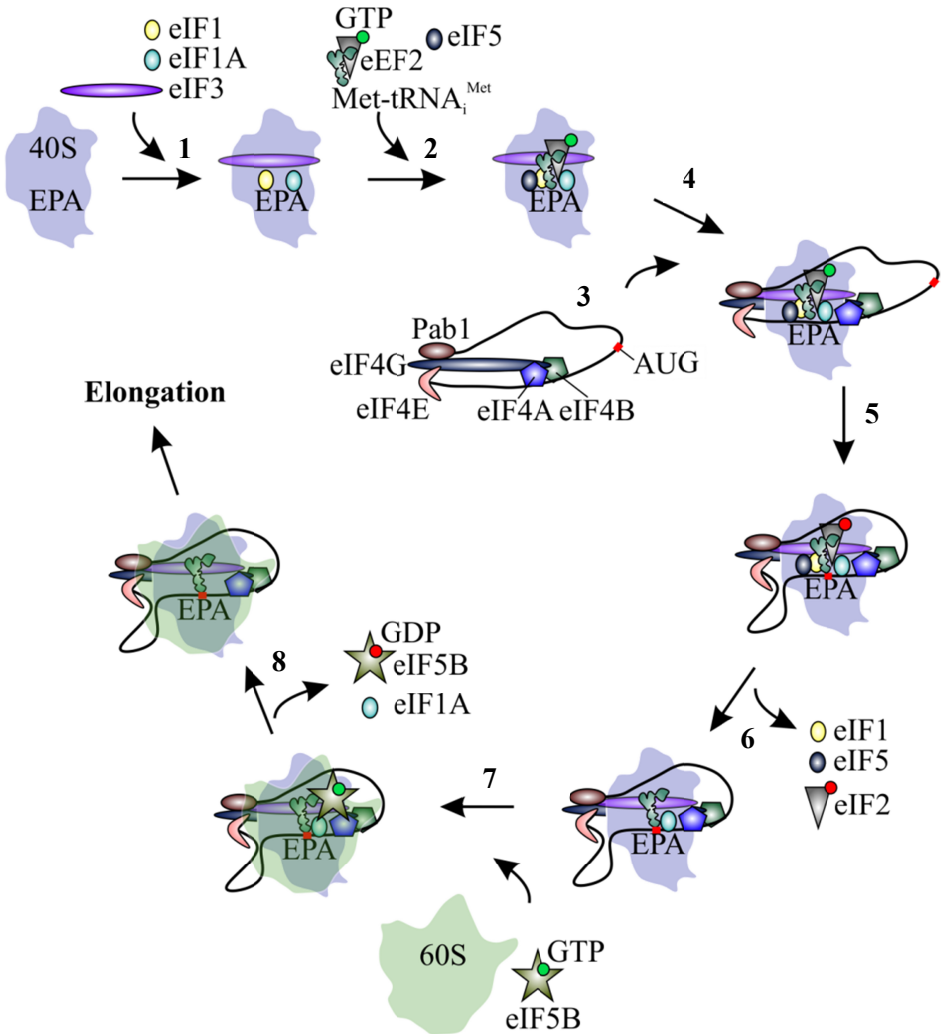


**Figure 14. Model of the eukaryotic initiation of translation.** Steps described in the main text are shown. **1 -** binding of factors eIF1, eIF1A and eIF3. **2** – docking of ternary complex to the small subunit. **3** – activation of mRNA by eIF4F complex. **4** – attachment of activated mRNA to the 43S preinitiation complex. **5** – scanning. **6** – recognition of start codon, dissociation of factors eIF1, GDP-bound eIF2 and eIF5. **7** – joining of ribosomal subunits promoted by the GTP-bound eIF5B. **8** – dissociation of eIF1A and GDP-bound eIF5B. Timing of eIF4F and eIF3 release is not shown. Adapted with modifications from Merrick and Pavitt, 2018.

Joining of ribosomal subunits depends on the correct formation of intersubunit bridges. Unfortunately, kinetics of intersubunit bridge formation in the eukaryotic ribosomes is yet not known. Time-resolved chemical probing and cryo-EM studies of bacterial subunit association in the absence of other ligands suggested a multi-step process of bridge formation (Hennelly et al. 2005; Shaikh et al. 2014). It has been proposed that conserved central bridges such as B2a, B3 and B7b are formed fist. Following that, formation of peripheral bridges B1a, B1b and B8 occurs. Lastly, bridges B2c, B4, B5 and B6 are formed (Shaikh et al. 2014). Alternatively, other time-resolved studies did not observe stepwise manner of the intersubunit bridge formation. These studies asserted that formation of intersubuni bridges is a one-step reaction completed within 60 ms (Nguyenle et al. 2006; Chen et al. 2015). In addition, recent study of bacterial subunit association implying 50S subunit and 30S initiation complex demonstrated that all intersubunit bridges are formed within 20–80 ms after mixing 50S and 30S initiation complex together (Kaledhonkar et al. 2018).

Apart from the time-resolved studies, sedimentation analyses of ribosomal particles in sucrose density gradients have been extensively used in association studies of bacterial ribosomes. *In vitro* reassociation of purified ribosomal subunits in the absence of particular bridges demonstrated that bridges B1a, B1b, B2a, B2b, B2c, B3, B7a and B8 are important for the correct association of subunits (Cukras & Green 2005; Ali et al. 2006; Liiv & O'Connor 2006; Kipper et al. 2009). These results are consistent with chemical modification studies that indicate requirement of bridges B2a, B2b, B3, B4, B5 and B7a for the formation of ribosomal particles (Maiväli et al. 2002; Pulk et al. 2006). Finally, sedimentation analysis of cell extract from bridge mutants showed the importance of bridges B3, B5, B7b and B8 for the association of subunits (Liiv & O'Connor 2006; Sun et al. 2011). Therefore, all intersubunit bridges, except for the B6, has been shown to be involved in the efficient subunit joining. However, loss of single bridge rarely causes lethal phenotype, probably due to compensatory actions of intact bridges. Negative effect of compromised bridge can also be outdone by addition of trans-acting factors such as mRNA and tRNAs. In this thesis, the importance of eukaryote-specific bridge eB12 and eB13 for the association of budding yeast ribosomal subunit was demonstrated both *in vivo* and *in vitro* (discussed in chapters 2.1.1. and 2.2.1.).

### 1.3.2. Translation elongation

Elongation of translation is a cyclic process of peptide bond formation, where each round results in the attachment of an amino acid to the growing polypeptide chain (reviewed in Dever et al. 2016; Dever et al. 2018). Elongation round starts with delivery of aminoacyl-tRNA by the GTP-bound eEF1A to a sense codon in the empty A site (Figure 15, step 1). Upon formation of the correct codon-anticodon interactions, 18S rRNA nucleotide residue G577 of the decoding center latches codon-anticodon helix. Codon recognition results in the

movement of eEF1, so the GTPase domain of the eEF1A becomes positioned at the sarcin/ricin loop (Ogle et al. 2001; Ogle et al. 2002; Demeshkina et al. 2012; Budkevich et al. 2014; Shao et al. 2016; Loveland et al. 2017). Following GTP hydrolysis, GDP-bound eEF1A dissociates from ribosome and is recycled into GTP-bound form by the nucleotide exchange factor eEF1B (Gromadski et al. 2007). Release of eEF1A allows proofreading of aminoacyl-tRNA – it is either accommodated to promote peptide bond synthesis or dissociates from ribosome (Figure 15, step 2). During accommodation, aminoacyl-tRNA is transferred from the A/T state to the A/A state, which allows acceptor arm of tRNA to reach peptidyl transferase center (Sanbonmatsu et al. 2005; Gromadski et al. 2006; Geggier et al. 2010; Whitford et al. 2010; Caulfield & Devkota 2012). Interestingly, cryo-EM reconstruction of mammalian ribosomes demonstrated that accommodation of tRNA is coupled with rolling of the small subunit (Budkevich *et al.* 2014). Rolling results in the narrowing of the A site intersubunit region and opening of the E site intersubunit region. Consequently, rolling most notably affects peripheral bridges: B6, B8 and eB13 at the A site side and eB8 at the E site side (Budkevich et al. 2014). In general, intersubunit bridges ensure correct conformation of ribosome required for the efficient initial selection of aminoacyl-tRNA, hydrolysis of eEF1A-bound GTP and/or proofreading of aminoacyl-tRNA. Several functional studies of bacterial and yeast ribosomes support this possibility, demonstrating that bridges B1a, B1b/c, B2c, B3, B5, B6, B7a, B7b and B8 are important for the selection of aminoacyl-tRNA (Cukras & Green 2005; Liiv & O'Connor 2006; McClory et al. 2010; Rhodin & Dinman 2011; Sun et al. 2011; Fagan et al. 2013; Musalgaonkar et al. 2014; Bowen et al. 2015).

Following accommodation of aminoacyl-tRNA, peptide bond formation occurs in the peptidyl transferase center: the α-amino group of the aminoacyl-tRNA attacks the carbonyl carbon of the peptidyl-tRNA with assistance of rRNA (Figure 15, step 3) (Rodnina et al. 2007). It has been recently suggested that factor eIF5A, located in the E site, orients acceptor arm of the P site tRNA for the reaction with the A site tRNA by the hypusine side chain (Saini et al. 2009; Melnikov et al. 2016; Shin et al. 2017). Growing peptide chain moves through the peptide exit tunnel. Upon peptide bond formation, A site is occupied by peptidyl-tRNA and P site is occupied by deacylated-tRNA. This conformation is not stable, so acceptor arms of the A and P site tRNAs dislocate into the P and E sites, respectively. However, anticodon ends of tRNAs remain bound to the A and P sites, which altogether results in the formation of A/P and P/E hybrid states. This process is coupled with the rotation of the small subunit (Ratje et al. 2010; Budkevich et al. 2011; Dunkle et al. 2011; Svidritskiy et al. 2014; Behrmann et al. 2015). Binding of the GTP-bound eEF2 to the GTPase associated center induces swiveling of the head domain. Factor eEF2 catalyzes translocation of tRNAs and mRNA (Figure 15, step 4) (Spahn et al. 2004a; Taylor et al. 2007; Sengupta et al. 2008; Munro et al. 2010; Achenbach & Nierhaus 2015). During translocation, diphthamide modification of eEF2 interacts with mRNA and decoding center to maintain reading frame and

prevent slippage of mRNA (Pellegrino et al. 2018). Upon translocation, peptidyl- and deacylated-tRNA molecules are in P/P and E/E states, respectively. Finally, GDP-bound eEF2 is released (Figure 11, step 5) (Taylor et al. 2007). Release of the deacylated-tRNA from the E site in the yeast ribosome is specifically promoted by the ATP-bound eEF3, which locates near the E site (Figure 15, step 6) (Triana-Alonso et al. 1995; Andersen et al. 2006). Interestingly, eEF3 also stimulates eEF1A-dependent delivery of the aminoacyl-tRNA (Triana-Alonso et al. 1995; Kovalchuke et al. 1998).

Several studies have demonstrated that rotation of the ribosomal subunits during translocation is regulated by intersubunit bridges. Intersubunit bridges contribute to the rotational equilibrium of ribosomes and regulate flow of information between subunit (Rhodin & Dinman 2011; Liu & Fredrick 2013; Musalgaonkar et al. 2014; Bock et al. 2015). The degree of rearrangements during rotation is the least at the central part, where rRNA-rRNA bridges lie, and increases at the periphery of ribosome. For example, the long C-terminal helical domain of proteins eL19 and eL24, that form the bulk of eukaryote-specific bridges eB12 and eB13, follow rotational movement of the small ribosomal subunit (Ben-Shem et al. 2011; Behrmann et al. 2015; Khatter et al. 2015). Thus, bridges eB12 and eB13 may coordinate rotation of the small subunit.

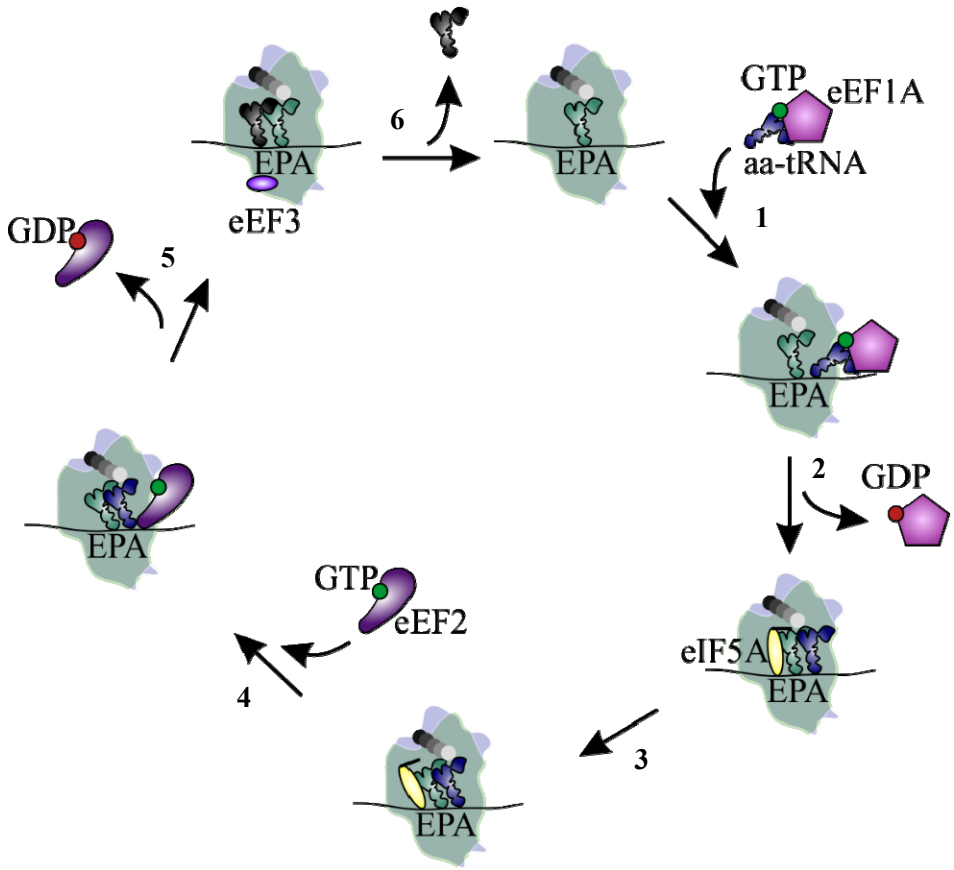


**Figure 15. Model of the eukaryotic elongation of translation.** Steps described in the main text are shown. **1** – delivery of aminoacyl-tRNA (aa-tRNA) by GTP-bound factor eEF1A. **2** – accommodation of aa-tRNA at the A site, release of the GDP-bound eEF1A. **3** – formation of peptide bond. **4** – binding of GTP-bound eEF2. **5** – translocation, release of GDP-bound eEF2. **6** – eEF3-promoted release of tRNA form E site. Timing of eIF5A and eEF3 release is not shown. Adapted with modifications from Dever et al, 2018.

### 1.3.3. Translation termination and ribosome recycling

Termination of translation occurs once stop codon (UAA, UAG or UGA) enters the A site of ribosome (reviewed in Dever & Green 2012; Dever et al. 2016; Hellen 2018). Stop codon is recognized by the N-terminal domain of factor eRF1, while the C-terminal domain of eRF1 is bound to the eRF3 (Figure 16, step 1) (Bertram et al. 2000; Mantsyzov et al. 2010; Conard et al. 2012; Preis et al. 2014; Blanchet et al. 2015; Brown et al. 2015; Shao et al. 2016). Once stop codon is recognized, hydrolysis of GTP by eRF3 occurs (Frolova et al. 1996; Salas-Marco & Bedwell 2004; Alkalaeva et al. 2006; Pisareva et al. 2006; Cheng et al. 2009; des Georges et al. 2014). Subsequently, conformational changes reorient eRF1 closely to the 3'CCA end of peptidyl-tRNA (Figure 16, step 2) (Matheisl et al. 2015; Muhs et al. 2015; Shao et al. 2016). This results in rearrangements in the peptidyl transferase center that lead to the hydrolysis and release of peptide (Figure 16, step 3) (Frolova et al. 1999; Song et al. 2000; Jin et al. 2010).

Budding yeast 80S ribosome is recycled by factor Rli1 (ABCE1 in mammalians). Cryo-EM studies of ribosome recycling complexes demonstrated that Rli1/ABCE1 binds to the translational GTPase binding site (Figure 16, step 4). It interacts with 25S rRNA sarcin-ricin loop, 18S rRNA (helices 5, 8, 14 and 15) and r-proteins eS6, eS24, uL6, uL10 and uL14 (Becker et al. 2012; Preis et al. 2014; Brown et al. 2015; Kiosze-Becker et al. 2016; Heuer et al. 2017a). FeS cluster domain of Rli1/ABCE1 interacts with eRF1, which is bound to the A site at the proximity to the central intersubunit bridges (Preis et al. 2014; Brown et al. 2015). Recent structural studies of pre- and post-recycling complexes suggested two steps of ribosome dissociation (Brown et al. 2015; Kiosze-Becker et al. 2016; Heuer et al. 2017a). First, movement of the FeS cluster domain of Rli1/ABCE1 pushes eRF1 into the intersubunit space, which destabilizes intersubunit bridges. Following that, FeS cluster domain clashes with protein uL14 near the helix 44 and therefore prevents formation of the B5 bridge (Heuer et al. 2017a)

The timing of Rli1/ABCE1 dissociation after release of the large subunit remains unknown. It is either dissociates immediately after release (Figure 16, step 5) or retains on the small subunit to promote recruitment of the initiation factors (Pisarev et al. 2010; Heuer et al. 2017a; Hellen 2018). In both scenarios, factors eIF1, eIF1A and eIF3 bind to the small subunit and promote dissociation of the non-initiator tRNA from the P site, which in turn leads to release of mRNA (Figure 16, step 6) (Pisarev et al. 2007; Pisarev et al. 2010). Finally, ribosomal subunits can proceed into next round of protein synthesis.

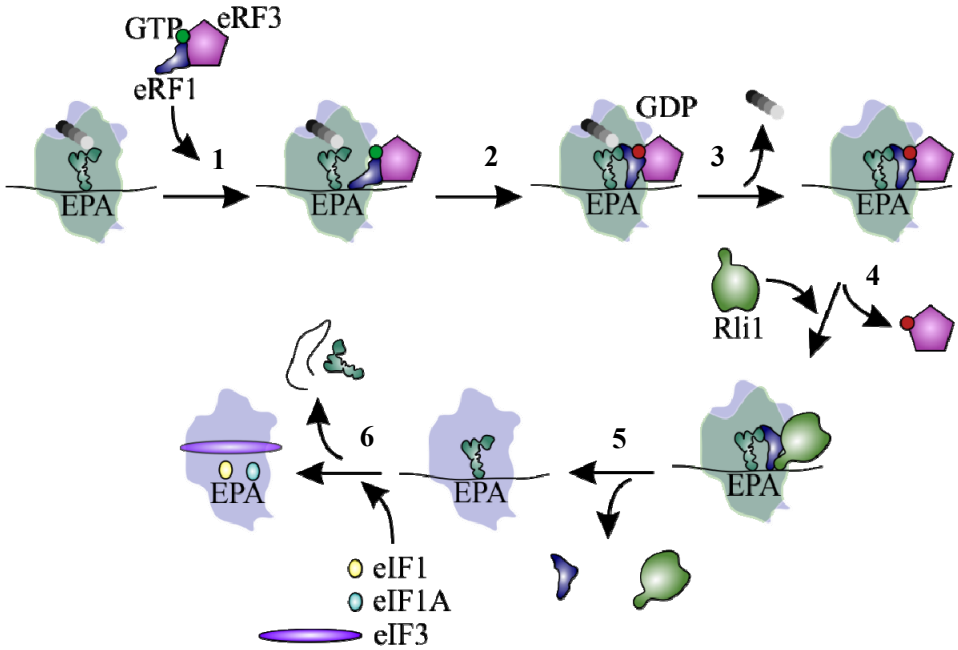


**Figure 16. Model of the eukaryotic termination of translation and ribosome recycling.** Steps described in the main text are shown. **1** – binding of factors eRF1 and GTP-bound eRF3. **2** – recognition of stop codon, hydrolysis of eRF3-bound GTP. **3** – release of peptide. **4** – release of the GDP-bound eRF3, binding of the factor Rli1. **5** – Rli1-promoted recycling of ribosomal subunits. Scenario with dissociation of the Rli1 is shown. **6** – binding of factors eIF1, eIF1A and eIF3; release of mRNA and tRNA. Adapted with modifications from Dever and Green, 2012 and Hellen et al, 2018.

# 2. RESULTS AND DISCUSSION

## Aims of the study

The high-resolution atomic models of eukaryotic ribosomes demonstrate that two r-proteins, eL19 and eL24, are distinctive by their position in the ribosome. Both proteins consist of three domains: an N-terminal globular domain, a middle/linker region and a C-terminal α-helical domain. The C-terminal α-helices of eL19 and eL24 are long antennae-like domains that form eukaryote-specific intersubunit bridges eB12 and eB13, respectively (chapter 1.1.3.). The main aim of the present study was to characterize functions of different domains of r-proteins eL19 and eL24 in the budding yeast ribosome.

Protein eL19 is essential for viability of budding yeast cells (Song *et al.* 1996). Previous study implying depletion of eL19 has revealed that this protein contributes to the cleavage of 27SB pre-rRNAs during assembly of the large ribosomal subunit (chapter 1.2.2.) (Poll et al. 2009). This study aspired to determine:

- domains of eL19 that are important for the cleavage of 27SB pre-rRNAs;
- functions of the intersubunit bridge eB12 in the budding yeast ribosome;
- whether contribution to the pre-rRNA cleavage or formation of the intersubunit bridge is an essential for cell viability function of eL19.

Second r-protein covered in this study, eL24, is nonessential for budding yeast cell viability (Baronas-Lowell & Warner 1990). However, the absence of eL24 leads to the reduced by 30 % growth rate, accumulation of halfmer ribosomes and altered elongation of translation (Baronas-Lowell & Warner 1990; Dresios et al. 2000; Dresios et al. 2001). The tasks of this study were to dissect:

- functions of the eB13 bridge in the budding yeast ribosome;
- functions of the N-terminal globular domain of the eL24.

## 2.1. Functions of the r-protein eL19 at the domain level (Ref I)

Essential r-protein eL19 belongs to the group of archaea/eukaryote-specific proteins (Table 1, Figure 8) (Lecompte et al. 2002; Ban et al. 2014). Structural studies demonstrated that the eukaryotic variant of eL19 is composed of three domains (Figure 17) (Ben-Shem et al. 2011; Anger et al. 2013; Behrmann et al. 2015). The globular N-terminal domain and the helical middle region of eL19 are archaea/eukaryote-specific and demonstrate similar conformation in ribosomes of both *Archaea* and *Eukarya* (Figure 17) (Ban et al. 2000; Ben-Shem et al. 2011; Anger et al. 2013; Armache et al. 2013; Gabdulkhakov et al. 2013; Behrmann et al. 2015; Khatter et al. 2015). In the budding yeast ribosome, these domains are buried within the 25S rRNA and do not interact with any other large subunit protein (Table 1, Figure 8) (Ben-Shem et al. 2011; Poirot & Timsit 2016). The third, C-terminal domain of eukaryotic eL19 is folded into a long eukaryote-specific α-helix (Figure 17). This domain extends far from the E-site side of the large subunit and forms eukaryote-specific bridge eB12 (Ref I Figure 1C, chapter 1.1.3.). By comparison, archaeal eL19 has a short, only ~17 amino acid residues long C-terminal helix and therefore it cannot reach the small subunit (Figure 17) (Armache et al. 2013). In the budding yeast ribosomes, a bulk of the eB12 bridge is formed by interactions between C-terminal α-helix of eL19 and ES6S of 18S rRNA. Bridge eB12 is additionally stabilized by interactions of α-helix with proteins uS17 (pre-translocational state) and eS7 (post-translocational state) (Table 4) (Ben-Shem et al. 2011). Based on the position of the eB12 bridge in the ribosome, involvement of this bridge in joining of subunit and shedding/releasing of factors during translation initiation has been suggested (Ben-Shem et al. 2011).

In order to study functions of different domains of eL19, we constructed several yeast mutants. To analyse the effect of eL19 depletion, we used a conditional null mutant system. We ectopically expressed *RPL19A* gene under the control of the galactose inducible *GAL1* promotor in *rpl19AΔrpl19BΔ* background (Ref I Materials and Methods, Supplemental Tables S1 and S2). To analyse the importance of the C-terminal α-helix of eL19, we constructed a set of eL19A variants that were expressed under the control of the native promotor in *rpl19AΔrpl19BΔ* background (Figure 17, Ref I Table 1). Full-length wild-type eL19A variant served as a control. The $eL19_{1\text{-}183}$ variant lacked amino acid residues interacting with protein eS7. The $eL19_{1\text{-}154}$ variant lacked the eB12 bridge forming region of the C-terminal α-helix of eL19. The $eL19_{1\text{-}146}$ variant mimicked the archaeal version of eL19 and was also not able to form the eB12 bridge. The $eL19_{1\text{-}133}$ variant lacked the entire C-terminal α-helix of eL19.

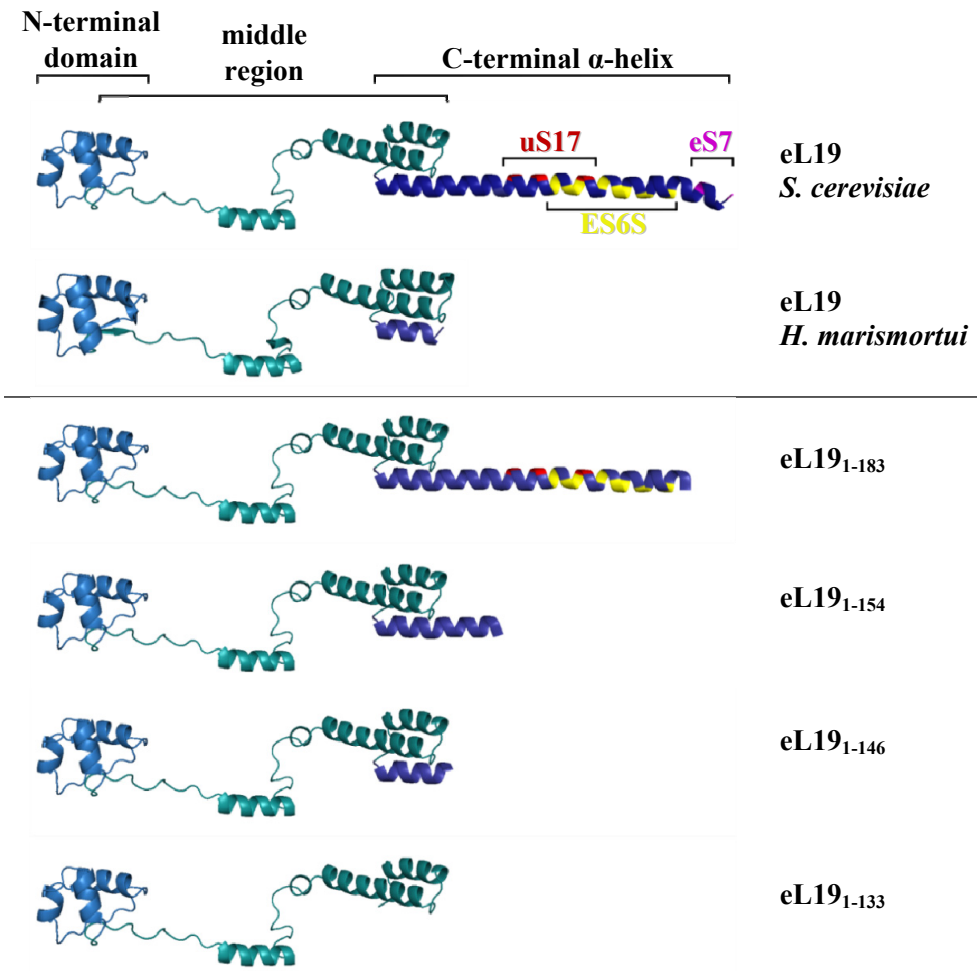


**Figure 17. Structure of the r-protein eL19.** Structures of the wild-type eL19 in eukaryotic (*Saccharomyces cerevisiae*) and archaeal (*Haloarcula marismortui*) ribosomes are shown in the upper panel. Variants of eL19 constructed in this study are shown in the lower panel. The N-terminal domains (light blue), the middle regions (teal) and the C-terminal α-helical domains (dark blue) of eL19 are indicated. Amino acid residues interacting with uS17 (red), 18S rRNA ES6S (yellow) and eS7 (purple) are indicated. Coordinates for eukaryotic (PDB entry 3U5E from Ben-Shem et al, 2011) and archaeal eL19 (PDB entry 4V9F from Gabdulkhakov et al, 2013) were rendered in PyMol.

### 2.1.1 The C-terminal α-helix of eL19 is required for the association of ribosomal subunits

We started our analysis with assessing the growth characteristics of all constructed mutants. In accordance with previous studies, protein eL19 was essential for yeast cell viability (Ref I Figure 3A) (Song et al. 1996). In contrast, all mutants expressing truncated variants of eL19, except for $eL19_{1-133}$, were viable (Ref I Figures 1D and 2A). This indicates that the eB12 bridge forming region of eL19 is not essential for yeast cell viability. In turn, the N-terminal domain, the middle region and the first 13 amino acid residues of C-terminal helix of eL19 are essential for viability (discussed in chapter 2.1.2.).

Next, we accessed the functional importance of the eB12 bridge for the budding yeast ribosome. More detailed growth analysis demonstrated that the loss of interactions between eL19 and eS7 (variant $eL19_{1-183}$) resulted in similar to wild-type growth (Ref I Figure 2A). In contrast, loss of the entire eB12 bridge upon truncation of C-terminal α-helix of eL19 led to slow growth at all analysed temperatures (variant $eL19_{1-154}$ and $eL19_{1-146}$) (Ref I Figure 2A). To more extensively characterize eL19 mutants, we evaluated global levels of translation (Figure 18). We determined incorporation of radioactive isotope labelled amino acids in newly synthesized proteins in exponentially growing mutant and control cells. No significant change in the translation levels was observed upon loss of interactions between eL19 and eS7 (variant $eL19_{1-183}$), if compared to eL19 control cells (Figure 18). Loss of the entire eB12 bridge (variants $eL19_{1-154}$ and $eL19_{1-146}$) reduced the level of translation by ~20 % (Figure 18). Taken together, our results demonstrate that growth phenotype of cells expressing $eL19_{1-183}$ variant is similar to that of control cells. This indicates that contacts between eL19 and eS7 have a minor role in ribosome functioning. Absence of the entire eB12 bridge, in turn, leads to reduced ribosome functionality, as can be deduced from slow growth and decreased global levels of translation.

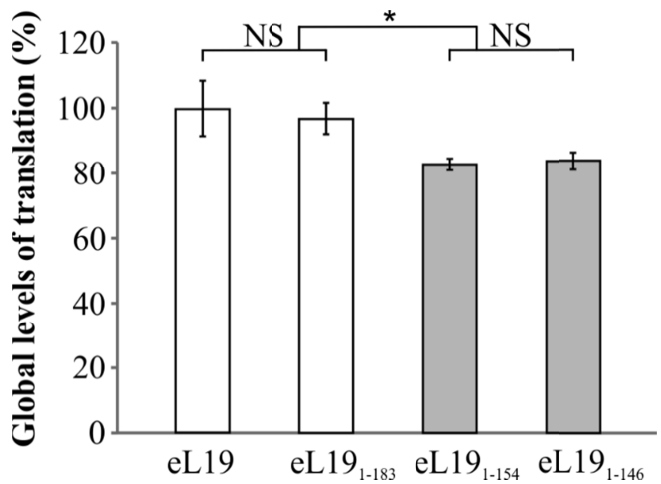


**Figure 18. Global levels of translation in cells with different variants of eL19.** *rpl19AΔrpl19BΔ* strains expressing wild-type (eL19) or mutant variants ($eL19_{1-183}$, $eL19_{1-154}$ and $eL19_{1-146}$**)** of eL19 were analysed. Radioactive isotope labelled amino acids were added to exponentially growing cells in synthetic minimal medium at 30 °C. Culture samples were taken at every 15 minute over 2 hours of incubation. Samples were TCA precipitated and incorporation of radioactive label was measured. Values of disintegrations per minute (DPM) were plotted and slope was calculated. The average (mean± SD) normalized slope values from at least four biological replicates are plotted. Statistical significance was determined by the unpaired two sample Student's t-test (* $p<0.01$; NS, not significant).

In order to test the impact of reduced ribosome functionality on the populations of ribosomal particles, we analysed ribosome-polysome profiles of cells with different variants of eL19 (Ref I Figure 2B). Populations of ribosomal particles were similar in cells expressing $eL19_{1-183}$ variant and control cells at both temperatures. Expression of $eL19_{1-154}$ and $eL19_{1-146}$ variants, not able to form bridge eB12, resulted in excess large ribosomal subunits when grown at 20 °C (Ref I Figure 2B). Interestingly, excess of large subunits at 20 °C was not accompanied by excess of neither small ribosomal subunits nor stalled preinitiation complexes referred to as halfmer. Both scenarios would be indicative of defects in joining of ribosomal subunits during translation initiation. To determine relative levels of large and small ribosomal subunits more precisely, we prepared extracts of control and mutant cells in low $Mg^{2+}$ conditions when grown at 20 °C (Figure 19). Low $Mg^{2+}$ conditions cause ribosomes to dissociate into subunits, which can be then separated by sucrose density gradient centrifugation. Relative amount of subunits were assessed by quantifications of areas under the peaks of small and large subunits. Consistent with ribosome-polysome profile analysis, expression of $eL19_{1-183}$ has no effect on the levels of ribosomal subunits, if compared to eL19 control (Figure 19). Loss of the entire

eB12 bridge (variants $eL19_{1-154}$ and $eL19_{1-146}$) led to increased ratio of 60S/40S, which reflects decreased level of small subunits. It has been shown that shortage of the functional large ribosomal subunits leads to turnover of small ribosomal subunits (Gregory et al. 2019). This may prevent formation of preinitiation complexes not able to form 80S ribosomes due to absence of functional large subunits. Excess preinitiation complexes could sequester mRNAs and distort protein synthesis (Gregory et al. 2019). It is possible that loss of the eB12 bridge leads to defects in subunit joining, which causes accumulation of free ribosomal subunits (Ref I Figure 2B). To secure the process of translation, free small subunits are degraded, resulting in increased 60S/40S ratio (Figure 19).

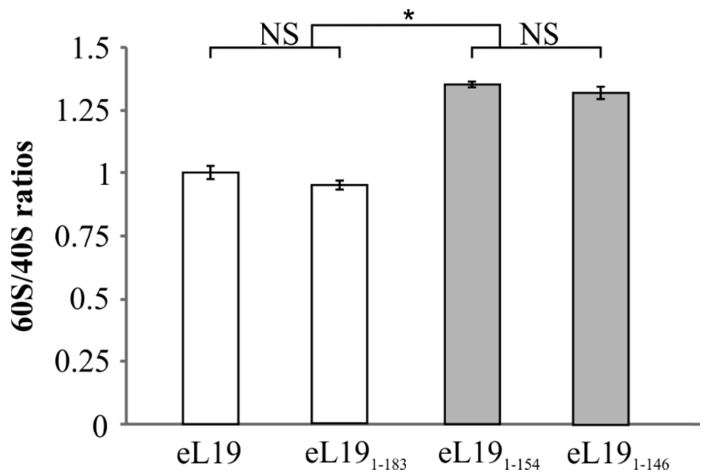


**Figure 19. Relative amounts of small (40S) and large (60S) ribosomal subunits in extracts of cells with different eL19 variants.** *rpl19AΔrpl19BΔ* strains expressing wild-type (eL19) or mutant variants ($eL19_{1-183,}$ $eL19_{1-154}$ and $eL19_{1-146}$**)** of eL19 were grown in YPD medium at 20 °C. The whole cell extracts were prepared at the low $Mg^{2+}$ conditions and analysed in 10% - 30% sucrose gradients. Areas under the small (40S) and large (60S) ribosomal subunit peaks were quantified by ImageJ and 60S/40S ratios were calculated. The average (mean ± SD) normalized ratios of two biological replicates are plotted. Statistical significance was determined by the unpaired two sample Student's t-test (* $p<0.01$; NS, not significant).

We speculate that increased amount of free large subunits upon loss of the eB12 bridge is caused by defects in subunit joining. To test this possibility, we analysed the necessity of eB12 bridge for the *in vitro* reassociation of ribosomal subunits (Ref I Figure 4). In this assay we used purified large and small ribosomal subunits obtained through dissociation of monosomes by treatment with 0.5 M KCl. The reassociation reactions were conducted at different $Mg^{2+}$ concentrations through mixing together large subunits containing either wild-type or mutant variants of eL19 with wild-type small subunits. The reassociation efficiencies were assessed by centrifugation in sucrose density gradient with corresponding $Mg^{2+}$ concentrations. Wild-type ribosomal subunits reassociated already at 5 mM $Mg^{2+}$. In the absence of contacts between eL19 and protein eS7 (variant $eL19_{1\text{-}183}$), reassociation of ribosomal subunits occurred similarly to wild-type (Ref I Figure 4). Deletion of the entire eB12 bridge forming region of eL19 (variant $eL19_{1\text{-}154}$ and $eL19_{1\text{-}146}$) resulted in the inability of large subunits to form 80S particles at all analysed $Mg^{2+}$ concentrations (Ref I Figure 4). We conclude that interactions between eL19 and eS7 have a minor role in the formation of 80S particle. In accordance, structural studies of the budding yeast ribosomes demonstrated that these are transient contacts occurring only in the pre-translocational state (Table 4) (Ben-Shem et al. 2011). The association of subunits largely relies on the extensive protein-rRNA interactions between C-terminal of eL19 and 18S rRNA expansion segment ES6S. These contacts are presented in both pre- and post-translocational states (Table 4) (Ben-Shem et al. 2011).

Altogether, loss of the eB12 bridge (variants $eL19_{1\text{-}154}$ and $eL19_{1\text{-}146}$) lead to a reduced ribosome functionality, as can be deduced from slow-growth of yeast cells, decreased global levels of translation and accumulation of excess large ribosomal subunits (Figure 18, Ref I Figure 2). Analysis of *in vitro* reassociation activities of ribosomal subunits demonstrated inability to form 80S particles when the eB12 bridge is absent (Ref I Figure 4). All these phenotypes may reflect the involvement of the eB12 bridge in the association of 80S ribosome during the subunit joining step of translation initiation. The role of this bridge in the subunit joining has been also suggested based on the structural studies (Ben-Shem et al. 2011). Additionally, it has been shown that the eB12 bridge forming region of eL19 is highly dynamical and follows movements of the small subunit during translocation (Figure 20) (Ben-Shem et al. 2011; Behrmann et al. 2015). Such position of the C-terminal domains of eL19 may allow it to regulate rotation of the small ribosomal subunits. Thus, eB12 may contribute to the elongation step of translation. However, this possibility remains to be examined.

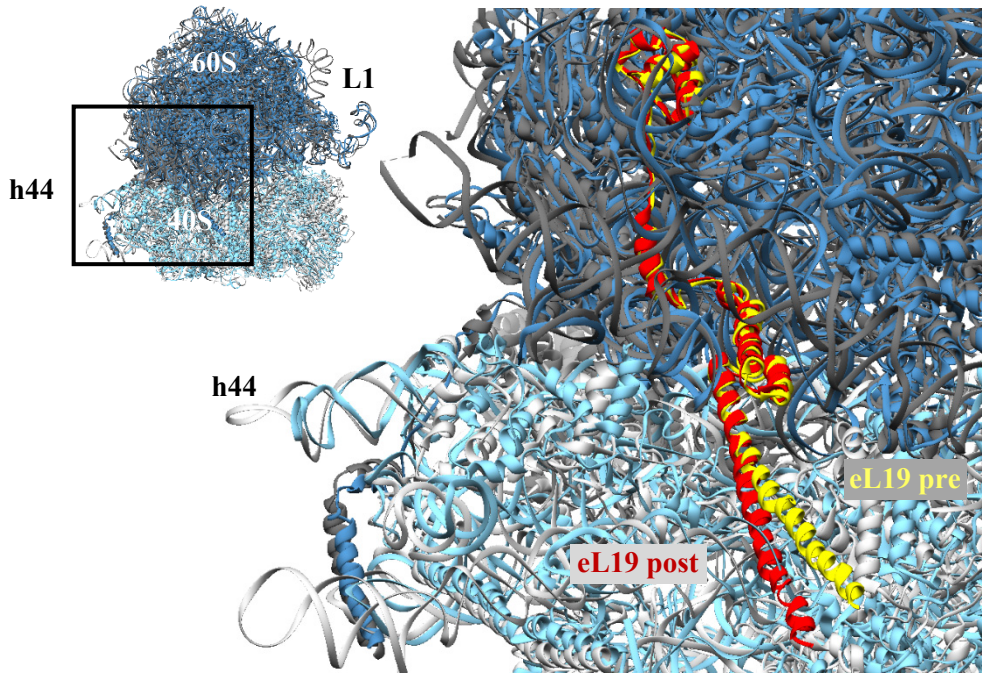


**Figure 20. Conformation of eL19 in pre-translocational (eL19 pre; yellow) and post-translocational (eL19 post; red) conformations of the human ribosome.** rRNAs and proteins of large subunit are dark blue (pre-translocation) and dark grey (post-translocation). rRNAs and proteins of small subunit are light blue (pre-translocation) and light grey (post-translocation). Small panel illustrates approximate position of the enlarged region (square) within 80S ribosome. Positions of helix 44 (h44) and L1 stalk (L1) are indicated. Human ribosomes in pre-translocational (PDB coordinates 4UG0 from Khatter et al, 2015) and post-translocational conformation (PDB coordinates 4V6X from Anger et al, 2013) were superimposed in Chimera.

### 2.1.2. The N-terminal domain and the middle region of eL19 are required for the assembly of the large ribosomal subunit

Our analysis of eL19 mutants demonstrated that N-terminal domain, the middle region and the first 13 amino acid residues of C-terminal helix of eL19 are essential for yeast cell viability (Ref I Figures 1D, 2A and 3A). Next, we analysed ribosome-polysome profiles of cells with depleted or truncated eL19 by sucrose density gradient centrifugation (Ref I Figures 2A and 3B). The depletion of eL19 led to the reduction of polysome and monosome fractions accompanied by accumulation of excess small ribosomal subunits (Ref I Figure 3B). This phenotype may reflect defects in the assembly of the large ribosomal subunit. Truncation of C-terminal α-helix of eL19, in turn, did not cause any changes in monosome and polysome fractions, if compared to control. Therefore, the eB12 bridge forming C-terminal domain of eL19 has no apparent role in assembly of large ribosomal subunit.

During assembly of the large ribosomal subunit, 35S pre-rRNA is cleaved and processed in several subsequent steps, where each step gives rise to a specific intermediate pre-rRNA species (chapter 1.2.2.). Relative amounts of such pre-rRNAs reflect efficiency of large subunit assembly, so changes in the amounts of pre-rRNAs may point to a defective assembly step. To access the steady-state levels of pre-rRNAs, we employed primer extension analysis of total RNA extracted from mutant cells (Ref I Figures 3C and 3D). We used two specific oligonucleotides that allowed us to determine relative amounts of $27SA_2$, $27SA_3$ and 25.5S pre-rRNA species. Unfortunately, we were not able to assess levels of 27SB and 7S pre-rRNAs separately, but only total levels of both pre-rRNAs. These are denoted as "$27SB_L$+$7S_L$"and "$27SB_S$+$7S_S$"(Ref I Figures 3C and 3D). Depletion of eL19 led to the slight reduction in levels of $27SA_2$ and $27SA_3$ pre-rRNAs and occurrence of a nonspecific stops at the ITS2 region. We also detected increase in total levels of 27SB and 7S pre-rRNAs, probably indicating increased levels of $27SB_L$ and $27SB_S$ pre-rRNAs (Ref I Figure 3D). In contrast, truncations of C-terminal domain of eL19 had no effect on the pre-rRNA processing, according to the primer extension analysis. These results demonstrate that cleavage at the $C_2$ cite depends on the presence of the N-terminal domain, the linker region and the first 13 amino acid residues of C-terminal domain of eL19. This is consistent with previous study that showed defects in cleavage of 27SB pre-rRNAs upon depletion of the whole eL19 (Poll et al. 2009).

Altogether, our data demonstrates that the N-terminal domain, the middle region and the first 13 amino acid residues of C-terminal domain of eL19 are essential for yeast cell viability. The essential function of these domains is in contribution to the cleavage of 27SB pre-rRNAs at the $C_2$ site. Interestingly, structural studies of pre-60S particles demonstrated that the N-terminal domain and the middle region of eL19 lie at the distance from the $C_2$ site (Wu et al. 2016; Kater et al. 2017). It remains to be shown how these domains of eL19 are linked with cleavage of ITS2. Depletion of eL19 has been recently

demonstrated to cause alterations in structure of 5.8S rRNA and decreased levels of r-proteins uL22, uL24, uL29 and eL31 (Biedka et al. 2018). Therefore, presence of eL19 may be important for the formation of the rim around the peptide exit tunnel (Biedka et al. 2018). Cleavage at the $C_2$ site is carried out by endonuclease Las1 (Gasse et al. 2015; Pillon et al. 2017). It has been suggested that maturation of the rim around the peptide exit tunnel is necessary for Las1 to bind to the pre-60S particle and to cleave ITS2 (Biedka et al. 2018).

## 2.2. Functions of the r-protein eL24 at the domain level (Ref II and III)

Nonessential for yeast cell viability r-protein eL24 is an archaea/eukaryote-specific protein (Table 1, Figure 8) (Lecompte et al. 2002; Ban et al. 2014). The N-terminal globular domain of eL24 lies on the surface of the large ribosomal subunit and has a similar structure in both archaeal and eukaryotic ribosomes (Figure 21) (Ban et al. 2000; Ben-Shem et al. 2011; Anger et al. 2013; Armache et al. 2013; Gabdulkhakov et al. 2013; Behrmann et al. 2015; Khatter et al. 2015). In the budding yeast ribosome, R43 and R47 of the N-terminal domain of eL24 form two contacts with 18S rRNA helix 44, giving rise to a universally conserved bridge B6 (Table 3, Figures 9 and 10) (Ben-Shem et al. 2011). The linker region and the C-terminal α-helix of eukaryotic eL24 are eukaryote-specific domains that extend to the small ribosomal subunit and form the eukaryote-specific intersubunit bridge eB13 (Table 4, Figures 9, 10 and 21). In the budding yeast ribosome, the best part of the eB13 bridge is formed by interactions of eL24 with r-protein eS6. In the post-translocational state, additional contacts of eL24 with 18S rRNA (helix 6, ES3S and ES12S) occur. Structural studies suggested that the eB13 bridge forming region of eL24 follows movements of the small ribosomal subunit (Figure 22). Therefore, the eB13 bridge may regulate rotation of this subunit (Ben-Shem et al. 2011; Behrmann et al. 2015).

In order to study functions of the r-protein eL24 at the domain level, we constructed several yeast mutants (Figure 21, Ref II Figure 1A and Table 2). To study the effects of the absence of the whole eL24, we deleted both paralogous genes (mutant eL24Δ). In the eL24 control cells, the full-length wild-type eL24A was expressed under the control of native promotor in *rpl24AΔrpl24BΔ* background. Every other strain was generated by expression of mutant eL24A variants. To assess the role of the eB13 bridge forming region of eL24, the set of C-terminal truncated variants of eL24 was generated (Figure 21). The 112–155Δ variant was not able to interact with 18S rRNA helix 6 and ES3S. The 81–155Δ variant lacked amino acid residues interacting with r-protein eS6 and 18S rRNA helix 6 and ES3S. The eB13Δ variant lacked the entire eB13 bridge forming region of eL24. This variant of eL24 contained only the N-terminal domain and therefore mimicked the archaeal variant of eL24. Additionally, we constructed two variants to study the importance of the B6 bridge (Figure 21). The B6Δ variant harbored R43A and R47A substitutions in its N-terminal domain, which disrupted interactions between eL24 and 18S rRNA helix 44. The eB13ΔB6Δ variant was not able to form both eB13 and B6 bridges.

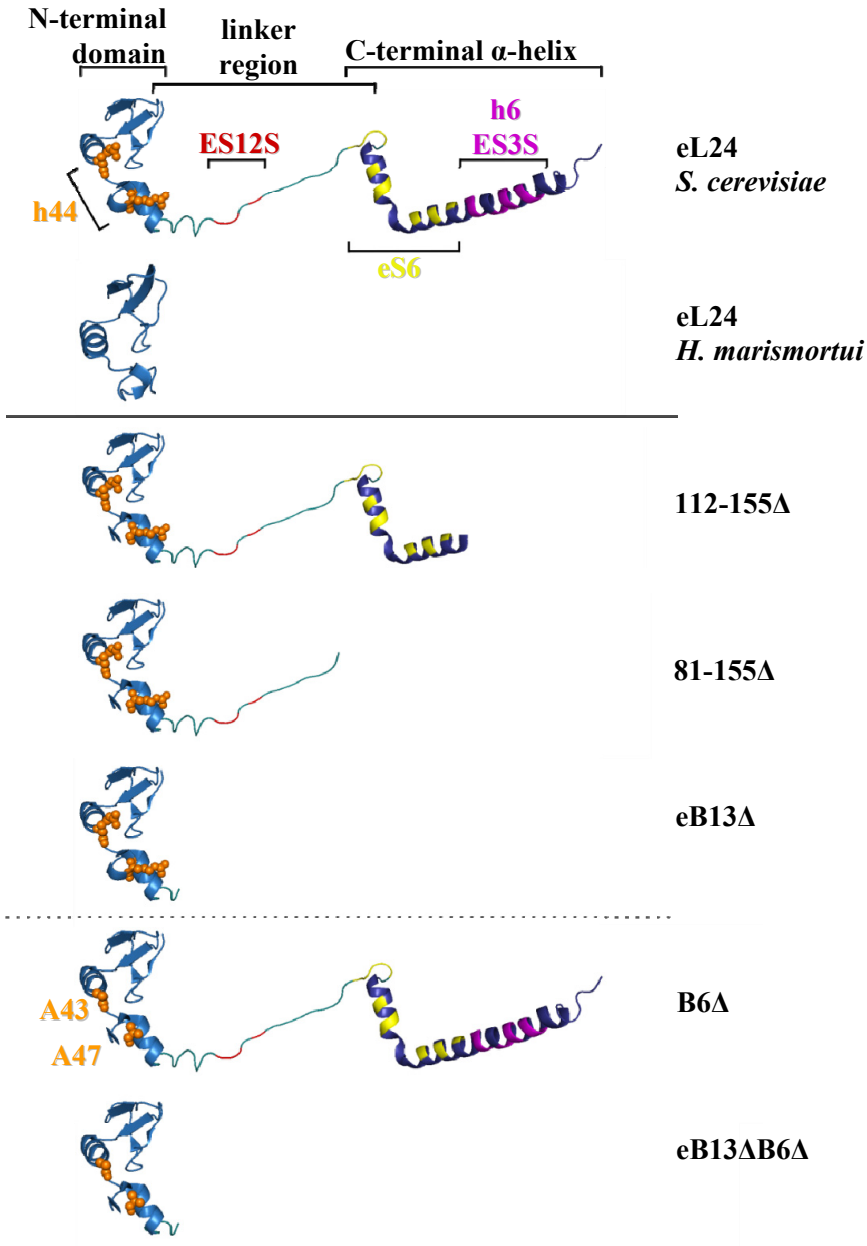


**Figure 21. Structure of the r-protein eL24.** Structures of wild-type eL24 in eukaryotic (*Saccharomyces cerevisiae*) and archaeal (*Haloarcula marismortui*) ribosomes are shown in the upper panel. The N-terminal domains (light blue), the middle regions (teal) and the C-terminal α-helical domains (dark blue) of eL24 are indicated. Amino acid residues interacting with 18S ES12S (red), protein eS6 (yellow) and 18S rRNA helix 6 and ES3S (purple) are indicated. Arginine residues that interact with 18S rRNA helix 44 (orange) and form B6 bridge are shown as orange spheres. Structures of the mutant

variants of eL24 constructed in this study are shown in the middle and lower panel. In variants B6Δ and eB13ΔB6Δ residues R43 and R47 that from bridge B6 were substitutes to residues A43 and A47. Coordinates for eukaryotic (PDB entry 3U5E from Ben-Shem et al, 2011) and archaeal eL24 (PDB entry 4V9F from Gabdulkhakov et al, 2013) were rendered in PyMol.

### 2.2.1. The C-terminal α-helix and the linker region of eL24 are important for both initiation and elongation steps of translation

The most prominent role of the eL24, carried out by its C-terminal domain and linker region, is in formation of the eukaryote-specific intersubunit bridge eB13. In order to access the importance of the eB13 bridge forming region of eL24 for the ribosome functionality, we constructed C-terminal truncated variants 112–155Δ, 81–155Δ and eB13Δ (Figure 21). Analysis of growth rates and global levels of translation in cells expressing truncated variants of eL24 allowed us to specify two phenotypic groups (Ref II Figure 2). First group contained variant 112–155Δ, which was not able to interact with 18S rRNA helix 6 and ES3S. Cells expressing this variant exhibited similar to the eL24 control cells growth rates and global levels of translation (Ref II Figure 2). This suggests that interactions of eL24 with 18S rRNA helix 6 and ES3S play a minor role in the functioning of the eB13 bridge. Second group consisted of variants 81–155Δ and eB13Δ. Both were not able to interact with protein eS6 and 18S rRNA helix 6 and ES3S. In addition, eB13Δ lacked contacts with 18S rRNA ES12S. This group demonstrated reduced ribosome functionality manifested in cold sensitivity and decreased global levels of translation by 15–20 % (Ref II Figure 2). These data indicates that functionality of the eB13 bridge mainly depends on the interactions between eL24 and eS6.

Additionally, we analyzed growth phenotypes of cells lacking the whole eL24 (eL24Δ) (Ref II Figure 2). These cells exhibited cold sensitivity and reduced by ~40 % global levels of translation, if compare to eL24 control cells. Interestingly, absence of the eL24 led to the intensified cold sensitivity and decreased by ~20 % global levels of translation, if compare to cells expressing eB13Δ variant of eL24 (Ref II Figure 2). This data suggests that the N-terminal domain of eL24 carries out additional functions. However, it is known that eL24 is incorporated into the large ribosomal subunit at the late, cytoplasmic step of maturation (Saveanu et al. 2003). Protein eL24 shares the same binding site with the essential biogenesis factor Rlp24 (Wu et al. 2016; Kater et al. 2017; Schuller et al. 2018). At the cytoplasmic step of maturation, factor Rlp24 is removed by AAA-ATPase Drg1, which is followed by incorporation of eL24 (Saveanu et al. 2003; Pertschy et al. 2007; Lo et al. 2010; Kappel et al. 2012). It is possible that C-terminal truncated variants of eL24 are incorporated into ribosomes less efficiently than full-length protein, leading to a mixed population of ribosomes either with truncated eL24 or without eL24. This would explain intermediate phenotype of cells expressing eB13Δ variant, if compared to

control and eL24Δ cells (Ref II Figure 2). In order to quantitatively analyze protein composition of ribosomes, we first optimized metabolic labelling of r-proteins, isolation of labeled ribosomes and mass spectrometric analysis of r-proteins (Ref III Materials and Methods). To metabolically label r-proteins, we employed stable isotope labelling by amino acids in yeast cell culture (SILAC). Budding yeast cells were grown in synthetic minimal medium containing either "light" L-lysine and L-arginine or "heavy" [$^{13}C_6/^{15}N_2$] L-lysine and [$^{13}C_6/^{15}N_4$] L-arginine (Ref III Materials and Methods). "Light" and "heavy" ribosomes were isolated through sucrose density gradient centrifugation (Ref III Materials and Methods, Figure 1). "Heavy" ribosomes served as a control that was mixed together with "light" ribosomes. Following that, r-proteins were digested by LysC/trypsin and "heavy/light" ratios for peptides were determined by HPLC-MS/MS (Ref III Materials and Methods). 75 out of 79 budding yeast r-protein were identified, with at least two peptides identified for each r-protein (Ref III Table S1). We conclude that SILAC combined with HPLC-MS/MS allows us to characterize protein composition of ribosomes. Next, ribosomes from eL24Δ cells and cells expressing eB13Δ variant of eL24 were analysed by mass spectrometry Proteins of mutant and control ribosomes were labelled by "light" and "heavy" amino acids, respectively (Ref II Materials and Methods). "Heavy/light" ratios of peptides were determined by HPLC-MS/MS. Stoichiometric ratios of r-proteins in the ribosomes from eL24Δ and eB13 bridge mutant cells were similar to that in the ribosomes of control cells (Ref II Figure 4). Moreover, eB13Δ variant of eL24 was incorporated into ribosomes similarly to the full-length eL24 (Ref II Figures 4 and S2). We also did not observe presence of biogenesis factors that are bound/released at the cytoplasmic step. This suggests that in cells lacking eL24 or expressing truncated variant of eL24 ribosome maturation occurs similarly to that in control cells. Altogether, we conclude that phenotypic difference between cells lacking eL24 and expressing eB13Δ variant indicates additional functions of the N-terminal domain of eL24. Functions of this domain are further discussed in chapter 2.2.2. Intermediate phenotype of cells expressing eB13Δ variant, if compared to control and eL24Δ cells, are caused by compromised eB13 bridge.

Next, we employed ribosome-polysome profile analysis to assess populations of ribosomal particles in cells expressing eB13Δ variant of eL24 (Ref II Figure 3). Compromised eB13 bridge formation led to the reduction of polysome/monosome ratio by ~37 % at 30 °C and by ~46 % at 20 °C, if compared to control (Ref II Figure 3B). Interestingly, we also detected accumulation of halfmers at 20 °C, which was specific for cells with compromised eB13 bridge formation (Ref II Figure 3A). Accumulation of halfmers may indicate impaired association of ribosomal subunits upon loss of the eB13 bridge. To test this possibility, we analysed the *in vitro* reassociation ability of the large ribosomal subunits impaired in the eB13 bridge formation as described in chapter 2.1.1. (Ref II Figure 5). Deletion of the eB13 bridge forming region of eL24 (variant eB13Δ) led to inability of large subunits to reassociate with small subunits at 5 mM $Mg^{2+}$ and to formation of intermediate particles at 10–

20 mM $Mg^{2+}$. We conclude that the eB13 bridge forming region of eL24 is important for the formation of 80S particles both *in vivo* and *in vitro*.

Association of ribosomal subunits occurs at the initiation step of translation. Thus, reduced association ability of ribosomal subunits (Ref II Figure 5) may cause a reduced rate of translation initiation. In order to test the importance of eB13 bridge for dynamics of translation in more detail, we examined *in vitro* cap- and polyA tail-dependent translation in cell-free translation extracts. In this assay, we analyzed the time course of synthesis of single Firefly luciferase over 80 minutes (Ref II Figures 6A and 6B). The slope of the linear part of the luciferase activity time course depends on the maximum rate of translation (Ref II Figure 6A-6C). Given that initiation is the rate-limiting step of translation, slope reflects the rate of initiation (Andersson & Kurland 1990; Bulmer 1991; Arava et al. 2003; Shah et al. 2013). In case of eB13Δ extracts, slope was ~1.6 times lower, if compared to control extracts (Ref II Figure 6C). This suggests that bridge eB13 contributes to the initiation step of translation.

Unfortunately, the use of single Firefly luciferase did not allow to access processivity of ribosomes and the rate of elongation. To overcome this limitation, we introduced novel system, where the time course of synthesis of fusion Renilla-Firefly luciferase was monitored. First, we determined the slopes of the linear parts of the obtained Renilla and Firefly luciferase time courses (Ref II Figures S4A-S4D). The ratio of slopes reflects processivity of ribosomes – the number of ribosomes that complete the Firefly moiety of fusion protein after completion of the Renilla moiety. Extracts of the eB13Δ mutant demonstrated similar to control extract slope ratios (Ref II Figures S4A-S4D). We conclude that apparent processivity of ribosomes with compromised eB13 bridge (variant eB13Δ) is similar to that of control ribosomes.

To assess elongation rates of ribosomes, time of first appearance (TFA) of Renilla and Firefly luminescence signals were measured in cell-free translation extracts (Ref II Figure 7). TFA of Renilla luminescence signal indicates the completion of synthesis of the Renilla moiety of the fusion protein, when Firefly part is not yet synthesized. TFA of Firefly luminescence signal, in turn, indicates the completion of synthesis of the whole fusion protein. Difference between Renilla and Firefly TFAs depends on the time needed to synthesize the Firefly moiety of the fusion protein and, consequently, reflects the rate of elongation. Ribosomes with compromised eB13 bridge needed ~1.3 times more time than control ribosomes to synthesize the Firefly moiety of protein (Ref II Figure 7). This data suggests that the eB13 bridge contributes to the elongation step of translation.

Taken together, our results indicate that presence of the eB13 bridge is important for the optimal ribosomal functionality (Ref II Figure 2). The principal contacts in this bridge are formed between the C-terminal helix and the linker region of eL24 and the r-protein eS6. Loss of the eB13 bridge leads to defects in association of ribosomal subunits, both *in vivo* and *in vitro* (Ref II Figure 3 and 5). This may lead to defects at the subunit joining step of translation initiation. Our *in vitro* translation experiments also support this

possibility, showing decreased rate of initiation upon loss of the eB13 bridge (Ref II Figures 6B and 6C). Additionally, *in vitro* translation experiments revealed that ribosomes with compromised eB13 bridge had decreased rate of elongation, if compared to control ribosomes (Ref II Figure 7). It has been previously demonstrated by structural studies that the eB13 bridge forming region of eL24 is highly dynamical and follows rotation of small subunit (Figure 22) (Ben-Shem et al. 2011; Behrmann et al. 2015; Khatter et al. 2015). Bridge eB13 is located in the vicinity of binding site for the eEF2 (Figure 22) (Anger et al. 2013). SHAPE analysis coupled with molecular dynamic simulations suggested that during translation elongation eB13 bridge transduces information between eEF2 binding site and small ribosomal subunit (Gulay et al. 2017). We speculate that reduced elongation rate in our *in vitro* translation experiments reflects involvement of the eB13 bridge in the regulation of small subunit rotation and flow of information between subunits.

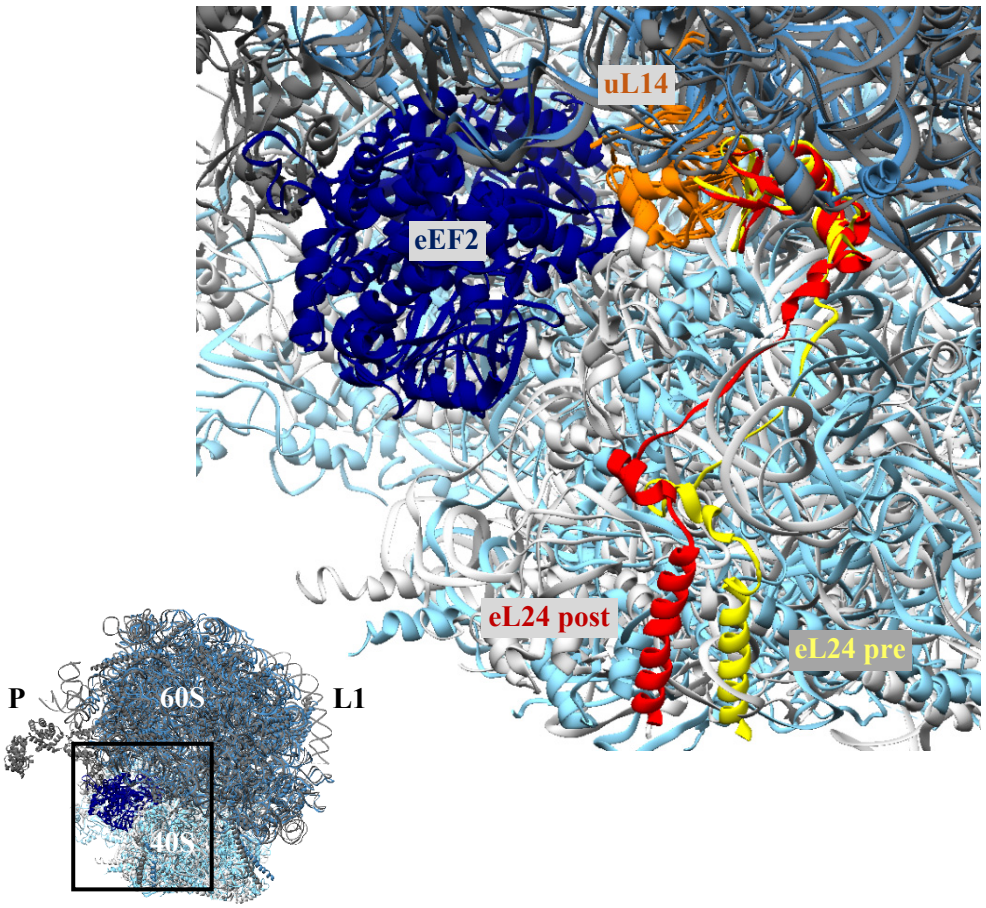


**Figure 22. Conformation of eL24 in pre-translocational (eL24 pre; yellow) and post-translocational (eL24 post; red) conformations.** rRNAs and proteins of large subunit are dark blue (pre-translocation) and dark grey (post-translocation). rRNAs and proteins of small subunit are light blue (pre-translocation) and light grey (post-translocation). R-protein uL14 (orange) have similar orientation in both conformations. Factor eEF2 (navy blue) is shown. Small panel illustrates approximate position of the enlarged region (square) within 80S ribosome. Landmarks of the large subunit are indicated (P, P stalk; L1, L1 stalk). Human ribosomes in pre-translocational (PDB coordinates 4UG0 from Khatter et al, 2015) and post-translocational conformation (PDB coordinates 4V6X from Anger et al, 2013) were superimposed in Chimera.

### 2.2.2. The N-terminal domain of eL24 is involved in the initiation of translation

Two budding yeast mutants employed in the present study allowed us to assess the functions of the N-terminal domain of eL24. Mutant eL24Δ lacked the whole eL24 protein. The eB13Δ mutant cells expressed variant of eL24 that carried deletion of the C-terminal helix and the linker region of eL24. Analysis of eL24Δ cells demonstrated the intensified cold sensitivity and decreased by ~20 % global level of translation, if compare to the eB13Δ mutant (chapter 2.2.1., Ref II Figure 2). This difference can be explained by the absence of the N-terminal domain of eL24 in the eL24Δ cells. It is known that the N-terminal domain forms intersubunit bridge B6 (chapter 1.1.3., Table 3). Therefore, difference of phenotypes may be provoked not by the deletion of the N-terminal domain per se, but by the concomitant loss of the B6 bridge. To test this hypothesis, we constructed B6Δ and eB13ΔB6Δ variants of eL24 that were not able to form the B6 bridge (Figure 21, Ref II Table 2 and Figure 2). In both variants, two arginine residues (R43 and R47) were substituted to alanine residues, which impaired B6 bridge formation (Figure 21, Ref II Figure 1). Cells expressing B6Δ variant displayed similar to control cells growth rates and global levels of translation (Ref II Table 2 and Figure 2). Phenotype of cells expressing eB13ΔB6Δ variant was similar to that of cells expressing eB13Δ variant. This indicates that bridge B6 has no apparent role in the budding yeast ribosome. The N-terminal domain of eL24, in turn, carries previously not known function.

In order to determine possible functions of the N-terminal domain of eL24, we first analysed ribosome-polysome profiles of cells lacking eL24. These cells demonstrated reduction of polysome/monosome ratios by ~35 % at 30 °C and by ~47 % at 20 °C, if compared to control cells (Ref II Figure 3). However, no changes in populations of ribosomal particles were detected, if compared to cells expressing eB13Δ variant of eL24 (Ref II Figure 3). Subsequent analysis of *in vitro* reassociation demonstrated that large ribosomal subunits lacking the whole eL24 protein (eL24Δ) were not able to form ribosomal particles at 10 mM $Mg^{2+}$, while large subunits with compromised eB13 bridge (eB13Δ) formed at this $Mg^{2+}$ concentration intermediate particles (Ref II Figure 5). This suggests that the N-terminal domain of eL24 is involved in the *in* vitro association of the ribosomal subunits. To access role of the N-terminal domain in more detail, we analysed *in vitro* translation in cell-free translational extracts as described in chapter 2.2.1. Analysis of the time course of synthesis of single Firefly luciferase demonstrated that rate of translation in eL24Δ extracts decreased by ~10 times, if compare to control extracts. Moreover, the rate of translation was ~6 times lower than that in the eB13Δ mutant extracts (Ref II Figures 6B and 6C). This suggests that the N-terminal domain of eL24 contributes to the initiation step of translation. Interestingly, processivity and rate of elongation of ribosomes lacking the N-terminal domain of eL24 were

similar to that of ribosomes impaired in eB13 bridge formation (Ref II Figures 7 and S4).

Altogether, our data suggests that the N-terminal domain of eL24 is important for the functionality of budding yeast ribosomes (Ref II Figure 2). This domain contributes to the *in vitro* association of ribosomal subunits (Ref II Figure 5). Defect in the association of ribosomal subunits may explain reduced rate of *in vitro* translation initiation (Ref II Figure 6C). Structural models of the eukaryotic ribosomes demonstrated that the N-terminal domain of the eL24 interacts with protein uL14, which has a unique position in the ribosome (Figure 22). First, uL14 resides closely to the main binding site for the translation factors. Two factors, eIF5B and eIF6, act at the subunit joining step of initiation. Factor eIF5B promotes joining of ribosomal subunits. In contrast, factor eIF6 sterically prevents formation of 80S particle. We speculate that presence of the N-terminal domain of eL24 is prerequisite for the efficient binding/dissociation of factors eIF5B and/or eIF6. Additionally, protein uL14 is involved in the formation of two conserved intersubunit bridges B5 and B8 (chapter 1.1.3., Table 3, Figures 9 and 10). Loss of the N-terminal domain of eL24 may affect formation of these bridges and consequently lead to the defective subunit joining. Altogether, the N-terminal domain of eL24 may contribute to the local structure of the large ribosomal subunit. The future cryo-EM studies will shed a light on this possibility.

## 2.3. The pleiotropic functions of r-proteins eL19 and eL24

R-proteins eL19 and eL24 belong to the group of archaea/eukaryote-specific proteins (chapter 1.1.2.). Eukaryotic variants of these proteins have a similar three-domain structure, consisting of an N-terminal domain, a middle/linker region and a C-terminal α-helical domain (Figures 17 and 21). These domains can be divided into archaea/eukaryote-specific and eukaryote-specific domains. The present study demonstrates that different domains of eL19 and eL24 bear distinctive functions. Interestingly, such distribution of functions reflects the evolutionary history of these proteins.

During the course of evolution, the complexity of ribosomes increased through the attachment of domain-specific structural elements. The transition from bacteria to archaea was accompanied by the appearance of the set of 35 proteins named archaea/eukaryote-specific (Lecompte et al. 2002; Ban et al. 2014). It has been proposed that archaea evolved from gram-positive bacteria as a result of antibiotic selection and search for vacant niches (Gupta 2000; Cavalier-Smith 2002; Valas & Bourne 2011). It is possible that archaea/ eukaryote-specific r-proteins were an evolutionary adaptation that enabled to maintain structure of ribosome and efficiency of protein synthesis in new, often extreme environments. In this study, functions of the archaea/eukaryote-specific domains of proteins eL19 and eL24 were examined in the eukaryotic ribosome. These domains fully resemble structures of the archaeal eL19 and eL24 (Figures 17 and 22). In the eukaryotic eL19, archaea/eukaryote-specific domains are the N-terminal domain and the middle region, both buried within the 25S rRNA. These domains of eL19 are essential for the assembly of the large ribosomal subunit (chapter 2.1.2.). In contrast, the archaea/eukaryote-specific N-terminal domain of eL24 lies on the surface of the large subunit and possibly contributes to the local structure of the large ribosomal subunit (chapter 2.2.2.). Thus, archaea/eukaryote-specific domains of eL19 and eL24 support formation of the proper structure of the large ribosomal subunit, which is important for the functionality of ribosome.

Although the origin of eukaryotes remains largely enigmatic, their emerging seems to be associated with endosymbiosis between archaeal host and eubacterial endosymbiont (McInerney et al. 2014; Martin et al. 2015). It has been proposed that archaeal superphylum Asgard (contains Lokiarchaeota, Thorarchaeota, Odinarchaeota and Heimdallarchaeota) is related to the archaeal host and thus comprises close archaeal relatives of eukaryotes (Spang et al. 2015; Zaremba-Niedzwiedzka et al. 2017; Spang et al. 2018). In accordance to the endosymbiotic theory, eukaryotic ribosomes has been suggested to be evolved from archaeal ribosomes through the attachment of additional structural elements such as eukaryote-specific rRNA and rRNA expansion segments, eukaryote-specific proteins and protein domains (Hartman et al. 2006). Eukaryote-specific structural elements formed a vast network of intra- and intersubunit interactions that possibly was an evolutionary adaptation to increased complexity of ribosomes and cells in general (Klinge et al. 2012; Anger et al. 2013; Poirot &

Timsit 2016). For example, eukaryotic r-proteins eL19 and eL24 contain long antennae-like eukaryote-specific domains that extend far from the large subunit and form eukaryote-specific bridges eB12 and eB13. Archaeal ribosomes lack these bridges (Armache et al. 2013). In this study, two archaea-like variants of eL19 and eL24 were constructed and examined. Variant $eL19_{1-146}$ lacked the C-terminal α-helix of the eL19 and was not able to form intersubunit bridge eB12. Variant eB13Δ lacked the C-terminal α-helix and the linker region of eL24, being impaired eB13 bridge formation. Analysis of these variants revealed that both eB12 and eB13 bridges are important for the optimal functionality of the budding yeast ribosome (chapters 2.1.1. and 2.2.1.). These bridges contribute to the formation of 80S particles and communication between subunits. Thus, eukaryote-specific domains of eL19 and eL24 support complex structure of eukaryotic ribosomes and may give an advantage in regulation of protein synthesis.

# CONCLUSIONS

The three-dimensional shape of ribosomes is mainly defined by a tertiary structure of ribosomal RNAs that serve as a framework for binding of r-proteins. R-proteins shape a vast network of interactions that contribute to a various aspects of the protein synthesis machinery, including assembly of ribosomes and interactions of ribosomal subunits. Two r-proteins in this network, eL19 and eL24, are distinctive by their structure and position in the eukaryotic ribosome. Both proteins consist of three domains: an N-terminal globular domain, a middle/linker region and a C-terminal α-helical domain. These domains can be divided into archaea/eukaryote-specific and eukaryote-specific domains. Eukaryote-specific domains of eL19 and eL24 are long antennae-like protein moieties that form the eukaryote-specific intersubunit bridges eB12 and eB13, respectively.

In the present study, the functions of different domains of r-proteins eL19 and eL24 in the budding yeast ribosome were assessed. The mutational analysis of the eL19 revealed that the N-terminal domain and the middle region contribute to the cleavage of 27SB pre-rRNAs during assembly of the large ribosomal subunit. These archaea/eukaryote-specific domains of eL19 are essential for cell viability. Formation of the eB12 bridge by the eukaryote-specific C-terminal α-helical domain is important for the optimal functionality of the budding yeast ribosomes. This bridge is required for the stable association of ribosomal subunits in the absence of other ligands. As for the eL24, eukaryote-specific domains of this protein form intersubunit bridge eB13, and are necessary for the formation of 80S ribosomes. The eB13 bridge is involved in both initiation and elongation steps of translation. The archaea/eukaryote-specific N-terminal domain of eL24, in turn, contributes to the initiation step of translation, possibly through the regulation of the local structure of large ribosomal subunit.

Our data demonstrate that different structural domains of eL19 and eL24 bear distinctive functions. The archaea/eukaryote-specific domains are important parts of the intrasubunit interaction network that ensures the proper formation of large ribosomal subunit structure. The eukaryote-specific domains of eL19 and eL24 contribute to the network of intersubunit interactions and support translation by stabilizing the association of ribosomal subunits. Altogether, our results broaden the knowledge about the principles of the structural organization of the eukaryotic ribosome. Moreover, the functional importance of the eukaryote-specific bridges eB12 and eB13 for the protein synthesis is shown for the first time.

# SUMMARY IN ESTONIAN

## Ribosoomi valkude eL19 ja eL24 funktsioonid pagaripärmi ribosoomis

Ribosoomid on makromolekulaarsed kompleksid, mis viivad läbi valgu sünteesi kõikides elusloodu domeenides (*Bacteria, Archaea* ja *Eukarya*). Eukarüoodi ribosoom (pagaripärmi *Saccharomyces cerevisiae* 80S ribosoomi näitel) koosneb neljast ribosomaalse RNA molekulist (rRNA) ja 79 valgust, mis on jagatud kahe ribosomaalse alaühiku vahel. Väikese (40S) alaühiku koostisesse kuulub 18S rRNA ja 33 valku. Selle alaühiku põhilisteks funktsionaalseteks üksusteks on dekodeerimistsenter, aminoatsüül-, peptidüül- ja väljuva transpordi RNA-de (tRNA) seondumiskohad ning informatsiooni RNA (mRNA) kanal. Translatsiooni initsiatsiooni käigus seob väike alaühik initsiatsioonifaktoreid, tänu millele seob ta initsiaator-tRNA-d ja skaneerib mRNA-d. Translatsiooni elongatsiooni käigus valitakse väikese alaühiku dekodeerimistsentris korrektne aminoatsüül-tRNA sõltuvalt mRNA järjestusest. Suure (60S) alaühiku koostisesse kuulub kolm rRNA molekuli (5S rRNA, 5,8S rRNA ja 25S rRNA) ning 46 valku. Suure alaühiku põhilisteks funktsionaalseteks tsentriteks on peptidüültransferaasne tsenter, tRNA-de seondumiskohad ning peptiidi kanal. Translatsiooni elongatsiooni käigus sünteesitakse peptidüültransferaasses tsentris peptiidside – protsess, mida katalüüsib rRNA. Seega arvatakse, et ribosoom on ürgne, RNA maailmast pärit ribosüüm.

Ribosoomi alaühikute kolmemõõtmelist struktuuri määrab peamiselt rRNA tertsiaarne struktuur. Valgud omakorda tagavad rRNA korrektse voltumise ja stabiliseerivad selle struktuuri. Üheskoos moodustavad rRNA-d ja valgud eukarüoodi ribosoomis ulatusliku interaktsioonide võrgustiku. Need on valk-valk, rRNA-valk ning rRNA-rRNA alaühikutesisesed ja -vahelised kontaktid, mis tagavad ribosoomi optimaalse funktsionaalsuse. Näiteks, pagaripärmi ribosoomis on kirjeldatud 17 alaühikutevahelist silda, millest 12 on konserveerunud ning 5 spetsiifilised eukarüoodi ribosoomi jaoks. Alaühikutevahelised sillad tagavad alaühikute koospüsimise ja liikumise translatsiooni käigus.

Eukarüoodi ribosoomi interaktsioonide võrgustikku kuulub kaks selle töö raames uuritud valku – eL19 ja eL24. Mõlemad valgud koosnevad kolmest domeenist: N-terminaalne domeen, keskmine regioon ja C-terminaalne α-heelikaalne domeen. Neid domeene saab jagada arhede- ja eukarüoodispetsiifilisteks ning eukarüoodispetsiifilisteks domeenideks. Valkude eL19 ja eL24 eripäraks on pikad C-terminaalsed domeenid, mis osalevad alaühikutevaheliste eukarüoodispetsiifiliste sildade eB12 ja eB13 moodustamisel. Vaatamata sellele, et valkude struktuur on teada, ei ole nende struktuursete domeenide funktsioone senini välja põhjalikult uuritud. Lisaks, on eukarüoodispetsiifiliste sildade eB12 ja eB13 roll suuresti teadmata. Käesolev töö keskendub valkude eL19 ja eL24 funktsioonidele pagaripärmi ribosoomis.

Pagaripärmi ribosoomi valku eL19 kodeerivad kaks paraloogset geeni: *RPL19A* ja *RPL19B*. Mõlema geeni kustutamine on rakkudele letaalne, mis

näitab, et valk eL19 on eluks hädavajalik. On teada, et valgu eL19 puudumine põhjustab suure ribosomaalse alaühiku kokkupakkimise defekte, kus 27SB pre-rRNA-d ei lõigata $C_2$ lõikekohast. Meie tulemused näitavad, et $C_2$ lõikamisel mängivad rolli eL19 valgu N-terminaalne domeen ja keskmine regioon. Just need arhede- ja eukarüoodispetsiifilised eL19 valgu domeenid on hädavajalikud pärmirakkude eluks. Teine eL19 valgu roll seisneb silla eB12 moodustamisel, mis toimub eL19 eukarüoodispetsiifilise C-terminaalse α-heelikaalse domeeni vahendusel. Valgu eL19 deletsioonimutantide analüüsil selgus, et eB12 silla funktsionaalsus peamiselt sõltub valk-rRNA interaktsioonidest valgu eL24 ja 18S rRNA lisasegmendi ES6S vahel. Kuigi eB12 sild ei ole eluks hädavajalik, on see erakordselt oluline ribosoomi optimaalseks toimimiseks. Biokeemiline analüüs näitas, et eB12 sild toetab ribosoomi alaühikute koospüsimist *in vitro.*

Pagaripärmi ribosoomi valku eL24 kodeerivad paraloogsed geenid *RPL24A* ja *RPL24B.* See valk ei ole eluks hädavajalik. Varasemast on teada, et valgu eL24 puudumisel aeglustub rakkude kasv, kuhjuvad poolteistmeersed ribosoomid ning langeb translatsiooni elongatsiooni kiirus. Meie analüüs näitab, et valgu eL24 N-terminaalne domeen mängib rolli translatsiooni initsiatsioonil. On võimalik, et see arhede- ja eukarüoodispetsiifiline domeen tagab suure alaühiku struktuuri korrektse moodustamise. Valgu eL24 keskmine regioon ja C-terminaalne α-helikaalne domeen on eukarüoodispetsiifilised domeenid, mis moodustavad silla eB13. Käesoleva töö raames selgus, et silla funktsioneerimise tagavad eelkõige valk-valk interaktsioonid valkude eL24 ja eS6 vahel. Sild eB13 on vajalik 80S ribosoomi moodustamiseks *in vivo* ja *in vitro*. Rakuvaba translatsiooni analüüs näitas, et eB13 sild mängib rolli nii translatsiooni initsiatsioonis kui ka elongatsioonis.

Saadud tulemuste põhjal saab järeldada, et valkude eL19 ja eL24 funktsioonid on jagatud struktuursete domeenide vahel. Arhede- ja eukarüoodispetsiifilised domeenid tagavad suure alaühiku struktuuri korrektse moodustamise. Eukarüoodispetsiifilised domeenid moodustavad alaühikutevahelisi sildasid eB12 ja eB13. Need sillad toetavad efektiivset valgusünteesi stabiliseerides ribosoomi alaühikute koospüsimist. Kokkuvõtteks, käesoleva doktoriväitekirja tulemused laiendavad meie teadmisi eukarüoodi ribosoomi struktuurse ülesehituse printsiipidest. Lisaks, doktoriväitekirjas näidatakse esmakordselt eukarüoodispetsiifiliste alaühikutevaheliste sildade olulisus ribosoomi funktsionaalsuse jaoks.

# ACKNOWLEDGEMENTS

First and foremost, I would like to thank my supervisors Jaanus Remme and Tiina Tamm for being the best supervisors I could wish for my graduate studies: supportive, positive, operative and always having a crafty plan. I am thankful to all members of our research lab (Aivar Liiv, Margus Leppik, Silva Lilleorg, Kaspar Reier and Pavel Volõnkin) for their help, research tips, critical reviewing of our results/manuscripts and for just having a great time in- and outside of the lab. I also owe many thanks to people from biochemistry lab, especially Natali Garber and Maie Loorits. I would like to thank all co-authors that have contributed to our research. Special thanks to Uno Mäeorg for taking a risk and letting me try organic synthesis in his lab. My gratitude goes to Arnold Kristjuhan for reviewing this thesis and important comments. I also thank Graduate School in Biomedicine and Biotechnology (Kristina Mäemets-Allas) and Archimedes Foundation for giving me a financial opportunity to attend conferences and practical courses. I would like to acknowledge administrative staff of our institute (Tiiu Rootslane, Lagle Lõhmus, Jaanika Vana and Teele Eensaar) for being always helpful.

My greatest gratitude goes to my school and university friends Vladimir, Mihail, Aleksandr and Kristina. Конечно же, я благодарен всей своей семье, моим родителям за их неоценимую помощь и поддержу.

# REFERENCES


Abou Elela S., Good L., Melekhovets Y.F. & Nazar R.N. (1994). Inhibition of protein synthesis by an efficiently expressed mutation in the yeast 5.8S ribosomal RNA. *Nucleic acids research*, 22, 686–93.

Abou Elela S. & Nazar R.N. (1997). Role of the 5.8S rRNA in ribosome translocation. *Nucleic acids research*, 25, 1788–94.

Abramson R.D., Dever T.E., Lawson T.G., Ray B.K., Thach R.E. & Merrick W.C. (1987). The ATP-dependent interaction of eukaryotic initiation factors with mRNA. *The Journal of biological chemistry*, 262, 3826–32.

Achenbach J. & Nierhaus K.H. (2015). The mechanics of ribosomal translocation. *Biochimie*, 114, 80–9.

Acker M.G., Shin B.S., Nanda J.S., Saini A.K., Dever T.E. & Lorsch J.R. (2009). Kinetic analysis of late steps of eukaryotic translation initiation. *Journal of molecular biology*, 385, 491–506.

Aitken C.E., Beznoskova P., Vlckova V., Chiu W.L., Zhou F., Valasek L.S., Hinnebusch A.G. & Lorsch J.R. (2016). Eukaryotic translation initiation factor 3 plays distinct roles at the mRNA entry and exit channels of the ribosomal preinitiation complex. *eLife*, 5.

Algire M.A., Maag D., Savio P., Acker M.G., Tarun S.Z., Jr., Sachs A.B., Asano K., Nielsen K.H., Olsen D.S., Phan L., Hinnebusch A.G. & Lorsch J.R. (2002). Development and characterization of a reconstituted yeast translation initiation system. *Rna*, 8, 382–97.

Ali I.K., Lancaster L., Feinberg J., Joseph S. & Noller H.F. (2006). Deletion of a conserved, central ribosomal intersubunit RNA bridge. *Molecular cell*, 23, 865–74.

Alkalaeva E.Z., Pisarev A.V., Frolova L.Y., Kisselev L.L. & Pestova T.V. (2006). In vitro reconstitution of eukaryotic translation reveals cooperativity between release factors eRF1 and eRF3. *Cell*, 125, 1125–36.

Allmang C. & Tollervey D. (1998). The role of the 3' external transcribed spacer in yeast pre-rRNA processing. *Journal of molecular biology*, 278, 67–78.

Andersen C.B., Becker T., Blau M., Anand M., Halic M., Balar B., Mielke T., Boesen T., Pedersen J.S., Spahn C.M., Kinzy T.G., Andersen G.R. & Beckmann R. (2006). Structure of eEF3 and the mechanism of transfer RNA release from the E-site. *Nature*, 443, 663–8.

Andersson S.G. & Kurland C.G. (1990). Codon preferences in free-living micro-organisms. *Microbiological reviews*, 54, 198–210.

Anger A.M., Armache J.P., Berninghausen O., Habeck M., Subklewe M., Wilson D.N. & Beckmann R. (2013). Structures of the human and Drosophila 80S ribosome. *Nature*, 497, 80–5.

Arava Y., Wang Y., Storey J.D., Liu C.L., Brown P.O. & Herschlag D. (2003). Genome-wide analysis of mRNA translation profiles in Saccharomyces cerevisiae. *Proceedings of the National Academy of Sciences of the United States of America*, 100, 3889–94.

Archer S.K., Shirokikh N.E., Hallwirth C.V., Beilharz T.H. & Preiss T. (2015). Probing the closed-loop model of mRNA translation in living cells. *RNA biology*, 12, 248–54.

Armache J.P., Anger A.M., Marquez V., Franckenberg S., Frohlich T., Villa E., Berninghausen O., Thomm M., Arnold G.J., Beckmann R. & Wilson D.N. (2013).

Promiscuous behaviour of archaeal ribosomal proteins: implications for eukaryotic ribosome evolution. *Nucleic acids research*, 41, 1284–93.

Armache J.P., Jarasch A., Anger A.M., Villa E., Becker T., Bhushan S., Jossinet F., Habeck M., Dindar G., Franckenberg S., Marquez V., Mielke T., Thomm M., Berninghausen O., Beatrix B., Soding J., Westhof E., Wilson D.N. & Beckmann R. (2010a). Cryo-EM structure and rRNA model of a translating eukaryotic 80S ribosome at 5.5-A resolution. *Proceedings of the National Academy of Sciences of the United States of America*, 107, 19748–53.

Armache J.P., Jarasch A., Anger A.M., Villa E., Becker T., Bhushan S., Jossinet F., Habeck M., Dindar G., Franckenberg S., Marquez V., Mielke T., Thomm M., Berninghausen O., Beatrix B., Soding J., Westhof E., Wilson D.N. & Beckmann R. (2010b). Localization of eukaryote-specific ribosomal proteins in a 5.5-A cryo-EM map of the 80S eukaryotic ribosome. *Proceedings of the National Academy of Sciences of the United States of America*, 107, 19754–9.

Axt K., French S.L., Beyer A.L. & Tollervey D. (2014). Kinetic analysis demonstrates a requirement for the Rat1 exonuclease in cotranscriptional pre-rRNA cleavage. *PloS one*, 9, e85703.

Aylett C.H., Boehringer D., Erzberger J.P., Schaefer T. & Ban N. (2015). Structure of a yeast 40S-eIF1-eIF1A-eIF3-eIF3j initiation complex. *Nature structural & molecular biology*, 22, 269–71.

Baba K., Tumuraya K., Tanaka I., Yao M. & Uchiumi T. (2013). Molecular dissection of the silkworm ribosomal stalk complex: the role of multiple copies of the stalk proteins. *Nucleic acids research*, 41, 3635–43.

Ban N., Beckmann R., Cate J.H., Dinman J.D., Dragon F., Ellis S.R., Lafontaine D.L., Lindahl L., Liljas A., Lipton J.M., McAlear M.A., Moore P.B., Noller H.F., Ortega J., Panse V.G., Ramakrishnan V., Spahn C.M., Steitz T.A., Tchorzewski M., Tollervey D., Warren A.J., Williamson J.R., Wilson D., Yonath A. & Yusupov M. (2014). A new system for naming ribosomal proteins. *Current opinion in structural biology*, 24, 165–9.

Ban N., Nissen P., Hansen J., Moore P.B. & Steitz T.A. (2000). The complete atomic structure of the large ribosomal subunit at 2.4 A resolution. *Science*, 289, 905–20.

Barandun J., Chaker-Margot M., Hunziker M., Molloy K.R., Chait B.T. & Klinge S. (2017). The complete structure of the small-subunit processome. *Nature structural & molecular biology*, 24, 944–953.

Baronas-Lowell D.M. & Warner J.R. (1990). Ribosomal protein L30 is dispensable in the yeast Saccharomyces cerevisiae. *Molecular and cellular biology*, 10, 5235–43.

Becker T., Franckenberg S., Wickles S., Shoemaker C.J., Anger A.M., Armache J.P., Sieber H., Ungewickell C., Berninghausen O., Daberkow I., Karcher A., Thomm M., Hopfner K.P., Green R. & Beckmann R. (2012). Structural basis of highly conserved ribosome recycling in eukaryotes and archaea. *Nature*, 482, 501–6.

Behrmann E., Loerke J., Budkevich T.V., Yamamoto K., Schmidt A., Penczek P.A., Vos M.R., Burger J., Mielke T., Scheerer P. & Spahn C.M. (2015). Structural snapshots of actively translating human ribosomes. *Cell*, 161, 845–57.

Ben-Shem A., Garreau de Loubresse N., Melnikov S., Jenner L., Yusupova G. & Yusupov M. (2011). The structure of the eukaryotic ribosome at 3.0 A resolution. *Science*, 334, 1524–9.

Bertram G., Bell H.A., Ritchie D.W., Fullerton G. & Stansfield I. (2000). Terminating eukaryote translation: domain 1 of release factor eRF1 functions in stop codon recognition. *Rna*, 6, 1236–47.

Biedka S., Micic J., Wilson D., Brown H., Diorio-Toth L. & Woolford J.L., Jr. (2018). Hierarchical recruitment of ribosomal proteins and assembly factors remodels nucleolar pre-60S ribosomes. *The Journal of cell biology*, 217, 2503–2518.

Blanchet S., Rowe M., Von der Haar T., Fabret C., Demais S., Howard M.J. & Namy O. (2015). New insights into stop codon recognition by eRF1. *Nucleic acids research*, 43, 3298–308.

Bock L.V., Blau C., Vaiana A.C. & Grubmuller H. (2015). Dynamic contact network between ribosomal subunits enables rapid large-scale rotation during spontaneous translocation. *Nucleic acids research*, 43, 6747–60.

Bogdanov A.A., Dontsova O.A., Dokudovskaya S.S. & Lavrik I.N. (1995). Structure and function of 5S rRNA in the ribosome. *Biochemistry and cell biology = Biochimie et biologie cellulaire*, 73, 869–76.

Bowen A.M., Musalgaonkar S., Moomau C.A., Gulay S.P., Mirvis M. & Dinman J.D. (2015). Ribosomal protein uS19 mutants reveal its role in coordinating ribosome structure and function. *Translation*, 3, e1117703.

Bradatsch B., Leidig C., Granneman S., Gnadig M., Tollervey D., Bottcher B., Beckmann R. & Hurt E. (2012). Structure of the pre-60S ribosomal subunit with nuclear export factor Arx1 bound at the exit tunnel. *Nature structural & molecular biology*, 19, 1234–41.

Brown A., Shao S., Murray J., Hegde R.S. & Ramakrishnan V. (2015). Structural basis for stop codon recognition in eukaryotes. *Nature*, 524, 493–496.

Budkevich T., Giesebrecht J., Altman R.B., Munro J.B., Mielke T., Nierhaus K.H., Blanchard S.C. & Spahn C.M. (2011). Structure and dynamics of the mammalian ribosomal pretranslocation complex. *Molecular cell*, 44, 214–24.

Budkevich T.V., Giesebrecht J., Behrmann E., Loerke J., Ramrath D.J., Mielke T., Ismer J., Hildebrand P.W., Tung C.S., Nierhaus K.H., Sanbonmatsu K.Y. & Spahn C.M. (2014). Regulation of the mammalian elongation cycle by subunit rolling: a eukaryotic-specific ribosome rearrangement. *Cell*, 158, 121–31.

Bulmer M. (1991). The selection-mutation-drift theory of synonymous codon usage. *Genetics*, 129, 897–907.

Bulygin K., Chavatte L., Frolova L., Karpova G. & Favre A. (2005). The first position of a codon placed in the A site of the human 80S ribosome contacts nucleotide C1696 of the 18S rRNA as well as proteins S2, S3, S3a, S30, and S15. *Biochemistry*, 44, 2153–62.

Calvino F.R., Kharde S., Ori A., Hendricks A., Wild K., Kressler D., Bange G., Hurt E., Beck M. & Sinning I. (2015). Symportin 1 chaperones 5S RNP assembly during ribosome biogenesis by occupying an essential rRNA-binding site. *Nature communications*, 6, 6510.

Castle C.D., Sardana R., Dandekar V., Borgianini V., Johnson A.W. & Denicourt C. (2013). Las1 interacts with Grc3 polynucleotide kinase and is required for ribosome synthesis in Saccharomyces cerevisiae. *Nucleic acids research*, 41, 1135–50.

Caulfield T. & Devkota B. (2012). Motion of transfer RNA from the A/T state into the A-site using docking and simulations. *Proteins*, 80, 2489–500.

Cavalier-Smith T. (2002). The neomuran origin of archaebacteria, the negibacterial root of the universal tree and bacterial megaclassification. *International journal of systematic and evolutionary microbiology*, 52, 7–76.

Chaker-Margot M. (2018). Assembly of the small ribosomal subunit in yeast: mechanism and regulation. *Rna*, 24, 881–891.

Chaker-Margot M., Hunziker M., Barandun J., Dill B.D. & Klinge S. (2015). Stage-specific assembly events of the 6-MDa small-subunit processome initiate eukaryotic ribosome biogenesis. *Nature structural & molecular biology*, 22, 920–3.

Chen B., Kaledhonkar S., Sun M., Shen B., Lu Z., Barnard D., Lu T.M., Gonzalez R.L., Jr. & Frank J. (2015). Structural dynamics of ribosome subunit association studied by mixing-spraying time-resolved cryogenic electron microscopy. *Structure*, 23, 1097–105.

Chen W., Xie Z., Yang F. & Ye K. (2017). Stepwise assembly of the earliest precursors of large ribosomal subunits in yeast. *Nucleic acids research*, 45, 6837–6847.

Cheng J., Kellner N., Berninghausen O., Hurt E. & Beckmann R. (2017). 3.2-A-resolution structure of the 90S preribosome before A1 pre-rRNA cleavage. *Nature structural & molecular biology*, 24, 954–964.

Cheng Z., Saito K., Pisarev A.V., Wada M., Pisareva V.P., Pestova T.V., Gajda M., Round A., Kong C., Lim M., Nakamura Y., Svergun D.I., Ito K. & Song H. (2009). Structural insights into eRF3 and stop codon recognition by eRF1. *Genes & development*, 23, 1106–18.

Cheung Y.N., Maag D., Mitchell S.F., Fekete C.A., Algire M.A., Takacs J.E., Shirokikh N., Pestova T., Lorsch J.R. & Hinnebusch A.G. (2007). Dissociation of eIF1 from the 40S ribosomal subunit is a key step in start codon selection in vivo. *Genes & development*, 21, 1217–30.

Chu S., Archer R.H., Zengel J.M. & Lindahl L. (1994). The RNA of RNase MRP is required for normal processing of ribosomal RNA. *Proceedings of the National Academy of Sciences of the United States of America*, 91, 659–63.

Cigan A.M., Feng L. & Donahue T.F. (1988). tRNAi(met) functions in directing the scanning ribosome to the start site of translation. *Science*, 242, 93–7.

Cole J.R., Wang Q., Fish J.A., Chai B., McGarrell D.M., Sun Y., Brown C.T., Porras-Alfaro A., Kuske C.R. & Tiedje J.M. (2014). Ribosomal Database Project: data and tools for high throughput rRNA analysis. *Nucleic acids research*, 42, D633–42.

Conard S.E., Buckley J., Dang M., Bedwell G.J., Carter R.L., Khass M. & Bedwell D.M. (2012). Identification of eRF1 residues that play critical and complementary roles in stop codon recognition. *Rna*, 18, 1210–21.

Cukras A.R. & Green R. (2005). Multiple effects of S13 in modulating the strength of intersubunit interactions in the ribosome during translation. *Journal of molecular biology*, 349, 47–59.

Demeshkina N., Jenner L., Westhof E., Yusupov M. & Yusupova G. (2012). A new understanding of the decoding principle on the ribosome. *Nature*, 484, 256–9.

Demeshkina N.A., Laletina E.S., Meshchaninova M.I., Repkova M.N., Ven'iaminova A.G., Graifer D.M. & Karpova G.G. (2003). [The mRNA codon environment at the P and E sites of human ribosomes deduced from photo crosslinking with pUUUGUU]. *Molekuliarnaia biologiia*, 37, 147–55.

des Georges A., Hashem Y., Unbehaun A., Grassucci R.A., Taylor D., Hellen C.U., Pestova T.V. & Frank J. (2014). Structure of the mammalian ribosomal pre-termination complex associated with eRF1.eRF3.GDPNP. *Nucleic acids research*, 42, 3409–18.

Dever T.E., Dinman J.D. & Green R. (2018). Translation Elongation and Recoding in Eukaryotes. *Cold Spring Harbor perspectives in biology*, 10.

Dever T.E. & Green R. (2012). The elongation, termination, and recycling phases of translation in eukaryotes. *Cold Spring Harbor perspectives in biology*, 4, a013706.

Dever T.E., Kinzy T.G. & Pavitt G.D. (2016). Mechanism and Regulation of Protein Synthesis in Saccharomyces cerevisiae. *Genetics*, 203, 65–107.
Dieci G., Fiorino G., Castelnuovo M., Teichmann M. & Pagano A. (2007). The expanding RNA polymerase III transcriptome. *Trends in genetics : TIG*, 23, 614–22.
Dinman J.D. (2005). 5S rRNA: Structure and Function from Head to Toe. *International journal of biomedical science : IJBS*, 1, 2–7.
Dragon F., Gallagher J.E., Compagnone-Post P.A., Mitchell B.M., Porwancher K.A., Wehner K.A., Wormsley S., Settlage R.E., Shabanowitz J., Osheim Y., Beyer A.L., Hunt D.F. & Baserga S.J. (2002). A large nucleolar U3 ribonucleoprotein required for 18S ribosomal RNA biogenesis. *Nature*, 417, 967–70.
Dresios J., Derkatch I.L., Liebman S.W. & Synetos D. (2000). Yeast ribosomal protein L24 affects the kinetics of protein synthesis and ribosomal protein L39 improves translational accuracy, while mutants lacking both remain viable. *Biochemistry*, 39, 7236–44.
Dresios J., Panopoulos P., Frantziou C.P. & Synetos D. (2001). Yeast ribosomal protein deletion mutants possess altered peptidyltransferase activity and different sensitivity to cycloheximide. *Biochemistry*, 40, 8101–8.
Dresios J., Panopoulos P., Suzuki K. & Synetos D. (2003). A dispensable yeast ribosomal protein optimizes peptidyltransferase activity and affects translocation. *The Journal of biological chemistry*, 278, 3314–22.
Dunkle J.A., Wang L., Feldman M.B., Pulk A., Chen V.B., Kapral G.J., Noeske J., Richardson J.S., Blanchard S.C. & Cate J.H. (2011). Structures of the bacterial ribosome in classical and hybrid states of tRNA binding. *Science*, 332, 981–4.
Fagan C.E., Dunkle J.A., Maehigashi T., Dang M.N., Devaraj A., Miles S.J., Qin D., Fredrick K. & Dunham C.M. (2013). Reorganization of an intersubunit bridge induced by disparate 16S ribosomal ambiguity mutations mimics an EF-Tu-bound state. *Proceedings of the National Academy of Sciences of the United States of America*, 110, 9716–21.
Fan-Minogue H. & Bedwell D.M. (2008). Eukaryotic ribosomal RNA determinants of aminoglycoside resistance and their role in translational fidelity. *Rna*, 14, 148–57.
Fedyukina D.V., Jennaro T.S. & Cavagnero S. (2014). Charge segregation and low hydrophobicity are key features of ribosomal proteins from different organisms. *The Journal of biological chemistry*, 289, 6740–50.
Fernandez-Pevida A., Kressler D. & de la Cruz J. (2015). Processing of preribosomal RNA in Saccharomyces cerevisiae. *Wiley interdisciplinary reviews. RNA*, 6, 191–209.
Fernandez I.S., Bai X.C., Hussain T., Kelley A.C., Lorsch J.R., Ramakrishnan V. & Scheres S.H.W. (2013). Molecular architecture of a eukaryotic translational initiation complex. *Science*, 342, 1240585.
Fox G.E. (2010). Origin and evolution of the ribosome. *Cold Spring Harbor perspectives in biology*, 2, a003483.
Frank J. & Agrawal R.K. (2000). A ratchet-like inter-subunit reorganization of the ribosome during translocation. *Nature*, 406, 318–22.
Frank J., Zhu J., Penczek P., Li Y., Srivastava S., Verschoor A., Radermacher M., Grassucci R., Lata R.K. & Agrawal R.K. (1995). A model of protein synthesis based on cryo-electron microscopy of the E. coli ribosome. *Nature*, 376, 441–4.
Fringer J.M., Acker M.G., Fekete C.A., Lorsch J.R. & Dever T.E. (2007). Coupled release of eukaryotic translation initiation factors 5B and 1A from 80S ribosomes following subunit joining. *Molecular and cellular biology*, 27, 2384–97.

Frolova L., Le Goff X., Zhouravleva G., Davydova E., Philippe M. & Kisselev L. (1996). Eukaryotic polypeptide chain release factor eRF3 is an eRF1- and ribosome-dependent guanosine triphosphatase. *Rna*, 2, 334–41.

Frolova L.Y., Tsivkovskii R.Y., Sivolobova G.F., Oparina N.Y., Serpinsky O.I., Blinov V.M., Tatkov S.I. & Kisselev L.L. (1999). Mutations in the highly conserved GGQ motif of class 1 polypeptide release factors abolish ability of human eRF1 to trigger peptidyl-tRNA hydrolysis. *Rna*, 5, 1014–20.

Fromm L., Falk S., Flemming D., Schuller J.M., Thoms M., Conti E. & Hurt E. (2017). Reconstitution of the complete pathway of ITS2 processing at the pre-ribosome. *Nature communications*, 8, 1787.

Fujii K., Susanto T.T., Saurabh S. & Barna M. (2018). Decoding the Function of Expansion Segments in Ribosomes. *Molecular cell*, 72, 1013–1020 e6.

Gabdulkhakov A., Nikonov S. & Garber M. (2013). Revisiting the Haloarcula marismortui 50S ribosomal subunit model. *Acta crystallographica. Section D, Biological crystallography*, 69, 997–1004.

Gadal O., Strauss D., Petfalski E., Gleizes P.E., Gas N., Tollervey D. & Hurt E. (2002). Rlp7p is associated with 60S preribosomes, restricted to the granular component of the nucleolus, and required for pre-rRNA processing. *The Journal of cell biology*, 157, 941–51.

Gamalinda M., Ohmayer U., Jakovljevic J., Kumcuoglu B., Woolford J., Mbom B., Lin L. & Woolford J.L., Jr. (2014). A hierarchical model for assembly of eukaryotic 60S ribosomal subunit domains. *Genes & development*, 28, 198–210.

Gao H., Sengupta J., Valle M., Korostelev A., Eswar N., Stagg S.M., Van Roey P., Agrawal R.K., Harvey S.C., Sali A., Chapman M.S. & Frank J. (2003). Study of the structural dynamics of the E coli 70S ribosome using real-space refinement. *Cell*, 113, 789–801.

Garreau de Loubresse N., Prokhorova I., Holtkamp W., Rodnina M.V., Yusupova G. & Yusupov M. (2014). Structural basis for the inhibition of the eukaryotic ribosome. *Nature*, 513, 517–22.

Gartmann M., Blau M., Armache J.P., Mielke T., Topf M. & Beckmann R. (2010). Mechanism of eIF6-mediated inhibition of ribosomal subunit joining. *The Journal of biological chemistry*, 285, 14848–51.

Gasse L., Flemming D. & Hurt E. (2015). Coordinated Ribosomal ITS2 RNA Processing by the Las1 Complex Integrating Endonuclease, Polynucleotide Kinase, and Exonuclease Activities. *Molecular cell*, 60, 808–815.

Geerlings T.H., Vos J.C. & Raue H.A. (2000). The final step in the formation of 25S rRNA in Saccharomyces cerevisiae is performed by 5'-->3' exonucleases. *Rna*, 6, 1698–703.

Geggier P., Dave R., Feldman M.B., Terry D.S., Altman R.B., Munro J.B. & Blanchard S.C. (2010). Conformational sampling of aminoacyl-tRNA during selection on the bacterial ribosome. *Journal of molecular biology*, 399, 576–95.

Gerbi S.A. (1986). The evolution of eukaryotic ribosomal DNA. *Bio Systems*, 19, 247–58.

Ghosh A. & Komar A.A. (2015). Eukaryote-specific extensions in ribosomal proteins of the small subunit: Structure and function. *Translation*, 3, e999576.

Gingras A.C., Raught B. & Sonenberg N. (1999). eIF4 initiation factors: effectors of mRNA recruitment to ribosomes and regulators of translation. *Annual review of biochemistry*, 68, 913–63.

Gomez Ramos L.M., Smeekens J.M., Kovacs N.A., Bowman J.C., Wartell R.M., Wu R. & Williams L.D. (2016). Yeast rRNA Expansion Segments: Folding and Function. *Journal of molecular biology*, 428, 4048–4059.

Graifer D., Molotkov M., Styazhkina V., Demeshkina N., Bulygin K., Eremina A., Ivanov A., Laletina E., Ven'yaminova A. & Karpova G. (2004). Variable and conserved elements of human ribosomes surrounding the mRNA at the decoding and upstream sites. *Nucleic acids research*, 32, 3282–93.

Granneman S., Petfalski E., Swiatkowska A. & Tollervey D. (2010). Cracking pre-40S ribosomal subunit structure by systematic analyses of RNA-protein cross-linking. *The EMBO journal*, 29, 2026–36.

Greber B.J., Boehringer D., Godinic-Mikulcic V., Crnkovic A., Ibba M., Weygand-Durasevic I. & Ban N. (2012). Cryo-EM structure of the archaeal 50S ribosomal subunit in complex with initiation factor 6 and implications for ribosome evolution. *Journal of molecular biology*, 418, 145–60.

Gregory B., Rahman N., Bommakanti A., Shamsuzzaman M., Thapa M., Lescure A., Zengel J.M. & Lindahl L. (2019). The small and large ribosomal subunits depend on each other for stability and accumulation. *Life science alliance*, 2.

Grifo J.A., Abramson R.D., Satler C.A. & Merrick W.C. (1984). RNA-stimulated ATPase activity of eukaryotic initiation factors. *The Journal of biological chemistry*, 259, 8648–54.

Gromadski K.B., Daviter T. & Rodnina M.V. (2006). A uniform response to mismatches in codon-anticodon complexes ensures ribosomal fidelity. *Molecular cell*, 21, 369–77.

Gromadski K.B., Schummer T., Stromgaard A., Knudsen C.R., Kinzy T.G. & Rodnina M.V. (2007). Kinetics of the interactions between yeast elongation factors 1A and 1Balpha, guanine nucleotides, and aminoacyl-tRNA. *The Journal of biological chemistry*, 282, 35629–37.

Gross J.D., Moerke N.J., von der Haar T., Lugovskoy A.A., Sachs A.B., McCarthy J.E. & Wagner G. (2003). Ribosome loading onto the mRNA cap is driven by conformational coupling between eIF4G and eIF4E. *Cell*, 115, 739–50.

Gulay S.P., Bista S., Varshney A., Kirmizialtin S., Sanbonmatsu K.Y. & Dinman J.D. (2017). Tracking fluctuation hotspots on the yeast ribosome through the elongation cycle. *Nucleic acids research*, 45, 4958–4971.

Gulen B., Petrov A.S., Okafor C.D., Vander Wood D., O'Neill E.B., Hud N.V. & Williams L.D. (2016). Ribosomal small subunit domains radiate from a central core. *Scientific reports*, 6, 20885.

Gupta R.S. (2000). The natural evolutionary relationships among prokaryotes. *Critical reviews in microbiology*, 26, 111–31.

Hackmann A., Gross T., Baierlein C. & Krebber H. (2011). The mRNA export factor Npl3 mediates the nuclear export of large ribosomal subunits. *EMBO reports*, 12, 1024–31.

Han Y., Yan C., Fishbain S., Ivanov I. & He Y. (2018). Structural visualization of RNA polymerase III transcription machineries. *Cell discovery*, 4, 40.

Hartman H., Favaretto P. & Smith T.F. (2006). The archaeal origins of the eukaryotic translational system. *Archaea*, 2, 1–9.

Hashem Y., des Georges A., Dhote V., Langlois R., Liao H.Y., Grassucci R.A., Hellen C.U., Pestova T.V. & Frank J. (2013). Structure of the mammalian ribosomal 43S preinitiation complex bound to the scanning factor DHX29. *Cell*, 153, 1108–19.

Hellen C.U.T. (2018). Translation Termination and Ribosome Recycling in Eukaryotes. *Cold Spring Harbor perspectives in biology*, 10.

Hennelly S.P., Antoun A., Ehrenberg M., Gualerzi C.O., Knight W., Lodmell J.S. & Hill W.E. (2005). A time-resolved investigation of ribosomal subunit association. *Journal of molecular biology*, 346, 1243–58.

Henras A.K., Plisson-Chastang C., O'Donohue M.F., Chakraborty A. & Gleizes P.E. (2015). An overview of pre-ribosomal RNA processing in eukaryotes. *Wiley interdisciplinary reviews. RNA*, 6, 225–42.

Henry Y., Wood H., Morrissey J.P., Petfalski E., Kearsey S. & Tollervey D. (1994). The 5' end of yeast 5.8S rRNA is generated by exonucleases from an upstream cleavage site. *The EMBO journal*, 13, 2452–63.

Heuer A., Gerovac M., Schmidt C., Trowitzsch S., Preis A., Kotter P., Berninghausen O., Becker T., Beckmann R. & Tampe R. (2017a). Structure of the 40S-ABCE1 post-splitting complex in ribosome recycling and translation initiation. *Nature structural & molecular biology*, 24, 453–460.

Heuer A., Thomson E., Schmidt C., Berninghausen O., Becker T., Hurt E. & Beckmann R. (2017b). Cryo-EM structure of a late pre-40S ribosomal subunit from Saccharomyces cerevisiae. *eLife*, 6.

Hussain T., Llacer J.L., Fernandez I.S., Munoz A., Martin-Marcos P., Savva C.G., Lorsch J.R., Hinnebusch A.G. & Ramakrishnan V. (2014). Structural changes enable start codon recognition by the eukaryotic translation initiation complex. *Cell*, 159, 597–607.

Jacq B. (1981). Sequence homologies between eukaryotic 5.8S rRNA and the 5' end of prokaryotic 23S rRNa: evidences for a common evolutionary origin. *Nucleic acids research*, 9, 2913–32.

Jeeninga R.E., Van Delft Y., de Graaff-Vincent M., Dirks-Mulder A., Venema J. & Raue H.A. (1997). Variable regions V13 and V3 of Saccharomyces cerevisiae contain structural features essential for normal biogenesis and stability of 5.8S and 25S rRNA. *Rna*, 3, 476–88.

Jennings M.D., Kershaw C.J., Adomavicius T. & Pavitt G.D. (2017). Fail-safe control of translation initiation by dissociation of eIF2alpha phosphorylated ternary complexes. *eLife*, 6.

Jennings M.D. & Pavitt G.D. (2010). eIF5 has GDI activity necessary for translational control by eIF2 phosphorylation. *Nature*, 465, 378–81.

Jin H., Kelley A.C., Loakes D. & Ramakrishnan V. (2010). Structure of the 70S ribosome bound to release factor 2 and a substrate analog provides insights into catalysis of peptide release. *Proceedings of the National Academy of Sciences of the United States of America*, 107, 8593–8.

Johnson A.W. (1997). Rat1p and Xrn1p are functionally interchangeable exoribonucleases that are restricted to and required in the nucleus and cytoplasm, respectively. *Molecular and cellular biology*, 17, 6122–30.

Kaledhonkar S., Fu Z., Caban K., Li W., Chen B., Sun M., Gonzalez Jr R.L. & Frank J. (2018). Real-time structural dynamics of late steps in bacterial translation initiation visualized using time-resolved cryogenic electron microscopy. *bioRxiv*.

Kaltschmidt E. (1971). Ribosomal proteins. XIV. Isoelectric points of ribosomal proteins of E. coli as determined by two-dimensional polyacrylamide gel electrophoresis. *Analytical biochemistry*, 43, 25–31.

Kaltschmidt E. & Wittmann H.G. (1970). Ribosomal proteins. XII. Number of proteins in small and large ribosomal subunits of Escherichia coli as determined by two-

dimensional gel electrophoresis. *Proceedings of the National Academy of Sciences of the United States of America*, 67, 1276–82.
Kapp L.D., Kolitz S.E. & Lorsch J.R. (2006). Yeast initiator tRNA identity elements cooperate to influence multiple steps of translation initiation. *Rna*, 12, 751–64.
Kapp L.D. & Lorsch J.R. (2004). GTP-dependent recognition of the methionine moiety on initiator tRNA by translation factor eIF2. *Journal of molecular biology*, 335, 923–36.
Kappel L., Loibl M., Zisser G., Klein I., Fruhmann G., Gruber C., Unterweger S., Rechberger G., Pertschy B. & Bergler H. (2012). Rlp24 activates the AAA-ATPase Drg1 to initiate cytoplasmic pre-60S maturation. *The Journal of cell biology*, 199, 771–82.
Karbstein K. (2013). Quality control mechanisms during ribosome maturation. *Trends in cell biology*, 23, 242–50.
Kater L., Thoms M., Barrio-Garcia C., Cheng J., Ismail S., Ahmed Y.L., Bange G., Kressler D., Berninghausen O., Sinning I., Hurt E. & Beckmann R. (2017). Visualizing the Assembly Pathway of Nucleolar Pre-60S Ribosomes. *Cell*, 171, 1599–1610 e14.
Kessler S.H. & Sachs A.B. (1998). RNA recognition motif 2 of yeast Pab1p is required for its functional interaction with eukaryotic translation initiation factor 4G. *Molecular and cellular biology*, 18, 51–7.
Khairulina J., Graifer D., Bulygin K., Ven'yaminova A., Frolova L. & Karpova G. (2010). Eukaryote-specific motif of ribosomal protein S15 neighbors A site codon during elongation and termination of translation. *Biochimie*, 92, 820–5.
Khatter H., Myasnikov A.G., Natchiar S.K. & Klaholz B.P. (2015). Structure of the human 80S ribosome. *Nature*, 520, 640–5.
Kief D.R. & Warner J.R. (1981). Coordinate control of syntheses of ribosomal ribonucleic acid and ribosomal proteins during nutritional shift-up in Saccharomyces cerevisiae. *Molecular and cellular biology*, 1, 1007–15.
Kiosze-Becker K., Ori A., Gerovac M., Heuer A., Nurenberg-Goloub E., Rashid U.J., Becker T., Beckmann R., Beck M. & Tampe R. (2016). Structure of the ribosome post-recycling complex probed by chemical cross-linking and mass spectrometry. *Nature communications*, 7, 13248.
Kipper K., Hetenyi C., Sild S., Remme J. & Liiv A. (2009). Ribosomal intersubunit bridge B2a is involved in factor-dependent translation initiation and translational processivity. *Journal of molecular biology*, 385, 405–22.
Klein D.J., Moore P.B. & Steitz T.A. (2004). The roles of ribosomal proteins in the structure assembly, and evolution of the large ribosomal subunit. *Journal of molecular biology*, 340, 141–77.
Klinge S., Voigts-Hoffmann F., Leibundgut M., Arpagaus S. & Ban N. (2011). Crystal structure of the eukaryotic 60S ribosomal subunit in complex with initiation factor 6. *Science*, 334, 941–8.
Klinge S., Voigts-Hoffmann F., Leibundgut M. & Ban N. (2012). Atomic structures of the eukaryotic ribosome. *Trends in biochemical sciences*, 37, 189–98.
Klinge S. & Woolford J.L., Jr. (2019). Ribosome assembly coming into focus. *Nature reviews. Molecular cell biology*, 20, 116–131.
Knorr A.G., Schmidt C., Tesina P., Berninghausen O., Becker T., Beatrix B. & Beckmann R. (2019). Ribosome-NatA architecture reveals that rRNA expansion segments coordinate N-terminal acetylation. *Nature structural & molecular biology*, 26, 35–39.

Komoda T., Sato N.S., Phelps S.S., Namba N., Joseph S. & Suzuki T. (2006). The A-site finger in 23 S rRNA acts as a functional attenuator for translocation. *The Journal of biological chemistry*, 281, 32303–9.

Konikkat S. & Woolford J.L., Jr. (2017). Principles of 60S ribosomal subunit assembly emerging from recent studies in yeast. *The Biochemical journal*, 474, 195–214.

Kornprobst M., Turk M., Kellner N., Cheng J., Flemming D., Kos-Braun I., Kos M., Thoms M., Berninghausen O., Beckmann R. & Hurt E. (2016). Architecture of the 90S Pre-ribosome: A Structural View on the Birth of the Eukaryotic Ribosome. *Cell*, 166, 380–393.

Kos M. & Tollervey D. (2010). Yeast pre-rRNA processing and modification occur cotranscriptionally. *Molecular cell*, 37, 809–20.

Kozak M. (1978). How do eucaryotic ribosomes select initiation regions in messenger RNA? *Cell*, 15, 1109–23.

Kovalchuke O., Kambampati R., Pladies E. & Chakraburtty K. (1998). Competition and cooperation amongst yeast elongation factors. *European journal of biochemistry / FEBS*, 258, 986–93.

Lamanna A.C. & Karbstein K. (2009). Nob1 binds the single-stranded cleavage site D at the 3'-end of 18S rRNA with its PIN domain. *Proceedings of the National Academy of Sciences of the United States of America*, 106, 14259–64.

Lamanna A.C. & Karbstein K. (2011). An RNA conformational switch regulates pre-18S rRNA cleavage. *Journal of molecular biology*, 405, 3–17.

Lebaron S., Schneider C., van Nues R.W., Swiatkowska A., Walsh D., Bottcher B., Granneman S., Watkins N.J. & Tollervey D. (2012). Proofreading of pre-40S ribosome maturation by a translation initiation factor and 60S subunits. *Nature structural & molecular biology*, 19, 744–53.

Lebreton A., Rousselle J.C., Lenormand P., Namane A., Jacquier A., Fromont-Racine M. & Saveanu C. (2008). 60S ribosomal subunit assembly dynamics defined by semi-quantitative mass spectrometry of purified complexes. *Nucleic acids research*, 36, 4988–99.

Lecompte O., Ripp R., Thierry J.C., Moras D. & Poch O. (2002). Comparative analysis of ribosomal proteins in complete genomes: an example of reductive evolution at the domain scale. *Nucleic acids research*, 30, 5382–90.

Leidig C., Thoms M., Holdermann I., Bradatsch B., Berninghausen O., Bange G., Sinning I., Hurt E. & Beckmann R. (2014). 60S ribosome biogenesis requires rotation of the 5S ribonucleoprotein particle. *Nature communications*, 5, 3491.

Liiv A. & O'Connor M. (2006). Mutations in the intersubunit bridge regions of 23 S rRNA. *The Journal of biological chemistry*, 281, 29850–62.

Liu Q. & Fredrick K. (2013). Contribution of intersubunit bridges to the energy barrier of ribosomal translocation. *Nucleic acids research*, 41, 565–74.

Llacer J.L., Hussain T., Marler L., Aitken C.E., Thakur A., Lorsch J.R., Hinnebusch A.G. & Ramakrishnan V. (2015). Conformational Differences between Open and Closed States of the Eukaryotic Translation Initiation Complex. *Molecular cell*, 59, 399–412.

Lo K.Y., Li Z., Bussiere C., Bresson S., Marcotte E.M. & Johnson A.W. (2010). Defining the pathway of cytoplasmic maturation of the 60S ribosomal subunit. *Molecular cell*, 39, 196–208.

Lo K.Y., Li Z., Wang F., Marcotte E.M. & Johnson A.W. (2009). Ribosome stalk assembly requires the dual-specificity phosphatase Yvh1 for the exchange of Mrt4 with P0. *The Journal of cell biology*, 186, 849–62.

Loveland A.B., Demo G., Grigorieff N. & Korostelev A.A. (2017). Ensemble cryo-EM elucidates the mechanism of translation fidelity. *Nature*, 546, 113–117.
Lygerou Z., Allmang C., Tollervey D. & Seraphin B. (1996). Accurate processing of a eukaryotic precursor ribosomal RNA by ribonuclease MRP in vitro. *Science*, 272, 268–70.
Ma C., Wu S., Li N., Chen Y., Yan K., Li Z., Zheng L., Lei J., Woolford J.L., Jr. & Gao N. (2017). Structural snapshot of cytoplasmic pre-60S ribosomal particles bound by Nmd3, Lsg1, Tif6 and Reh1. *Nature structural & molecular biology*, 24, 214–220.
Madru C., Lebaron S., Blaud M., Delbos L., Pipoli J., Pasmant E., Rety S. & Leulliot N. (2015). Chaperoning 5S RNA assembly. *Genes & development*, 29, 1432–46.
Maiväli U., Pulk A., Loogvali E.L. & Remme J. (2002). Accessibility of phosphates in domain I of 23 S rRNA in the ribosomal 50 S subunit as detected by R(P) phosphorothioates. *Biochimica et biophysica acta*, 1579, 1–7.
Majumdar R., Bandyopadhyay A. & Maitra U. (2003). Mammalian translation initiation factor eIF1 functions with eIF1A and eIF3 in the formation of a stable 40 S preinitiation complex. *The Journal of biological chemistry*, 278, 6580–7.
Mantsyzov A.B., Ivanova E.V., Birdsall B., Alkalaeva E.Z., Kryuchkova P.N., Kelly G., Frolova L.Y. & Polshakov V.I. (2010). NMR solution structure and function of the C-terminal domain of eukaryotic class 1 polypeptide chain release factor. *The FEBS journal*, 277, 2611–27.
Martin W.F., Garg S. & Zimorski V. (2015). Endosymbiotic theories for eukaryote origin. *Philosophical transactions of the Royal Society of London. Series B, Biological sciences*, 370, 20140330.
Matheisl S., Berninghausen O., Becker T. & Beckmann R. (2015). Structure of a human translation termination complex. *Nucleic acids research*, 43, 8615–26.
Matsuo Y., Granneman S., Thoms M., Manikas R.G., Tollervey D. & Hurt E. (2014). Coupled GTPase and remodelling ATPase activities form a checkpoint for ribosome export. *Nature*, 505, 112–116.
McClory S.P., Leisring J.M., Qin D. & Fredrick K. (2010). Missense suppressor mutations in 16S rRNA reveal the importance of helices h8 and h14 in aminoacyl-tRNA selection. *Rna*, 16, 1925–34.
McInerney J.O., O'Connell M.J. & Pisani D. (2014). The hybrid nature of the Eukaryota and a consilient view of life on Earth. *Nature reviews. Microbiology*, 12, 449–55.
Melnikov S., Ben-Shem A., Garreau de Loubresse N., Jenner L., Yusupova G. & Yusupov M. (2012). One core, two shells: bacterial and eukaryotic ribosomes. *Nature structural & molecular biology*, 19, 560–7.
Melnikov S., Mailliot J., Shin B.S., Rigger L., Yusupova G., Micura R., Dever T.E. & Yusupov M. (2016). Crystal Structure of Hypusine-Containing Translation Factor eIF5A Bound to a Rotated Eukaryotic Ribosome. *Journal of molecular biology*, 428, 3570–3576.
Melnikov S., Manakongtreecheep K. & Soll D. (2018). Revising the Structural Diversity of Ribosomal Proteins Across the Three Domains of Life. *Molecular biology and evolution*, 35, 1588–1598.
Merrick W.C. & Pavitt G.D. (2018). Protein Synthesis Initiation in Eukaryotic Cells. *Cold Spring Harbor perspectives in biology*, 10.
Meskauskas A., Harger J.W., Jacobs K.L. & Dinman J.D. (2003). Decreased peptidyl-transferase activity correlates with increased programmed -1 ribosomal frame-shifting and viral maintenance defects in the yeast Saccharomyces cerevisiae. *Rna*, 9, 982–92.

Miller O.L., Jr. & Beatty B.R. (1969). Visualization of nucleolar genes. *Science*, 164, 955–7.
Mitchell P., Petfalski E., Shevchenko A., Mann M. & Tollervey D. (1997). The exosome: a conserved eukaryotic RNA processing complex containing multiple 3'-->5' exoribonucleases. *Cell*, 91, 457–66.
Mohan S. & Noller H.F. (2017). Recurring RNA structural motifs underlie the mechanics of L1 stalk movement. *Nature communications*, 8, 14285.
Muhs M., Hilal T., Mielke T., Skabkin M.A., Sanbonmatsu K.Y., Pestova T.V. & Spahn C.M. (2015). Cryo-EM of ribosomal 80S complexes with termination factors reveals the translocated cricket paralysis virus IRES. *Molecular cell*, 57, 422–32.
Munro J.B., Wasserman M.R., Altman R.B., Wang L. & Blanchard S.C. (2010). Correlated conformational events in EF-G and the ribosome regulate translocation. *Nature structural & molecular biology*, 17, 1470–7.
Musalgaonkar S., Moomau C.A. & Dinman J.D. (2014). Ribosomes in the balance: structural equilibrium ensures translational fidelity and proper gene expression. *Nucleic acids research*, 42, 13384–92.
Neyer S., Kunz M., Geiss C., Hantsche M., Hodirnau V.V., Seybert A., Engel C., Scheffer M.P., Cramer P. & Frangakis A.S. (2016). Structure of RNA polymerase I transcribing ribosomal DNA genes. *Nature*, 540, 607–610.
Nguyenle T., Laurberg M., Brenowitz M. & Noller H.F. (2006). Following the dynamics of changes in solvent accessibility of 16 S and 23 S rRNA during ribosomal subunit association using synchrotron-generated hydroxyl radicals. *Journal of molecular biology*, 359, 1235–48.
Nissen P., Hansen J., Ban N., Moore P.B. & Steitz T.A. (2000). The structural basis of ribosome activity in peptide bond synthesis. *Science*, 289, 920–30.
Noller H.F. (2005). RNA structure: reading the ribosome. *Science*, 309, 1508–14.
Noller H.F. (2012). Evolution of protein synthesis from an RNA world. *Cold Spring Harbor perspectives in biology*, 4, a003681.
Nomura N., Honda T., Baba K., Naganuma T., Tanzawa T., Arisaka F., Noda M., Uchiyama S., Tanaka I., Yao M. & Uchiumi T. (2012). Archaeal ribosomal stalk protein interacts with translation factors in a nucleotide-independent manner via its conserved C terminus. *Proceedings of the National Academy of Sciences of the United States of America*, 109, 3748–53.
O'Leary S.E., Petrov A., Chen J. & Puglisi J.D. (2013). Dynamic recognition of the mRNA cap by Saccharomyces cerevisiae eIF4E. *Structure*, 21, 2197–207.
Oeffinger M., Dlakic M. & Tollervey D. (2004). A pre-ribosome-associated HEAT-repeat protein is required for export of both ribosomal subunits. *Genes & development*, 18, 196–209.
Oeffinger M., Zenklusen D., Ferguson A., Wei K.E., El Hage A., Tollervey D., Chait B.T., Singer R.H. & Rout M.P. (2009). Rrp17p is a eukaryotic exonuclease required for 5' end processing of Pre-60S ribosomal RNA. *Molecular cell*, 36, 768–81.
Ogle J.M., Brodersen D.E., Clemons W.M., Jr., Tarry M.J., Carter A.P. & Ramakrishnan V. (2001). Recognition of cognate transfer RNA by the 30S ribosomal subunit. *Science*, 292, 897–902.
Ogle J.M., Murphy F.V., Tarry M.J. & Ramakrishnan V. (2002). Selection of tRNA by the ribosome requires a transition from an open to a closed form. *Cell*, 111, 721–32.
Olsen D.S., Savner E.M., Mathew A., Zhang F., Krishnamoorthy T., Phan L. & Hinnebusch A.G. (2003). Domains of eIF1A that mediate binding to eIF2, eIF3 and

eIF5B and promote ternary complex recruitment in vivo. *The EMBO journal*, 22, 193–204.

Osheim Y.N., French S.L., Keck K.M., Champion E.A., Spasov K., Dragon F., Baserga S.J. & Beyer A.L. (2004). Pre-18S ribosomal RNA is structurally compacted into the SSU processome prior to being cleaved from nascent transcripts in Saccharomyces cerevisiae. *Molecular cell*, 16, 943–54.

Panse V.G. & Johnson A.W. (2010). Maturation of eukaryotic ribosomes: acquisition of functionality. *Trends in biochemical sciences*, 35, 260–6.

Passmore L.A., Schmeing T.M., Maag D., Applefield D.J., Acker M.G., Algire M.A., Lorsch J.R. & Ramakrishnan V. (2007). The eukaryotic translation initiation factors eIF1 and eIF1A induce an open conformation of the 40S ribosome. *Molecular cell*, 26, 41–50.

Pellegrino S., Demeshkina N., Mancera-Martinez E., Melnikov S., Simonetti A., Myasnikov A., Yusupov M., Yusupova G. & Hashem Y. (2018). Structural Insights into the Role of Diphthamide on Elongation Factor 2 in mRNA Reading-Frame Maintenance. *Journal of molecular biology*, 430, 2677–2687.

Perez-Fernandez J., Martin-Marcos P. & Dosil M. (2011). Elucidation of the assembly events required for the recruitment of Utp20, Imp4 and Bms1 onto nascent preribosomes. *Nucleic acids research*, 39, 8105–21.

Perez-Fernandez J., Roman A., De Las Rivas J., Bustelo X.R. & Dosil M. (2007). The 90S preribosome is a multimodular structure that is assembled through a hierarchical mechanism. *Molecular and cellular biology*, 27, 5414–29.

Pertschy B., Saveanu C., Zisser G., Lebreton A., Tengg M., Jacquier A., Liebminger E., Nobis B., Kappel L., van der Klei I., Hogenauer G., Fromont-Racine M. & Bergler H. (2007). Cytoplasmic recycling of 60S preribosomal factors depends on the AAA protein Drg1. *Molecular and cellular biology*, 27, 6581–92.

Petrov A.S., Bernier C.R., Gulen B., Waterbury C.C., Hershkovits E., Hsiao C., Harvey S.C., Hud N.V., Fox G.E., Wartell R.M. & Williams L.D. (2014a). Secondary structures of rRNAs from all three domains of life. *PloS one*, 9, e88222.

Petrov A.S., Bernier C.R., Hershkovits E., Xue Y., Waterbury C.C., Hsiao C., Stepanov V.G., Gaucher E.A., Grover M.A., Harvey S.C., Hud N.V., Wartell R.M., Fox G.E. & Williams L.D. (2013). Secondary structure and domain architecture of the 23S and 5S rRNAs. *Nucleic acids research*, 41, 7522–35.

Petrov A.S., Bernier C.R., Hsiao C., Norris A.M., Kovacs N.A., Waterbury C.C., Stepanov V.G., Harvey S.C., Fox G.E., Wartell R.M., Hud N.V. & Williams L.D. (2014b). Evolution of the ribosome at atomic resolution. *Proceedings of the National Academy of Sciences of the United States of America*, 111, 10251–6.

Pillon M.C., Sobhany M., Borgnia M.J., Williams J.G. & Stanley R.E. (2017). Grc3 programs the essential endoribonuclease Las1 for specific RNA cleavage. *Proceedings of the National Academy of Sciences of the United States of America*, 114, E5530-E5538.

Pisarev A.V., Hellen C.U. & Pestova T.V. (2007). Recycling of eukaryotic posttermination ribosomal complexes. *Cell*, 131, 286–99.

Pisarev A.V., Kolupaeva V.G., Yusupov M.M., Hellen C.U. & Pestova T.V. (2008). Ribosomal position and contacts of mRNA in eukaryotic translation initiation complexes. *The EMBO journal*, 27, 1609–21.

Pisarev A.V., Skabkin M.A., Pisareva V.P., Skabkina O.V., Rakotondrafara A.M., Hentze M.W., Hellen C.U. & Pestova T.V. (2010). The role of ABCE1 in eukaryotic posttermination ribosomal recycling. *Molecular cell*, 37, 196–210.

Pisareva V.P., Pisarev A.V., Hellen C.U., Rodnina M.V. & Pestova T.V. (2006). Kinetic analysis of interaction of eukaryotic release factor 3 with guanine nucleotides. *The Journal of biological chemistry*, 281, 40224–35.

Planta R.J. & Mager W.H. (1998). The list of cytoplasmic ribosomal proteins of Saccharomyces cerevisiae. *Yeast*, 14, 471–7.

Poirot O. & Timsit Y. (2016). Neuron-Like Networks Between Ribosomal Proteins Within the Ribosome. *Scientific reports*, 6, 26485.

Polikanov Y.S., Aleksashin N.A., Beckert B. & Wilson D.N. (2018). The Mechanisms of Action of Ribosome-Targeting Peptide Antibiotics. *Frontiers in molecular biosciences*, 5, 48.

Poll G., Braun T., Jakovljevic J., Neueder A., Jakob S., Woolford J.L., Jr., Tschochner H. & Milkereit P. (2009). rRNA maturation in yeast cells depleted of large ribosomal subunit proteins. *PloS one*, 4, e8249.

Preis A., Heuer A., Barrio-Garcia C., Hauser A., Eyler D.E., Berninghausen O., Green R., Becker T. & Beckmann R. (2014). Cryoelectron microscopic structures of eukaryotic translation termination complexes containing eRF1-eRF3 or eRF1-ABCE1. *Cell reports*, 8, 59–65.

Pulk A., Maivali U. & Remme J. (2006). Identification of nucleotides in E. coli 16S rRNA essential for ribosome subunit association. *Rna*, 12, 790–6.

Quast C., Pruesse E., Yilmaz P., Gerken J., Schweer T., Yarza P., Peplies J. & Glockner F.O. (2013). The SILVA ribosomal RNA gene database project: improved data processing and web-based tools. *Nucleic acids research*, 41, D590–6.

Rabl J., Leibundgut M., Ataide S.F., Haag A. & Ban N. (2011). Crystal structure of the eukaryotic 40S ribosomal subunit in complex with initiation factor 1. *Science*, 331, 730–6.

Rakauskaite R. & Dinman J.D. (2006). An arc of unpaired "hinge bases" facilitates information exchange among functional centers of the ribosome. *Molecular and cellular biology*, 26, 8992–9002.

Ramesh M. & Woolford J.L., Jr. (2016). Eukaryote-specific rRNA expansion segments function in ribosome biogenesis. *Rna*, 22, 1153–62.

Ratje A.H., Loerke J., Mikolajka A., Brunner M., Hildebrand P.W., Starosta A.L., Donhofer A., Connell S.R., Fucini P., Mielke T., Whitford P.C., Onuchic J.N., Yu Y., Sanbonmatsu K.Y., Hartmann R.K., Penczek P.A., Wilson D.N. & Spahn C.M. (2010). Head swivel on the ribosome facilitates translocation by means of intra-subunit tRNA hybrid sites. *Nature*, 468, 713–6.

Reblova K., Sponer J. & Lankas F. (2012). Structure and mechanical properties of the ribosomal L1 stalk three-way junction. *Nucleic acids research*, 40, 6290–303.

Rhodin M.H. & Dinman J.D. (2011). An extensive network of information flow through the B1b/c intersubunit bridge of the yeast ribosome. *PloS one*, 6, e20048.

Rodnina M.V., Beringer M. & Wintermeyer W. (2007). How ribosomes make peptide bonds. *Trends in biochemical sciences*, 32, 20–6.

Rozen F., Edery I., Meerovitch K., Dever T.E., Merrick W.C. & Sonenberg N. (1990). Bidirectional RNA helicase activity of eucaryotic translation initiation factors 4A and 4F. *Molecular and cellular biology*, 10, 1134–44.

Saini A.K., Nanda J.S., Lorsch J.R. & Hinnebusch A.G. (2010). Regulatory elements in eIF1A control the fidelity of start codon selection by modulating tRNA(i)(Met) binding to the ribosome. *Genes & development*, 24, 97–110.

Saini P., Eyler D.E., Green R. & Dever T.E. (2009). Hypusine-containing protein eIF5A promotes translation elongation. *Nature*, 459, 118–21.

Salas-Marco J. & Bedwell D.M. (2004). GTP hydrolysis by eRF3 facilitates stop codon decoding during eukaryotic translation termination. *Molecular and cellular biology*, 24, 7769–78.

Sanbonmatsu K.Y., Joseph S. & Tung C.S. (2005). Simulating movement of tRNA into the ribosome during decoding. *Proceedings of the National Academy of Sciences of the United States of America*, 102, 15854–9.

Sanghai Z.A., Miller L., Molloy K.R., Barandun J., Hunziker M., Chaker-Margot M., Wang J., Chait B.T. & Klinge S. (2018). Modular assembly of the nucleolar pre-60S ribosomal subunit. *Nature*, 556, 126–129.

Sarkar A., Pech M., Thoms M., Beckmann R. & Hurt E. (2016). Ribosome-stalk biogenesis is coupled with recruitment of nuclear-export factor to the nascent 60S subunit. *Nature structural & molecular biology*, 23, 1074–1082.

Saveanu C., Namane A., Gleizes P.E., Lebreton A., Rousselle J.C., Noaillac-Depeyre J., Gas N., Jacquier A. & Fromont-Racine M. (2003). Sequential protein association with nascent 60S ribosomal particles. *Molecular and cellular biology*, 23, 4449–60.

Scaiola A., Pena C., Weisser M., Bohringer D., Leibundgut M., Klingauf-Nerurkar P., Gerhardy S., Panse V.G. & Ban N. (2018). Structure of a eukaryotic cytoplasmic pre-40S ribosomal subunit. *The EMBO journal*, 37.

Schillewaert S., Wacheul L., Lhomme F. & Lafontaine D.L. (2012). The evolutionarily conserved protein Las1 is required for pre-rRNA processing at both ends of ITS2. *Molecular and cellular biology*, 32, 430–44.

Schluenzen F., Tocilj A., Zarivach R., Harms J., Gluehmann M., Janell D., Bashan A., Bartels H., Agmon I., Franceschi F. & Yonath A. (2000). Structure of functionally activated small ribosomal subunit at 3.3 angstroms resolution. *Cell*, 102, 615–23.

Schuller J.M., Falk S., Fromm L., Hurt E. & Conti E. (2018). Structure of the nuclear exosome captured on a maturing preribosome. *Science*, 360, 219–222.

Sengupta J., Nilsson J., Gursky R., Kjeldgaard M., Nissen P. & Frank J. (2008). Visualization of the eEF2–80S ribosome transition-state complex by cryo-electron microscopy. *Journal of molecular biology*, 382, 179–87.

Sergiev P.V., Kiparisov S.V., Burakovsky D.E., Lesnyak D.V., Leonov A.A., Bogdanov A.A. & Dontsova O.A. (2005). The conserved A-site finger of the 23S rRNA: just one of the intersubunit bridges or a part of the allosteric communication pathway? *Journal of molecular biology*, 353, 116–23.

Shah P., Ding Y., Niemczyk M., Kudla G. & Plotkin J.B. (2013). Rate-limiting steps in yeast protein translation. *Cell*, 153, 1589–601.

Shaikh T.R., Yassin A.S., Lu Z., Barnard D., Meng X., Lu T.M., Wagenknecht T. & Agrawal R.K. (2014). Initial bridges between two ribosomal subunits are formed within 9.4 milliseconds, as studied by time-resolved cryo-EM. *Proceedings of the National Academy of Sciences of the United States of America*, 111, 9822–7.

Shao S., Murray J., Brown A., Taunton J., Ramakrishnan V. & Hegde R.S. (2016). Decoding Mammalian Ribosome-mRNA States by Translational GTPase Complexes. *Cell*, 167, 1229–1240 e15.

Shi X., Khade P.K., Sanbonmatsu K.Y. & Joseph S. (2012). Functional role of the sarcin-ricin loop of the 23S rRNA in the elongation cycle of protein synthesis. *Journal of molecular biology*, 419, 125–38.

Shimizu T., Nakagaki M., Nishi Y., Kobayashi Y., Hachimori A. & Uchiumi T. (2002). Interaction among silkworm ribosomal proteins P1, P2 and P0 required for functional protein binding to the GTPase-associated domain of 28S rRNA. *Nucleic acids research*, 30, 2620–7.

Shin B.S., Katoh T., Gutierrez E., Kim J.R., Suga H. & Dever T.E. (2017). Amino acid substrates impose polyamine, eIF5A, or hypusine requirement for peptide synthesis. *Nucleic acids research*, 45, 8392–8402.

Simonetti A., Brito Querido J., Myasnikov A.G., Mancera-Martinez E., Renaud A., Kuhn L. & Hashem Y. (2016). eIF3 Peripheral Subunits Rearrangement after mRNA Binding and Start-Codon Recognition. *Molecular cell*, 63, 206–217.

Smith M.W., Meskauskas A., Wang P., Sergiev P.V. & Dinman J.D. (2001). Saturation mutagenesis of 5S rRNA in Saccharomyces cerevisiae. *Molecular and cellular biology*, 21, 8264–75.

Sonenberg N., Morgan M.A., Merrick W.C. & Shatkin A.J. (1978). A polypeptide in eukaryotic initiation factors that crosslinks specifically to the 5'-terminal cap in mRNA. *Proceedings of the National Academy of Sciences of the United States of America*, 75, 4843–7.

Song H., Mugnier P., Das A.K., Webb H.M., Evans D.R., Tuite M.F., Hemmings B.A. & Barford D. (2000). The crystal structure of human eukaryotic release factor eRF1--mechanism of stop codon recognition and peptidyl-tRNA hydrolysis. *Cell*, 100, 311–21.

Song J.M., Cheung E. & Rabinowitz J.C. (1996). Organization and characterization of the two yeast ribosomal protein YL19 genes. *Current genetics*, 30, 273–8.

Spahn C.M., Beckmann R., Eswar N., Penczek P.A., Sali A., Blobel G. & Frank J. (2001). Structure of the 80S ribosome from Saccharomyces cerevisiae--tRNA-ribosome and subunit-subunit interactions. *Cell*, 107, 373–86.

Spahn C.M., Gomez-Lorenzo M.G., Grassucci R.A., Jorgensen R., Andersen G.R., Beckmann R., Penczek P.A., Ballesta J.P. & Frank J. (2004a). Domain movements of elongation factor eEF2 and the eukaryotic 80S ribosome facilitate tRNA translocation. *The EMBO journal*, 23, 1008–19.

Spahn C.M., Jan E., Mulder A., Grassucci R.A., Sarnow P. & Frank J. (2004b). Cryo-EM visualization of a viral internal ribosome entry site bound to human ribosomes: the IRES functions as an RNA-based translation factor. *Cell*, 118, 465–75.

Spang A., Eme L., Saw J.H., Caceres E.F., Zaremba-Niedzwiedzka K., Lombard J., Guy L. & Ettema T.J.G. (2018). Asgard archaea are the closest prokaryotic relatives of eukaryotes. *PLoS genetics*, 14, e1007080.

Spang A., Saw J.H., Jorgensen S.L., Zaremba-Niedzwiedzka K., Martijn J., Lind A.E., van Eijk R., Schleper C., Guy L. & Ettema T.J.G. (2015). Complex archaea that bridge the gap between prokaryotes and eukaryotes. *Nature*, 521, 173–179.

Stage-Zimmermann T., Schmidt U. & Silver P.A. (2000). Factors affecting nuclear export of the 60S ribosomal subunit in vivo. *Molecular biology of the cell*, 11, 3777–89.

Strunk B.S. & Karbstein K. (2009). Powering through ribosome assembly. *Rna*, 15, 2083–104.

Strunk B.S., Novak M.N., Young C.L. & Karbstein K. (2012). A translation-like cycle is a quality control checkpoint for maturing 40S ribosome subunits. *Cell*, 150, 111–21.

Sun Q., Zhu X., Qi J., An W., Lan P., Tan D., Chen R., Wang B., Zheng S., Zhang C., Chen X., Zhang W., Chen J., Dong M.Q. & Ye K. (2017). Molecular architecture of the 90S small subunit pre-ribosome. *eLife*, 6.

Sun Q., Vila-Sanjurjo A. & O'Connor M. (2011). Mutations in the intersubunit bridge regions of 16S rRNA affect decoding and subunit-subunit interactions on the 70S ribosome. *Nucleic acids research*, 39, 3321–30.

Sweeney R., Chen L. & Yao M.C. (1994). An rRNA variable region has an evolutionarily conserved essential role despite sequence divergence. *Molecular and cellular biology*, 14, 4203–15.

Svidritskiy E., Brilot A.F., Koh C.S., Grigorieff N. & Korostelev A.A. (2014). Structures of yeast 80S ribosome-tRNA complexes in the rotated and nonrotated conformations. *Structure*, 22, 1210–1218.

Zaremba-Niedzwiedzka K., Caceres E.F., Saw J.H., Backstrom D., Juzokaite L., Vancaester E., Seitz K.W., Anantharaman K., Starnawski P., Kjeldsen K.U., Stott M.B., Nunoura T., Banfield J.F., Schramm A., Baker B.J., Spang A. & Ettema T.J. (2017). Asgard archaea illuminate the origin of eukaryotic cellular complexity. *Nature*, 541, 353–358.

Zhang F., Saini A.K., Shin B.S., Nanda J. & Hinnebusch A.G. (2015). Conformational changes in the P site and mRNA entry channel evoked by AUG recognition in yeast translation preinitiation complexes. *Nucleic acids research*, 43, 2293–312.

Zhang J., Harnpicharnchai P., Jakovljevic J., Tang L., Guo Y., Oeffinger M., Rout M.P., Hiley S.L., Hughes T. & Woolford J.L., Jr. (2007). Assembly factors Rpf2 and Rrs1 recruit 5S rRNA and ribosomal proteins rpL5 and rpL11 into nascent ribosomes. *Genes & development*, 21, 2580–92.

Zhang L., Wu C., Cai G., Chen S. & Ye K. (2016). Stepwise and dynamic assembly of the earliest precursors of small ribosomal subunits in yeast. *Genes & development*, 30, 718–32.

Zheng A., Yu J., Yamamoto R., Ose T., Tanaka I. & Yao M. (2014). X-ray structures of eIF5B and the eIF5B-eIF1A complex: the conformational flexibility of eIF5B is restricted on the ribosome by interaction with eIF1A. *Acta crystallographica. Section D, Biological crystallography*, 70, 3090–8.

Zhou D., Zhu X., Zheng S., Tan D., Dong M.Q. & Ye K. (2019). Cryo-EM structure of an early precursor of large ribosomal subunit reveals a half-assembled intermediate. *Protein & cell*, 10, 120–130.

Taylor D., Unbehaun A., Li W., Das S., Lei J., Liao H.Y., Grassucci R.A., Pestova T.V. & Frank J. (2012). Cryo-EM structure of the mammalian eukaryotic release factor eRF1-eRF3-associated termination complex. *Proceedings of the National Academy of Sciences of the United States of America*, 109, 18413–8.

Taylor D.J., Nilsson J., Merrill A.R., Andersen G.R., Nissen P. & Frank J. (2007). Structures of modified eEF2 80S ribosome complexes reveal the role of GTP hydrolysis in translocation. *The EMBO journal*, 26, 2421–31.

Tchorzewski M., Krokowski D., Boguszewska A., Liljas A. & Grankowski N. (2003). Structural characterization of yeast acidic ribosomal P proteins forming the P1A-P2B heterocomplex. *Biochemistry*, 42, 3399–408.

Thomson E. & Tollervey D. (2010). The final step in 5.8S rRNA processing is cytoplasmic in Saccharomyces cerevisiae. *Molecular and cellular biology*, 30, 976–84.

Trabuco L.G., Schreiner E., Eargle J., Cornish P., Ha T., Luthey-Schulten Z. & Schulten K. (2010). The role of L1 stalk-tRNA interaction in the ribosome elongation cycle. *Journal of molecular biology*, 402, 741–60.

Triana-Alonso F.J., Chakraburtty K. & Nierhaus K.H. (1995). The elongation factor 3 unique in higher fungi and essential for protein biosynthesis is an E site factor. *The Journal of biological chemistry*, 270, 20473–8.

Uchiumi T., Honma S., Nomura T., Dabbs E.R. & Hachimori A. (2002). Translation elongation by a hybrid ribosome in which proteins at the GTPase center of the

Escherichia coli ribosome are replaced with rat counterparts. *The Journal of biological chemistry*, 277, 3857–62.
Unbehaun A., Borukhov S.I., Hellen C.U. & Pestova T.V. (2004). Release of initiation factors from 48S complexes during ribosomal subunit joining and the link between establishment of codon-anticodon base-pairing and hydrolysis of eIF2-bound GTP. *Genes & development*, 18, 3078–93.
Valas R.E. & Bourne P.E. (2011). The origin of a derived superkingdom: how a gram-positive bacterium crossed the desert to become an archaeon. *Biology direct*, 6, 16.
Valasek L.S., Zeman J., Wagner S., Beznoskova P., Pavlikova Z., Mohammad M.P., Hronova V., Herrmannova A., Hashem Y. & Gunisova S. (2017). Embraced by eIF3: structural and functional insights into the roles of eIF3 across the translation cycle. *Nucleic acids research*, 45, 10948–10968.
Vanrobays E., Gelugne J.P., Caizergues-Ferrer M. & Lafontaine D.L. (2004). Dim2p, a KH-domain protein required for small ribosomal subunit synthesis. *Rna*, 10, 645–56.
Warner J.R. (1999). The economics of ribosome biosynthesis in yeast. *Trends in biochemical sciences*, 24, 437–40.
Warringer J. & Blomberg A. (2006). Evolutionary constraints on yeast protein size. *BMC evolutionary biology*, 6, 61.
Wells S.E., Hillner P.E., Vale R.D. & Sachs A.B. (1998). Circularization of mRNA by eukaryotic translation initiation factors. *Molecular cell*, 2, 135–40.
Whitford P.C., Geggier P., Altman R.B., Blanchard S.C., Onuchic J.N. & Sanbonmatsu K.Y. (2010). Accommodation of aminoacyl-tRNA into the ribosome involves reversible excursions along multiple pathways. *Rna*, 16, 1196–204.
Wilson D.N. & Beckmann R. (2011). The ribosomal tunnel as a functional environment for nascent polypeptide folding and translational stalling. *Current opinion in structural biology*, 21, 274–82.
von der Haar T. (2008). A quantitative estimation of the global translational activity in logarithmically growing yeast cells. *BMC systems biology*, 2, 87.
Wu S., Tutuncuoglu B., Yan K., Brown H., Zhang Y., Tan D., Gamalinda M., Yuan Y., Li Z., Jakovljevic J., Ma C., Lei J., Dong M.Q., Woolford J.L., Jr. & Gao N. (2016). Diverse roles of assembly factors revealed by structures of late nuclear pre-60S ribosomes. *Nature*, 534, 133–7.
Yamamoto H., Unbehaun A., Loerke J., Behrmann E., Collier M., Burger J., Mielke T. & Spahn C.M. (2014). Structure of the mammalian 80S initiation complex with initiation factor 5B on HCV-IRES RNA. *Nature structural & molecular biology*, 21, 721–7.
Yokoyama T. & Suzuki T. (2008). Ribosomal RNAs are tolerant toward genetic insertions: evolutionary origin of the expansion segments. *Nucleic acids research*, 36, 3539–51.
Yusupov M.M., Yusupova G.Z., Baucom A., Lieberman K., Earnest T.N., Cate J.H. & Noller H.F. (2001). Crystal structure of the ribosome at 5.5 A resolution. *Science*, 292, 883–96.
Yusupova G.Z., Yusupov M.M., Cate J.H. & Noller H.F. (2001). The path of messenger RNA through the ribosome. *Cell*, 106, 233–41.

# PUBLICATIONS

# CURRICULUM VITAE


Name: Ivan Kisly
Date of birth: May 31, 1989
Citizenship: Estonia
Address: Institute of Molecular and Cell Biology, University of Tartu, Riia Str. 23C, 51010, Tartu, Estonia
E-mail: kisly.ivan@gmail.com


**Education:**

| | |
|---|---|
| 2014– | University of Tartu, Institute of Molecular and Cell biology, PhD studies, molecular biology |
| 2012–2014 | University of Tartu, Institute of Molecular and Cell biology, MSc, gene technology |
| 2011–2012 | University of Tartu, Institute of Molecular and Cell biology, BSc, biology |
| 2008–2012 | University of Tartu, Institute of Education, BA, educational science (sciences) |
| 1996–2008 | Narva Centre Gymnasium |

**Language skills:** Russian, Estonian, English

**Additional studies:**

| | |
|---|---|
| 20.03–23.03.2018 | EMBL Course "RNA Sequencing Library Preparation – How Low Can You Go?" EMBL Heidelberg, Germany |
| 11.03–16.03.2018 | EMBL Course "Analysis and Integration of Transcriptome and Proteome Data", EMBL Heidelberg, Germany |

**Publications:**

1. **Kisly I.**, Remme J., Tamm T. (2019). Ribosomal protein eL24, involved in two intersubunit bridges, stimulates translation initiation and elongation. Nucleic Acids Research. 47(1): 406–420.
2. **Kisly I.**, Gulay S.P., Maeorg U., Dinman J.D., Remme J., Tamm T. (2016). The functional role of eL19 and eB12 intersubunit bridge in the eukaryotic ribosome. Journal of Molecular Biology. 428(10): 2203–2216.
3. Piir K., Tamm T., **Kisly I.**, Tammsalu T., Remme J. S. (2014). Stepwise splitting of ribosomal proteins from yeast ribosomes by LiCl. PLoS One. 9(7):e101561.

**Conference presentations:**

| | |
|---|---|
| 17–19.06.2019 | FEBS3+ conference of Latvian, Lithuanian and Estonian Biochemical Societies, Riga, Latvia; oral presentation "Dual role of the ribosomal protein eL24" |

03–06.10.2018 EMBO|EMBL Symposium "The Complex Life of RNA", Heidelberg, Germany; poster presentation "The functional importance of ribosomal eukaryote-specific intersubunit bridges eB12 and eB13 for the mRNA translation"

06–09.09.2017 EMBO Conference "Protein synthesis and translational control", Heidelberg, Germany; poster presentation "Dual role of the ribosomal protein eL24"

06–10.07.2016 EMBO Conference "Ribosome Structure and Function 2016", Strasbourg, France; poster presentation "The functional role of eL19 and eB12 intersubunit bridge in the eukaryotic ribosome"

**Scholarships:**

2019 Olev and Talvi Maimets stipendium, "Protein Synthesis and Translation Control" conference attendance, 4–7 September 2019, Heidelberg, Germany

2016 Kristjan Jaak scholarship, "Ribosome Structure and Function 2016" conference attendance

**Teaching:**

- Practical Course in Chemistry of Nucleic Acids
- Protein Biosynthesis, lecture "Regulation of translation in eukaryotes"
- Seminar in Biology and Biodiversity Conservation, problem solving in genetics and molecular biology
- Practical Course "Laboratory Projects", supervision of student project
- Project "Isolation and identification of Estonian yeast strains", lecture "Sequencing data visualization and analysis, identification of yeast species"

**Supervision:**

2 BSc students
ERASMUS+ summer intern
2 high school students

**Membership in professional organizations:**

Student member of the Estonian Biochemical Society

# ELULOOKIRJELDUS


Nimi: Ivan Kisly
Sünniaeg: 31. mai 1989
Kodakondsus: Eesti
Aadress: Molekulaar- ja Rakubioloogia instituut, Tartu Ülikool, Riia 23C, 51010, Tartu, Eesti
E-mail: kisly.ivan@gmail.com


**Haridus:**

| | |
|---|---|
| 2014– | Tartu Ülikool, Molekulaar- ja Rakubioloogia Instituut, doktoriõpe molekulaarbioloogia erialal |
| 2012–2014 | Tartu Ülikool, Molekulaar- ja Rakubioloogia Instituut, MSc, geenitehnoloogia |
| 2011–2012 | Tartu Ülikool, Molekulaar- ja Rakubioloogia Instituut, BSc, bioloogia |
| 2008–2012 | Tartu Ülikool, Haridusteaduste Instituut, BA, haridusteadus (loodusteaduslikud ained) |
| 1996–2008 | Narva Kesklinna Gümnaasium |

**Keelteoskus:** Vene, Eesti, Inglise

**Täiendõpe:**

| | |
|---|---|
| 20.03–23.03.2018 | EMBL Kursus "RNA Sequencing Library Preparation – How Low Can You Go?", EMBL Heidelberg, Saksamaa |
| 11.03–16.03.2018 | EMBL Kursus "Analysis and Integration of Transcriptome and Proteome Data", EMBL Heidelberg, Saksamaa |

**Publikatsioonide loetelu:**

1. Kisly I., Remme J., Tamm T. (2019). Ribosomal protein eL24, involved in two intersubunit bridges, stimulates translation initiation and elongation. Nucleic Acids Research. 47(1): 406–420.
2. Kisly I., Gulay S.P., Maeorg U., Dinman J.D., Remme J., Tamm T. (2016). The functional role of eL19 and eB12 intersubunit bridge in the eukaryotic ribosome. Journal of Molecular Biology. 428(10): 2203–2216.
3. Piir K., Tamm T., Kisly I., Tammsalu T., Remme J. S. (2014). Stepwise splitting of ribosomal proteins from yeast ribosomes by LiCl. PLoS One. 9(7):e101561.

**Konverentsiettekanded:**

| | |
|---|---|
| 17–19.06.2019 | FEBS3+ Läti, Leedu ja Eesti biokeemia seltside konverents, Riia, Läti; suuline ettekanne „Dual role of the ribosomal protein eL24" |

03–06.10.2018 EMBO|EMBL sümpoosion “The Complex Life of RNA”, Heidelberg, Saksamaa; stendiettekanne “The functional importance of ribosomal eukaryote-specific intersubunit bridges eB12 and eB13 for the mRNA translation”

06–09.09.2017 EMBO konverents “Protein synthesis and translational control”, Heidelberg, Saksamaa; stendiettekanne “Dual role of the ribosomal protein eL24”

06–10.07.2016 EMBO konverents “Ribosome Structure and Function 2016”, Strasbourg, Prantsusmaa; stendiettekanne “The functional role of eL19 and eB12 intersubunit bridge in the eukaryotic ribosome”

**Stipendiumid:**

2019 Olev ja Talvi Maimetsa stipendium, osalemiseks konverentsil „Protein synthesis and translational control“, 4.–7. september 2019, Heidelberg, Saksamaa

2016 Kristjan Jaagu stipendium, osalemiseks konverentsil “Ribosome Structure and Function 2016”

**Õppetöö:**

- Nukleiinhapete keemia praktikumi juhendamine
- Valgu biosünteesi kursuse raames loeng “Translatsiooni regulatsioon eukarüootides”
- Bioloogia ning elustiku kaitse erialaseminar, geneetika ja molekulaarbioloogia probleemülesanne
- Praktiline kursus „Laboratoorsed projektid“, üliõpilase projekti juhendamine
- Projekt “101 pärmitüve Eesti loodusest”, loeng “Sekveneerimistulemuste visualiseerimine ja analüüs ning pärmiliigi määramine”

**Juhendamised:**

2 bakalaureuseüliõpilast
ERASMUS+ väliskülalisüliõpilane
2 gümnaasiumiõpilast

**Erialaline liikmelisus:**

Eesti Biokeemia Seltsi üliõpilasliige

# DISSERTATIONES BIOLOGICAE UNIVERSITATIS TARTUENSIS

1. **Toivo Maimets**. Studies of human oncoprotein p53. Tartu, 1991, 96 p.
2. **Enn K. Seppet**. Thyroid state control over energy metabolism, ion transport and contractile functions in rat heart. Tartu, 1991, 135 p.
3. **Kristjan Zobel**. Epifüütsete makrosamblike väärtus õhu saastuse indikaatoritena Hamar-Dobani boreaalsetes mägimetsades. Tartu, 1992, 131 lk.
4. **Andres Mäe**. Conjugal mobilization of catabolic plasmids by transposable elements in helper plasmids. Tartu, 1992, 91 p.
5. **Maia Kivisaar**. Studies on phenol degradation genes of *Pseudomonas* sp. strain EST 1001. Tartu, 1992, 61 p.
6. **Allan Nurk**. Nucleotide sequences of phenol degradative genes from *Pseudomonas sp.* strain EST 1001 and their transcriptional activation in *Pseudomonas putida.* Tartu, 1992, 72 p.
7. **Ülo Tamm**. The genus *Populus* L. in Estonia: variation of the species biology and introduction. Tartu, 1993, 91 p.
8. **Jaanus Remme**. Studies on the peptidyltransferase centre of the *E.coli* ribosome. Tartu, 1993, 68 p.
9. **Ülo Langel**. Galanin and galanin antagonists. Tartu, 1993, 97 p.
10. **Arvo Käärd**. The development of an automatic online dynamic fluorescense-based pH-dependent fiber optic penicillin flowthrought biosensor for the control of the benzylpenicillin hydrolysis. Tartu, 1993, 117 p.
11. **Lilian Järvekülg**. Antigenic analysis and development of sensitive immunoassay for potato viruses. Tartu, 1993, 147 p.
12. **Jaak Palumets**. Analysis of phytomass partition in Norway spruce. Tartu, 1993, 47 p.
13. **Arne Sellin**. Variation in hydraulic architecture of *Picea abies* (L.) Karst. trees grown under different enviromental conditions. Tartu, 1994, 119 p.
13. **Mati Reeben**. Regulation of light neurofilament gene expression. Tartu, 1994, 108 p.
14. **Urmas Tartes**. Respiration rhytms in insects. Tartu, 1995, 109 p.
15. **Ülo Puurand**. The complete nucleotide sequence and infections *in vitro* transcripts from cloned cDNA of a potato A potyvirus. Tartu, 1995, 96 p.
16. **Peeter Hõrak**. Pathways of selection in avian reproduction: a functional framework and its application in the population study of the great tit (*Parus major*). Tartu, 1995, 118 p.
17. **Erkki Truve**. Studies on specific and broad spectrum virus resistance in transgenic plants. Tartu, 1996, 158 p.
18. **Illar Pata**. Cloning and characterization of human and mouse ribosomal protein S6-encoding genes. Tartu, 1996, 60 p.
19. **Ülo Niinemets**. Importance of structural features of leaves and canopy in determining species shade-tolerance in temperature deciduous woody taxa. Tartu, 1996, 150 p.

20. **Ants Kurg**. Bovine leukemia virus: molecular studies on the packaging region and DNA diagnostics in cattle. Tartu, 1996, 104 p.
21. **Ene Ustav**. E2 as the modulator of the BPV1 DNA replication. Tartu, 1996, 100 p.
22. **Aksel Soosaar**. Role of helix-loop-helix and nuclear hormone receptor transcription factors in neurogenesis. Tartu, 1996, 109 p.
23. **Maido Remm**. Human papillomavirus type 18: replication, transformation and gene expression. Tartu, 1997, 117 p.
24. **Tiiu Kull**. Population dynamics in *Cypripedium calceolus* L. Tartu, 1997, 124 p.
25. **Kalle Olli**. Evolutionary life-strategies of autotrophic planktonic microorganisms in the Baltic Sea. Tartu, 1997, 180 p.
26. **Meelis Pärtel**. Species diversity and community dynamics in calcareous grassland communities in Western Estonia. Tartu, 1997, 124 p.
27. **Malle Leht**. The Genus *Potentilla* L. in Estonia, Latvia and Lithuania: distribution, morphology and taxonomy. Tartu, 1997, 186 p.
28. **Tanel Tenson**. Ribosomes, peptides and antibiotic resistance. Tartu, 1997, 80 p.
29. **Arvo Tuvikene**. Assessment of inland water pollution using biomarker responses in fish *in vivo* and *in vitro.* Tartu, 1997, 160 p.
30. **Urmas Saarma**. Tuning ribosomal elongation cycle by mutagenesis of 23S rRNA. Tartu, 1997, 134 p.
31. **Henn Ojaveer**. Composition and dynamics of fish stocks in the gulf of Riga ecosystem. Tartu, 1997, 138 p.
32. **Lembi Lõugas**. Post-glacial development of vertebrate fauna in Estonian water bodies. Tartu, 1997, 138 p.
33. **Margus Pooga**. Cell penetrating peptide, transportan, and its predecessors, galanin-based chimeric peptides. Tartu, 1998, 110 p.
34. **Andres Saag**. Evolutionary relationships in some cetrarioid genera (Lichenized Ascomycota). Tartu, 1998, 196 p.
35. **Aivar Liiv**. Ribosomal large subunit assembly *in vivo*. Tartu, 1998, 158 p.
36. **Tatjana Oja**. Isoenzyme diversity and phylogenetic affinities among the eurasian annual bromes (*Bromus* L., Poaceae). Tartu, 1998, 92 p.
37. **Mari Moora**. The influence of arbuscular mycorrhizal (AM) symbiosis on the competition and coexistence of calcareous grassland plant species. Tartu, 1998, 78 p.
38. **Olavi Kurina**. Fungus gnats in Estonia (*Diptera: Bolitophilidae, Keroplatidae, Macroceridae, Ditomyiidae, Diadocidiidae, Mycetophilidae*). Tartu, 1998, 200 p.
39. **Andrus Tasa**. Biological leaching of shales: black shale and oil shale. Tartu, 1998, 98 p.
40. **Arnold Kristjuhan**. Studies on transcriptional activator properties of tumor suppressor protein p53. Tartu, 1998, 86 p.
41. **Sulev Ingerpuu**. Characterization of some human myeloid cell surface and nuclear differentiation antigens. Tartu, 1998, 163 p.

42. **Veljo Kisand**. Responses of planktonic bacteria to the abiotic and biotic factors in the shallow lake Võrtsjärv. Tartu, 1998, 118 p.
43. **Kadri Põldmaa**. Studies in the systematics of hypomyces and allied genera (Hypocreales, Ascomycota). Tartu, 1998, 178 p.
44. **Markus Vetemaa**. Reproduction parameters of fish as indicators in environmental monitoring. Tartu, 1998, 117 p.
45. **Heli Talvik**. Prepatent periods and species composition of different *Oesophagostomum* spp. populations in Estonia and Denmark. Tartu, 1998, 104 p.
46. **Katrin Heinsoo**. Cuticular and stomatal antechamber conductance to water vapour diffusion in *Picea abies* (L.) karst. Tartu, 1999, 133 p.
47. **Tarmo Annilo**. Studies on mammalian ribosomal protein S7. Tartu, 1998, 77 p.
48. **Indrek Ots**. Health state indicies of reproducing great tits (*Parus major*): sources of variation and connections with life-history traits. Tartu, 1999, 117 p.
49. **Juan Jose Cantero**. Plant community diversity and habitat relationships in central Argentina grasslands. Tartu, 1999, 161 p.
50. **Rein Kalamees**. Seed bank, seed rain and community regeneration in Estonian calcareous grasslands. Tartu, 1999, 107 p.
51. **Sulev Kõks**. Cholecystokinin (CCK) – induced anxiety in rats: influence of environmental stimuli and involvement of endopioid mechanisms and serotonin. Tartu, 1999, 123 p.
52. **Ebe Sild**. Impact of increasing concentrations of $O_3$ and $CO_2$ on wheat, clover and pasture. Tartu, 1999, 123 p.
53. **Ljudmilla Timofejeva**. Electron microscopical analysis of the synaptonemal complex formation in cereals. Tartu, 1999, 99 p.
54. **Andres Valkna**. Interactions of galanin receptor with ligands and G-proteins: studies with synthetic peptides. Tartu, 1999, 103 p.
55. **Taavi Virro**. Life cycles of planktonic rotifers in lake Peipsi. Tartu, 1999, 101 p.
56. **Ana Rebane**. Mammalian ribosomal protein S3a genes and intron-encoded small nucleolar RNAs U73 and U82. Tartu, 1999, 85 p.
57. **Tiina Tamm**. Cocksfoot mottle virus: the genome organisation and translational strategies. Tartu, 2000, 101 p.
58. **Reet Kurg**. Structure-function relationship of the bovine papilloma virus E2 protein. Tartu, 2000, 89 p.
59. **Toomas Kivisild**. The origins of Southern and Western Eurasian populations: an mtDNA study. Tartu, 2000, 121 p.
60. **Niilo Kaldalu**. Studies of the TOL plasmid transcription factor XylS. Tartu, 2000, 88 p.
61. **Dina Lepik**. Modulation of viral DNA replication by tumor suppressor protein p53. Tartu, 2000, 106 p.

62. **Kai Vellak**. Influence of different factors on the diversity of the bryophyte vegetation in forest and wooded meadow communities. Tartu, 2000, 122 p.
63. **Jonne Kotta**. Impact of eutrophication and biological invasionas on the structure and functions of benthic macrofauna. Tartu, 2000, 160 p.
64. **Georg Martin**. Phytobenthic communities of the Gulf of Riga and the inner sea the West-Estonian archipelago. Tartu, 2000, 139 p.
65. **Silvia Sepp**. Morphological and genetical variation of *Alchemilla L.* in Estonia. Tartu, 2000. 124 p.
66. **Jaan Liira**. On the determinants of structure and diversity in herbaceous plant communities. Tartu, 2000, 96 p.
67. **Priit Zingel**. The role of planktonic ciliates in lake ecosystems. Tartu, 2001, 111 p.
68. **Tiit Teder**. Direct and indirect effects in Host-parasitoid interactions: ecological and evolutionary consequences. Tartu, 2001, 122 p.
69. **Hannes Kollist**. Leaf apoplastic ascorbate as ozone scavenger and its transport across the plasma membrane. Tartu, 2001, 80 p.
70. **Reet Marits**. Role of two-component regulator system PehR-PehS and extracellular protease PrtW in virulence of *Erwinia Carotovora* subsp. *Carotovora*. Tartu, 2001, 112 p.
71. **Vallo Tilgar**. Effect of calcium supplementation on reproductive performance of the pied flycatcher *Ficedula hypoleuca* and the great tit *Parus major,* breeding in Nothern temperate forests. Tartu, 2002, 126 p.
72. **Rita Hõrak**. Regulation of transposition of transposon Tn*4652* in *Pseudomonas putida*. Tartu, 2002, 108 p.
73. **Liina Eek-Piirsoo**. The effect of fertilization, mowing and additional illumination on the structure of a species-rich grassland community. Tartu, 2002, 74 p.
74. **Krõõt Aasamaa**. Shoot hydraulic conductance and stomatal conductance of six temperate deciduous tree species. Tartu, 2002, 110 p.
75. **Nele Ingerpuu**. Bryophyte diversity and vascular plants. Tartu, 2002, 112 p.
76. **Neeme Tõnisson**. Mutation detection by primer extension on oligonucleotide microarrays. Tartu, 2002, 124 p.
77. **Margus Pensa**. Variation in needle retention of Scots pine in relation to leaf morphology, nitrogen conservation and tree age. Tartu, 2003, 110 p.
78. **Asko Lõhmus**. Habitat preferences and quality for birds of prey: from principles to applications. Tartu, 2003, 168 p.
79. **Viljar Jaks**. p53 – a switch in cellular circuit. Tartu, 2003, 160 p.
80. **Jaana Männik**. Characterization and genetic studies of four ATP-binding cassette (ABC) transporters. Tartu, 2003, 140 p.
81. **Marek Sammul**. Competition and coexistence of clonal plants in relation to productivity. Tartu, 2003, 159 p
82. **Ivar Ilves**. Virus-cell interactions in the replication cycle of bovine papillomavirus type 1. Tartu, 2003, 89 p.

83. **Andres Männik**. Design and characterization of a novel vector system based on the stable replicator of bovine papillomavirus type 1. Tartu, 2003, 109 p.
84. **Ivika Ostonen**. Fine root structure, dynamics and proportion in net primary production of Norway spruce forest ecosystem in relation to site conditions. Tartu, 2003, 158 p.
85. **Gudrun Veldre**. Somatic status of 12–15-year-old Tartu schoolchildren. Tartu, 2003, 199 p.
86. **Ülo Väli**. The greater spotted eagle *Aquila clanga* and the lesser spotted eagle *A. pomarina*: taxonomy, phylogeography and ecology. Tartu, 2004, 159 p.
87. **Aare Abroi**. The determinants for the native activities of the bovine papillomavirus type 1 E2 protein are separable. Tartu, 2004, 135 p.
88. **Tiina Kahre**. Cystic fibrosis in Estonia. Tartu, 2004, 116 p.
89. **Helen Orav-Kotta**. Habitat choice and feeding activity of benthic suspension feeders and mesograzers in the northern Baltic Sea. Tartu, 2004, 117 p.
90. **Maarja Öpik**. Diversity of arbuscular mycorrhizal fungi in the roots of perennial plants and their effect on plant performance. Tartu, 2004, 175 p.
91. **Kadri Tali**. Species structure of *Neotinea ustulata*. Tartu, 2004, 109 p.
92. **Kristiina Tambets**. Towards the understanding of post-glacial spread of human mitochondrial DNA haplogroups in Europe and beyond: a phylogeographic approach. Tartu, 2004, 163 p.
93. **Arvi Jõers**. Regulation of p53-dependent transcription. Tartu, 2004, 103 p.
94. **Lilian Kadaja**. Studies on modulation of the activity of tumor suppressor protein p53. Tartu, 2004, 103 p.
95. **Jaak Truu**. Oil shale industry wastewater: impact on river microbial community and possibilities for bioremediation. Tartu, 2004, 128 p.
96. **Maire Peters**. Natural horizontal transfer of the *pheBA* operon. Tartu, 2004, 105 p.
97. **Ülo Maiväli**. Studies on the structure-function relationship of the bacterial ribosome. Tartu, 2004, 130 p.
98. **Merit Otsus**. Plant community regeneration and species diversity in dry calcareous grasslands. Tartu, 2004, 103 p.
99. **Mikk Heidemaa**. Systematic studies on sawflies of the genera *Dolerus, Empria,* and *Caliroa* (Hymenoptera: Tenthredinidae). Tartu, 2004, 167 p.
100. **Ilmar Tõnno**. The impact of nitrogen and phosphorus concentration and N/P ratio on cyanobacterial dominance and $N_2$ fixation in some Estonian lakes. Tartu, 2004, 111 p.
101. **Lauri Saks**. Immune function, parasites, and carotenoid-based ornaments in greenfinches. Tartu, 2004, 144 p.
102. **Siiri Rootsi**. Human Y-chromosomal variation in European populations. Tartu, 2004, 142 p.
103. **Eve Vedler**. Structure of the 2,4-dichloro-phenoxyacetic acid-degradative plasmid pEST4011. Tartu, 2005. 106 p.

104. **Andres Tover**. Regulation of transcription of the phenol degradation *pheBA* operon in *Pseudomonas putida*. Tartu, 2005, 126 p.
105. **Helen Udras**. Hexose kinases and glucose transport in the yeast *Hansenula polymorpha*. Tartu, 2005, 100 p.
106. **Ave Suija**. Lichens and lichenicolous fungi in Estonia: diversity, distribution patterns, taxonomy. Tartu, 2005, 162 p.
107. **Piret Lõhmus**. Forest lichens and their substrata in Estonia. Tartu, 2005, 162 p.
108. **Inga Lips**. Abiotic factors controlling the cyanobacterial bloom occurrence in the Gulf of Finland. Tartu, 2005, 156 p.
109. **Kaasik, Krista**. Circadian clock genes in mammalian clockwork, metabolism and behaviour. Tartu, 2005, 121 p.
110. **Juhan Javoiš**. The effects of experience on host acceptance in ovipositing moths. Tartu, 2005, 112 p.
111. **Tiina Sedman**. Characterization of the yeast *Saccharomyces cerevisiae* mitochondrial DNA helicase Hmi1. Tartu, 2005, 103 p.
112. **Ruth Aguraiuja**. Hawaiian endemic fern lineage *Diellia* (Aspleniaceae): distribution, population structure and ecology. Tartu, 2005, 112 p.
113. **Riho Teras**. Regulation of transcription from the fusion promoters generated by transposition of Tn*4652* into the upstream region of *pheBA* operon in *Pseudomonas putida*. Tartu, 2005, 106 p.
114. **Mait Metspalu**. Through the course of prehistory in India: tracing the mtDNA trail. Tartu, 2005, 138 p.
115. **Elin Lõhmussaar**. The comparative patterns of linkage disequilibrium in European populations and its implication for genetic association studies. Tartu, 2006, 124 p.
116. **Priit Kupper**. Hydraulic and environmental limitations to leaf water relations in trees with respect to canopy position. Tartu, 2006, 126 p.
117. **Heili Ilves**. Stress-induced transposition of Tn*4652* in *Pseudomonas Putida.* Tartu, 2006, 120 p.
118. **Silja Kuusk**. Biochemical properties of Hmi1p, a DNA helicase from *Saccharomyces cerevisiae* mitochondria. Tartu, 2006, 126 p.
119. **Kersti Püssa**. Forest edges on medium resolution landsat thematic mapper satellite images. Tartu, 2006, 90 p.
120. **Lea Tummeleht**. Physiological condition and immune function in great tits (*Parus major* l.): Sources of variation and trade-offs in relation to growth. Tartu, 2006, 94 p.
121. **Toomas Esperk**. Larval instar as a key element of insect growth schedules. Tartu, 2006, 186 p.
122. **Harri Valdmann**. Lynx (*Lynx lynx*) and wolf (*Canis lupus*) in the Baltic region: Diets, helminth parasites and genetic variation. Tartu, 2006. 102 p.
123. **Priit Jõers**. Studies of the mitochondrial helicase Hmi1p in *Candida albicans* and *Saccharomyces cerevisia*. Tartu, 2006. 113 p.
124. **Kersti Lilleväli**. Gata3 and Gata2 in inner ear development. Tartu, 2007, 123 p.

125. **Kai Rünk**. Comparative ecology of three fern species: *Dryopteris carthusiana* (Vill.) H.P. Fuchs, *D. expansa* (C. Presl) Fraser-Jenkins & Jermy and *D. dilatata* (Hoffm.) A. Gray (Dryopteridaceae). Tartu, 2007, 143 p.
126. **Aveliina Helm**. Formation and persistence of dry grassland diversity: role of human history and landscape structure. Tartu, 2007, 89 p.
127. **Leho Tedersoo**. Ectomycorrhizal fungi: diversity and community structure in Estonia, Seychelles and Australia. Tartu, 2007, 233 p.
128. **Marko Mägi**. The habitat-related variation of reproductive performance of great tits in a deciduous-coniferous forest mosaic: looking for causes and consequences. Tartu, 2007, 135 p.
129. **Valeria Lulla**. Replication strategies and applications of Semliki Forest virus. Tartu, 2007, 109 p.
130. **Ülle Reier**. Estonian threatened vascular plant species: causes of rarity and conservation. Tartu, 2007, 79 p.
131. **Inga Jüriado**. Diversity of lichen species in Estonia: influence of regional and local factors. Tartu, 2007, 171 p.
132. **Tatjana Krama**. Mobbing behaviour in birds: costs and reciprocity based cooperation. Tartu, 2007, 112 p.
133. **Signe Saumaa**. The role of DNA mismatch repair and oxidative DNA damage defense systems in avoidance of stationary phase mutations in *Pseudomonas putida.* Tartu, 2007, 172 p.
134. **Reedik Mägi**. The linkage disequilibrium and the selection of genetic markers for association studies in european populations. Tartu, 2007, 96 p.
135. **Priit Kilgas**. Blood parameters as indicators of physiological condition and skeletal development in great tits (*Parus major*): natural variation and application in the reproductive ecology of birds. Tartu, 2007, 129 p.
136. **Anu Albert**. The role of water salinity in structuring eastern Baltic coastal fish communities. Tartu, 2007, 95 p.
137. **Kärt Padari**. Protein transduction mechanisms of transportans. Tartu, 2008, 128 p.
138. **Siiri-Lii Sandre**. Selective forces on larval colouration in a moth. Tartu, 2008, 125 p.
139. **Ülle Jõgar**. Conservation and restoration of semi-natural floodplain meadows and their rare plant species. Tartu, 2008, 99 p.
140. **Lauri Laanisto**. Macroecological approach in vegetation science: generality of ecological relationships at the global scale. Tartu, 2008, 133 p.
141. **Reidar Andreson**. Methods and software for predicting PCR failure rate in large genomes. Tartu, 2008, 105 p.
142. **Birgot Paavel**. Bio-optical properties of turbid lakes. Tartu, 2008, 175 p.
143. **Kaire Torn**. Distribution and ecology of charophytes in the Baltic Sea. Tartu, 2008, 98 p.
144. **Vladimir Vimberg**. Peptide mediated macrolide resistance. Tartu, 2008, 190 p.
145. **Daima Örd**. Studies on the stress-inducible pseudokinase TRB3, a novel inhibitor of transcription factor ATF4. Tartu, 2008, 108 p.

146. **Lauri Saag**. Taxonomic and ecologic problems in the genus *Lepraria* (*Stereocaulaceae*, lichenised *Ascomycota*). Tartu, 2008, 175 p.
147. **Ulvi Karu**. Antioxidant protection, carotenoids and coccidians in greenfinches – assessment of the costs of immune activation and mechanisms of parasite resistance in a passerine with carotenoid-based ornaments. Tartu, 2008, 124 p.
148. **Jaanus Remm**. Tree-cavities in forests: density, characteristics and occupancy by animals. Tartu, 2008, 128 p.
149. **Epp Moks**. Tapeworm parasites *Echinococcus multilocularis* and *E. granulosus* in Estonia: phylogenetic relationships and occurrence in wild carnivores and ungulates. Tartu, 2008, 82 p.
150. **Eve Eensalu**. Acclimation of stomatal structure and function in tree canopy: effect of light and $CO_2$ concentration. Tartu, 2008, 108 p.
151. **Janne Pullat**. Design, functionlization and application of an *in situ* synthesized oligonucleotide microarray. Tartu, 2008, 108 p.
152. **Marta Putrinš**. Responses of *Pseudomonas putida* to phenol-induced metabolic and stress signals. Tartu, 2008, 142 p.
153. **Marina Semtšenko**. Plant root behaviour: responses to neighbours and physical obstructions. Tartu, 2008, 106 p.
154. **Marge Starast**. Influence of cultivation techniques on productivity and fruit quality of some *Vaccinium* and *Rubus* taxa. Tartu, 2008, 154 p.
155. **Age Tats**. Sequence motifs influencing the efficiency of translation. Tartu, 2009, 104 p.
156. **Radi Tegova**. The role of specialized DNA polymerases in mutagenesis in *Pseudomonas putida.* Tartu, 2009, 124 p.
157. **Tsipe Aavik**. Plant species richness, composition and functional trait pattern in agricultural landscapes – the role of land use intensity and landscape structure. Tartu, 2009, 112 p.
158. **Kaja Kiiver**. Semliki forest virus based vectors and cell lines for studying the replication and interactions of alphaviruses and hepaciviruses. Tartu, 2009, 104 p.
159. **Meelis Kadaja**. Papillomavirus Replication Machinery Induces Genomic Instability in its Host Cell. Tartu, 2009, 126 p.
160. **Pille Hallast**. Human and chimpanzee Luteinizing hormone/Chorionic Gonadotropin beta (*LHB/CGB*) gene clusters: diversity and divergence of young duplicated genes. Tartu, 2009, 168 p.
161. **Ain Vellak**. Spatial and temporal aspects of plant species conservation. Tartu, 2009, 86 p.
162. **Triinu Remmel**. Body size evolution in insects with different colouration strategies: the role of predation risk. Tartu, 2009, 168 p.
163. **Jaana Salujõe**. Zooplankton as the indicator of ecological quality and fish predation in lake ecosystems. Tartu, 2009, 129 p.
164. **Ele Vahtmäe**. Mapping benthic habitat with remote sensing in optically complex coastal environments. Tartu, 2009, 109 p.

165. **Liisa Metsamaa**. Model-based assessment to improve the use of remote sensing in recognition and quantitative mapping of cyanobacteria. Tartu, 2009, 114 p.
166. **Pille Säälik**. The role of endocytosis in the protein transduction by cell-penetrating peptides. Tartu, 2009, 155 p.
167. **Lauri Peil**. Ribosome assembly factors in *Escherichia coli.* Tartu, 2009, 147 p.
168. **Lea Hallik**. Generality and specificity in light harvesting, carbon gain capacity and shade tolerance among plant functional groups. Tartu, 2009, 99 p.
169. **Mariliis Tark**. Mutagenic potential of DNA damage repair and tolerance mechanisms under starvation stress. Tartu, 2009, 191 p.
170. **Riinu Rannap**. Impacts of habitat loss and restoration on amphibian populations. Tartu, 2009, 117 p.
171. **Maarja Adojaan**. Molecular variation of HIV-1 and the use of this knowledge in vaccine development. Tartu, 2009, 95 p.
172. **Signe Altmäe**. Genomics and transcriptomics of human induced ovarian folliculogenesis. Tartu, 2010, 179 p.
173. **Triin Suvi**. Mycorrhizal fungi of native and introduced trees in the Seychelles Islands. Tartu, 2010, 107 p.
174. **Velda Lauringson**. Role of suspension feeding in a brackish-water coastal sea. Tartu, 2010, 123 p.
175. **Eero Talts**. Photosynthetic cyclic electron transport – measurement and variably proton-coupled mechanism. Tartu, 2010, 121 p.
176. **Mari Nelis**. Genetic structure of the Estonian population and genetic distance from other populations of European descent. Tartu, 2010, 97 p.
177. **Kaarel Krjutškov**. Arrayed Primer Extension-2 as a multiplex PCR-based method for nucleic acid variation analysis: method and applications. Tartu, 2010, 129 p.
178. **Egle Köster**. Morphological and genetical variation within species complexes: *Anthyllis vulneraria* s. l. and *Alchemilla vulgaris* (coll.). Tartu, 2010, 101 p.
179. **Erki Õunap**. Systematic studies on the subfamily Sterrhinae (Lepidoptera: Geometridae). Tartu, 2010, 111 p.
180. **Merike Jõesaar**. Diversity of key catabolic genes at degradation of phenol and *p*-cresol in pseudomonads. Tartu, 2010, 125 p.
181. **Kristjan Herkül**. Effects of physical disturbance and habitat-modifying species on sediment properties and benthic communities in the northern Baltic Sea. Tartu, 2010, 123 p.
182. **Arto Pulk**. Studies on bacterial ribosomes by chemical modification approaches. Tartu, 2010, 161 p.
183. **Maria Põllupüü**. Ecological relations of cladocerans in a brackish-water ecosystem. Tartu, 2010, 126 p.
184. **Toomas Silla**. Study of the segregation mechanism of the Bovine Papillomavirus Type 1. Tartu, 2010, 188 p.

185. **Gyaneshwer Chaubey**. The demographic history of India: A perspective based on genetic evidence. Tartu, 2010, 184 p.
186. **Katrin Kepp**. Genes involved in cardiovascular traits: detection of genetic variation in Estonian and Czech populations. Tartu, 2010, 164 p.
187. **Virve Sõber**. The role of biotic interactions in plant reproductive performance. Tartu, 2010, 92 p.
188. **Kersti Kangro**. The response of phytoplankton community to the changes in nutrient loading. Tartu, 2010, 144 p.
189. **Joachim M. Gerhold**. Replication and Recombination of mitochondrial DNA in Yeast. Tartu, 2010, 120 p.
190. **Helen Tammert**. Ecological role of physiological and phylogenetic diversity in aquatic bacterial communities. Tartu, 2010, 140 p.
191. **Elle Rajandu**. Factors determining plant and lichen species diversity and composition in Estonian *Calamagrostis* and *Hepatica* site type forests. Tartu, 2010, 123 p.
192. **Paula Ann Kivistik**. ColR-ColS signalling system and transposition of Tn*4652* in the adaptation of *Pseudomonas putida.* Tartu, 2010, 118 p.
193. **Siim Sõber**. Blood pressure genetics: from candidate genes to genome-wide association studies. Tartu, 2011, 120 p.
194. **Kalle Kipper**. Studies on the role of helix 69 of 23S rRNA in the factor-dependent stages of translation initiation, elongation, and termination. Tartu, 2011, 178 p.
195. **Triinu Siibak**. Effect of antibiotics on ribosome assembly is indirect. Tartu, 2011, 134 p.
196. **Tambet Tõnissoo**. Identification and molecular analysis of the role of guanine nucleotide exchange factor RIC-8 in mouse development and neural function. Tartu, 2011, 110 p.
197. **Helin Räägel**. Multiple faces of cell-penetrating peptides – their intracellular trafficking, stability and endosomal escape during protein transduction. Tartu, 2011, 161 p.
198. **Andres Jaanus**. Phytoplankton in Estonian coastal waters – variability, trends and response to environmental pressures. Tartu, 2011, 157 p.
199. **Tiit Nikopensius**. Genetic predisposition to nonsyndromic orofacial clefts. Tartu, 2011, 152 p.
200. **Signe Värv**. Studies on the mechanisms of RNA polymerase II-dependent transcription elongation. Tartu, 2011, 108 p.
201. **Kristjan Välk**. Gene expression profiling and genome-wide association studies of non-small cell lung cancer. Tartu, 2011, 98 p.
202. **Arno Põllumäe**. Spatio-temporal patterns of native and invasive zooplankton species under changing climate and eutrophication conditions. Tartu, 2011, 153 p.
203. **Egle Tammeleht**. Brown bear (*Ursus arctos*) population structure, demographic processes and variations in diet in northern Eurasia. Tartu, 2011, 143 p.

205. **Teele Jairus**. Species composition and host preference among ectomycorrhizal fungi in Australian and African ecosystems. Tartu, 2011, 106 p.
206. **Kessy Abarenkov**. PlutoF – cloud database and computing services supporting biological research. Tartu, 2011, 125 p.
207. **Marina Grigorova**. Fine-scale genetic variation of follicle-stimulating hormone beta-subunit coding gene (*FSHB*) and its association with reproductive health. Tartu, 2011, 184 p.
208. **Anu Tiitsaar**. The effects of predation risk and habitat history on butterfly communities. Tartu, 2011, 97 p.
209. **Elin Sild**. Oxidative defences in immunoecological context: validation and application of assays for nitric oxide production and oxidative burst in a wild passerine. Tartu, 2011, 105 p.
210. **Irja Saar**. The taxonomy and phylogeny of the genera *Cystoderma* and *Cystodermella* (Agaricales, Fungi). Tartu, 2012, 167 p.
211. **Pauli Saag**. Natural variation in plumage bacterial assemblages in two wild breeding passerines. Tartu, 2012, 113 p.
212. **Aleksei Lulla**. Alphaviral nonstructural protease and its polyprotein substrate: arrangements for the perfect marriage. Tartu, 2012, 143 p.
213. **Mari Järve**. Different genetic perspectives on human history in Europe and the Caucasus: the stories told by uniparental and autosomal markers. Tartu, 2012, 119 p.
214. **Ott Scheler**. The application of tmRNA as a marker molecule in bacterial diagnostics using microarray and biosensor technology. Tartu, 2012, 93 p.
215. **Anna Balikova**. Studies on the functions of tumor-associated mucin-like leukosialin (CD43) in human cancer cells. Tartu, 2012, 129 p.
216. **Triinu Kõressaar**. Improvement of PCR primer design for detection of prokaryotic species. Tartu, 2012, 83 p.
217. **Tuul Sepp**. Hematological health state indices of greenfinches: sources of individual variation and responses to immune system manipulation. Tartu, 2012, 117 p.
218. **Rya Ero**. Modifier view of the bacterial ribosome. Tartu, 2012, 146 p.
219. **Mohammad Bahram**. Biogeography of ectomycorrhizal fungi across different spatial scales. Tartu, 2012, 165 p.
220. **Annely Lorents**. Overcoming the plasma membrane barrier: uptake of amphipathic cell-penetrating peptides induces influx of calcium ions and downstream responses. Tartu, 2012, 113 p.
221. **Katrin Männik**. Exploring the genomics of cognitive impairment: whole-genome SNP genotyping experience in Estonian patients and general population. Tartu, 2012, 171 p.
222. **Marko Prous**. Taxonomy and phylogeny of the sawfly genus *Empria* (Hymenoptera, Tenthredinidae). Tartu, 2012, 192 p.
223. **Triinu Visnapuu**. Levansucrases encoded in the genome of *Pseudomonas syringae* pv. tomato DC3000: heterologous expression, biochemical characterization, mutational analysis and spectrum of polymerization products. Tartu, 2012, 160 p.

224. **Nele Tamberg**. Studies on Semliki Forest virus replication and pathogenesis. Tartu, 2012, 109 p.
225. **Tõnu Esko**. Novel applications of SNP array data in the analysis of the genetic structure of Europeans and in genetic association studies. Tartu, 2012, 149 p.
226. **Timo Arula**. Ecology of early life-history stages of herring *Clupea harengus membras* in the northeastern Baltic Sea. Tartu, 2012, 143 p.
227. **Inga Hiiesalu**. Belowground plant diversity and coexistence patterns in grassland ecosystems. Tartu, 2012, 130 p.
228. **Kadri Koorem**. The influence of abiotic and biotic factors on small-scale plant community patterns and regeneration in boreonemoral forest. Tartu, 2012, 114 p.
229. **Liis Andresen**. Regulation of virulence in plant-pathogenic pectobacteria. Tartu, 2012, 122 p.
230. **Kaupo Kohv**. The direct and indirect effects of management on boreal forest structure and field layer vegetation. Tartu, 2012, 124 p.
231. **Mart Jüssi**. Living on an edge: landlocked seals in changing climate. Tartu, 2012, 114 p.
232. **Riina Klais**. Phytoplankton trends in the Baltic Sea. Tartu, 2012, 136 p.
233. **Rauno Veeroja**. Effects of winter weather, population density and timing of reproduction on life-history traits and population dynamics of moose (*Alces alces*) in Estonia. Tartu, 2012, 92 p.
234. **Marju Keis**. Brown bear (*Ursus arctos*) phylogeography in northern Eurasia. Tartu, 2013, 142 p.
235. **Sergei Põlme**. Biogeography and ecology of *alnus*- associated ectomycorrhizal fungi – from regional to global scale. Tartu, 2013, 90 p.
236. **Liis Usküla**. Placental gene expression in normal and complicated pregnancy. Tartu, 2013, 173 p.
237. **Marko Lõoke**. Studies on DNA replication initiation in *Saccharomyces cerevisiae.* Tartu, 2013, 112 p.
238. **Anne Aan**. Light- and nitrogen-use and biomass allocation along productivity gradients in multilayer plant communities. Tartu, 2013, 127 p.
239. **Heidi Tamm**. Comprehending phylogenetic diversity – case studies in three groups of ascomycetes. Tartu, 2013, 136 p.
240. **Liina Kangur**. High-Pressure Spectroscopy Study of Chromophore-Binding Hydrogen Bonds in Light-Harvesting Complexes of Photosynthetic Bacteria. Tartu, 2013, 150 p.
241. **Margus Leppik**. Substrate specificity of the multisite specific pseudouridine synthase RluD. Tartu, 2013, 111 p.
242. **Lauris Kaplinski**. The application of oligonucleotide hybridization model for PCR and microarray optimization. Tartu, 2013, 103 p.
243. **Merli Pärnoja**. Patterns of macrophyte distribution and productivity in coastal ecosystems: effect of abiotic and biotic forcing. Tartu, 2013, 155 p.
244. **Tõnu Margus**. Distribution and phylogeny of the bacterial translational GTPases and the Mqsr/YgiT regulatory system. Tartu, 2013, 126 p.

245. **Pille Mänd**. Light use capacity and carbon and nitrogen budget of plants: remote assessment and physiological determinants. Tartu, 2013, 128 p.
246. **Mario Plaas**. Animal model of Wolfram Syndrome in mice: behavioural, biochemical and psychopharmacological characterization. Tartu, 2013, 144 p.
247. **Georgi Hudjašov**. Maps of mitochondrial DNA, Y-chromosome and tyrosinase variation in Eurasian and Oceanian populations. Tartu, 2013, 115 p.
248. **Mari Lepik**. Plasticity to light in herbaceous plants and its importance for community structure and diversity. Tartu, 2013, 102 p.
249. **Ede Leppik**. Diversity of lichens in semi-natural habitats of Estonia. Tartu, 2013, 151 p.
250. **Ülle Saks**. Arbuscular mycorrhizal fungal diversity patterns in boreonemoral forest ecosystems. Tartu, 2013, 151 p.
251. **Eneli Oitmaa**. Development of arrayed primer extension microarray assays for molecular diagnostic applications. Tartu, 2013, 147 p.
252. **Jekaterina Jutkina**. The horizontal gene pool for aromatics degradation: bacterial catabolic plasmids of the Baltic Sea aquatic system. Tartu, 2013, 121 p.
253. **Helen Vellau**. Reaction norms for size and age at maturity in insects: rules and exceptions. Tartu, 2014, 132 p.
254. **Randel Kreitsberg**. Using biomarkers in assessment of environmental contamination in fish – new perspectives. Tartu, 2014, 107 p.
255. **Krista Takkis**. Changes in plant species richness and population performance in response to habitat loss and fragmentation.Tartu, 2014, 141 p.
256. **Liina Nagirnaja**. Global and fine-scale genetic determinants of recurrent pregnancy loss. Tartu, 2014, 211 p.
257. **Triin Triisberg**. Factors influencing the re-vegetation of abandoned extracted peatlands in Estonia. Tartu, 2014, 133 p.
258. **Villu Soon**. A phylogenetic revision of the *Chrysis ignita* species group (Hymenoptera: Chrysididae) with emphasis on the northern European fauna. Tartu, 2014, 211 p.
259. **Andrei Nikonov**. RNA-Dependent RNA Polymerase Activity as a Basis for the Detection of Positive-Strand RNA Viruses by Vertebrate Host Cells. Tartu, 2014, 207 p.
260. **Eele Õunapuu-Pikas**. Spatio-temporal variability of leaf hydraulic conductance in woody plants: ecophysiological consequences. Tartu, 2014, 135 p.
261. **Marju Männiste**. Physiological ecology of greenfinches: information content of feathers in relation to immune function and behavior. Tartu, 2014, 121 p.
262. **Katre Kets**. Effects of elevated concentrations of $CO_2$ and $O_3$ on leaf photosynthetic parameters in *Populus tremuloides*: diurnal, seasonal and interannual patterns. Tartu, 2014, 115 p.

263. **Külli Lokko**. Seasonal and spatial variability of zoopsammon communities in relation to environmental parameters. Tartu, 2014, 129 p.
264. **Olga Žilina**. Chromosomal microarray analysis as diagnostic tool: Estonian experience. Tartu, 2014, 152 p.
265. **Kertu Lõhmus**. Colonisation ecology of forest-dwelling vascular plants and the conservation value of rural manor parks. Tartu, 2014, 111 p.
266. **Anu Aun**. Mitochondria as integral modulators of cellular signaling. Tartu, 2014, 167 p.
267. **Chandana Basu Mallick**. Genetics of adaptive traits and gender-specific demographic processes in South Asian populations. Tartu, 2014, 160 p.
268. **Riin Tamme**. The relationship between small-scale environmental heterogeneity and plant species diversity. Tartu, 2014, 130 p.
269. **Liina Remm**. Impacts of forest drainage on biodiversity and habitat quality: implications for sustainable management and conservation. Tartu, 2015, 126 p.
270. **Tiina Talve**. Genetic diversity and taxonomy within the genus *Rhinanthus.* Tartu, 2015, 106 p.
271. **Mehis Rohtla**. Otolith sclerochronological studies on migrations, spawning habitat preferences and age of freshwater fishes inhabiting the Baltic Sea. Tartu, 2015, 137 p.
272. **Alexey Reshchikov**. The world fauna of the genus *Lathrolestes* (Hymenoptera, Ichneumonidae). Tartu, 2015, 247 p.
273. **Martin Pook**. Studies on artificial and extracellular matrix protein-rich surfaces as regulators of cell growth and differentiation. Tartu, 2015, 142 p.
274. **Mai Kukumägi**. Factors affecting soil respiration and its components in silver birch and Norway spruce stands. Tartu, 2015, 155 p.
275. **Helen Karu**. Development of ecosystems under human activity in the North-East Estonian industrial region: forests on post-mining sites and bogs. Tartu, 2015, 152 p.
276. **Hedi Peterson**. Exploiting high-throughput data for establishing relationships between genes. Tartu, 2015, 186 p.
277. **Priit Adler**. Analysis and visualisation of large scale microarray data, Tartu, 2015, 126 p.
278. **Aigar Niglas**. Effects of environmental factors on gas exchange in deciduous trees: focus on photosynthetic water-use efficiency. Tartu, 2015, 152 p.
279. **Silja Laht**. Classification and identification of conopeptides using profile hidden Markov models and position-specific scoring matrices. Tartu, 2015, 100 p.
280. **Martin Kesler**. Biological characteristics and restoration of Atlantic salmon *Salmo salar* populations in the Rivers of Northern Estonia. Tartu, 2015, 97 p.
281. **Pratyush Kumar Das**. Biochemical perspective on alphaviral nonstructural protein 2: a tale from multiple domains to enzymatic profiling. Tartu, 2015, 205 p

282. **Priit Palta**. Computational methods for DNA copy number detection. Tartu, 2015, 130 p.
283. **Julia Sidorenko**. Combating DNA damage and maintenance of genome integrity in pseudomonads. Tartu, 2015, 174 p.
284. **Anastasiia Kovtun-Kante**. Charophytes of Estonian inland and coastal waters: distribution and environmental preferences. Tartu, 2015, 97 p.
285. **Ly Lindman**. The ecology of protected butterfly species in Estonia. Tartu, 2015, 171 p.
286. **Jaanis Lodjak**. Association of Insulin-like Growth Factor I and Corticosterone with Nestling Growth and Fledging Success in Wild Passerines. Tartu, 2016, 113 p.
287. **Ann Kraut**. Conservation of Wood-Inhabiting Biodiversity – Semi-Natural Forests as an Opportunity. Tartu, 2016, 141 p.
288. **Tiit Örd**. Functions and regulation of the mammalian pseudokinase TRIB3. Tartu, 2016, 182. p.
289. **Kairi Käiro**. Biological Quality According to Macroinvertebrates in Streams of Estonia (Baltic Ecoregion of Europe): Effects of Human-induced Hydromorphological Changes. Tartu, 2016, 126 p.
290. **Leidi Laurimaa**. *Echinococcus multilocularis* and other zoonotic parasites in Estonian canids. Tartu, 2016, 144 p.
291. **Helerin Margus**. Characterization of cell-penetrating peptide/nucleic acid nanocomplexes and their cell-entry mechanisms. Tartu, 2016, 173 p.
292. **Kadri Runnel**. Fungal targets and tools for forest conservation. Tartu, 2016, 157 p.
293. **Urmo Võsa**. MicroRNAs in disease and health: aberrant regulation in lung cancer and association with genomic variation. Tartu, 2016, 163 p.
294. **Kristina Mäemets-Allas**. Studies on cell growth promoting AKT signaling pathway – a promising anti-cancer drug target. Tartu, 2016, 146 p.
295. **Janeli Viil**. Studies on cellular and molecular mechanisms that drive normal and regenerative processes in the liver and pathological processes in Dupuytren's contracture. Tartu, 2016, 175 p.
296. **Ene Kook**. Genetic diversity and evolution of *Pulmonaria angustifolia* L. and *Myosotis laxa sensu lato* (Boraginaceae). Tartu, 2016, 106 p.
297. **Kadri Peil**. RNA polymerase II-dependent transcription elongation in *Saccharomyces cerevisiae*. Tartu, 2016, 113 p.
298. **Katrin Ruisu**. The role of RIC8A in mouse development and its function in cell-matrix adhesion and actin cytoskeletal organisation. Tartu, 2016, 129 p.
299. **Janely Pae**. Translocation of cell-penetrating peptides across biological membranes and interactions with plasma membrane constituents. Tartu, 2016, 126 p.
300. **Argo Ronk**. Plant diversity patterns across Europe: observed and dark diversity. Tartu, 2016, 153 p.

301. **Kristiina Mark**. Diversification and species delimitation of lichenized fungi in selected groups of the family Parmeliaceae (Ascomycota). Tartu, 2016, 181 p.
302. **Jaak-Albert Metsoja**. Vegetation dynamics in floodplain meadows: influence of mowing and sediment application. Tartu, 2016, 140 p.
303. **Hedvig Tamman**. The GraTA toxin-antitoxin system of *Pseudomonas putida*: regulation and role in stress tolerance. Tartu, 2016, 154 p.
304. **Kadri Pärtel**. Application of ultrastructural and molecular data in the taxonomy of helotialean fungi. Tartu, 2016, 183 p.
305. **Maris Hindrikson**. Grey wolf (*Canis lupus*) populations in Estonia and Europe: genetic diversity, population structure and -processes, and hybridization between wolves and dogs. Tartu, 2016, 121 p.
306. **Polina Degtjarenko**. Impacts of alkaline dust pollution on biodiversity of plants and lichens: from communities to genetic diversity. Tartu, 2016, 126 p.
307. **Liina Pajusalu**. The effect of $CO_2$ enrichment on net photosynthesis of macrophytes in a brackish water environment. Tartu, 2016, 126 p.
308. **Stoyan Tankov**. Random walks in the stringent response. Tartu, 2016, 94 p.
309. **Liis Leitsalu**. Communicating genomic research results to population-based biobank participants. Tartu, 2016, 158 p.
310. **Richard Meitern**. Redox physiology of wild birds: validation and application of techniques for detecting oxidative stress. Tartu, 2016, 134 p.
311. **Kaie Lokk**. Comparative genome-wide DNA methylation studies of healthy human tissues and non-small cell lung cancer tissue. Tartu, 2016, 127 p.
312. **Mihhail Kurašin**. Processivity of cellulases and chitinases. Tartu, 2017, 132 p.
313. **Carmen Tali**. Scavenger receptors as a target for nucleic acid delivery with peptide vectors. Tartu, 2017, 155 p.
314. **Katarina Oganjan**. Distribution, feeding and habitat of benthic suspension feeders in a shallow coastal sea. Tartu, 2017, 132 p.
315. **Taavi Paal**. Immigration limitation of forest plants into wooded landscape corridors. Tartu, 2017, 145 p.
316. **Kadri Õunap**. The Williams-Beuren syndrome chromosome region protein WBSCR22 is a ribosome biogenesis factor. Tartu, 2017, 135 p.
317. **Riin Tamm**. In-depth analysis of factors affecting variability in thiopurine methyltransferase activity. Tartu, 2017, 170 p.
318. **Keiu Kask**. The role of RIC8A in the development and regulation of mouse nervous system. Tartu, 2017, 184 p.
319. **Tiia Möller**. Mapping and modelling of the spatial distribution of benthic macrovegetation in the NE Baltic Sea with a special focus on the eelgrass *Zostera marina* Linnaeus, 1753. Tartu, 2017, 162 p.
320. **Silva Kasela**. Genetic regulation of gene expression: detection of tissue- and cell type-specific effects. Tartu, 2017, 150 p.

321. **Karmen Süld**. Food habits, parasites and space use of the raccoon dog *Nyctereutes procyonoides*: the role of an alien species as a predator and vector of zoonotic diseases in Estonia. Tartu, 2017, p.
322. **Ragne Oja**. Consequences of supplementary feeding of wild boar – concern for ground-nesting birds and endoparasite infection. Tartu, 2017, 141 p.
323. **Riin Kont**. The acquisition of cellulose chain by a processive cellobiohydrolase. Tartu, 2017, 117 p.
324. **Liis Kasari**. Plant diversity of semi-natural grasslands: drivers, current status and conservation challenges. Tartu, 2017, 141 p.
325. **Sirgi Saar**. Belowground interactions: the roles of plant genetic relatedness, root exudation and soil legacies. Tartu, 2017, 113 p.
326. **Sten Anslan**. Molecular identification of Collembola and their fungal associates. Tartu, 2017, 125 p.
327. **Imre Taal**. Causes of variation in littoral fish communities of the Eastern Baltic Sea: from community structure to individual life histories. Tartu, 2017, 118 p.
328. **Jürgen Jalak**. Dissecting the Mechanism of Enzymatic Degradation of Cellulose Using Low Molecular Weight Model Substrates. Tartu, 2017, 137 p.
329. **Kairi Kiik**. Reproduction and behaviour of the endangered European mink (*Mustela lutreola*) in captivity. Tartu, 2018, 112 p.
330. **Ivan Kuprijanov**. Habitat use and trophic interactions of native and invasive predatory macroinvertebrates in the northern Baltic Sea. Tartu, 2018, 117 p.
331. **Hendrik Meister**. Evolutionary ecology of insect growth: from geographic patterns to biochemical trade-offs. Tartu, 2018, 147 p.
332. **Ilja Gaidutšik.** Irc3 is a mitochondrial branch migration enzyme in *Saccharomyces cerevisiae.* Tartu, 2018, 161 p.
333. **Lena Neuenkamp**. The dynamics of plant and arbuscular mycorrhizal fungal communities in grasslands under changing land use. Tartu, 2018, 241 p.
334. **Laura Kasak.** Genome structural variation modulating the placenta and pregnancy maintenance. Tartu, 2018, 181 p.
335. **Kersti Riibak.** Importance of dispersal limitation in determining dark diversity of plants across spatial scales. Tartu, 2018, 133 p.
336. **Liina Saar.** Dynamics of grassland plant diversity in changing landscapes. Tartu, 2018, 206 p.
337. **Hanna Ainelo.** Fis regulates *Pseudomonas putida* biofilm formation by controlling the expression of *lapA*. Tartu, 2018, 143 p.
338. **Natalia Pervjakova.** Genomic imprinting in complex traits. Tartu, 2018, 176 p.
339. **Andrio Lahesaare.** The role of global regulator Fis in regulating the expression of *lapF* and the hydrophobicity of soil bacterium *Pseudomonas putida*. Tartu, 2018, 124 p.

340. **Märt Roosaare.** *K*-mer based methods for the identification of bacteria and plasmids. Tartu, 2018, 117 p.
341. **Maria Abakumova.** The relationship between competitive behaviour and the frequency and identity of neighbours in temperate grassland plants. Tartu, 2018, 104 p.
342. **Margus Vilbas.** Biotic interactions affecting habitat use of myrmecophilous butterflies in Northern Europe. Tartu, 2018, 142 p.
343. **Liina Kinkar**. Global patterns of genetic diversity and phylogeography of *Echinococcus granulosus* sensu stricto – a tapeworm species of significant public health concern. Tartu, 2018, 147 p.
344. **Teivi Laurimäe.** Taxonomy and genetic diversity of zoonotic tapeworms in the species complex of *Echinococcus granulosus* sensu lato. Tartu, 2018, 143 p.
345. **Tatjana Jatsenko.** Role of translesion DNA polymerases in mutagenesis and DNA damage tolerance in Pseudomonads. Tartu, 2018, 216 p.
346. **Katrin Viigand.** Utilization of α-glucosidic sugars by *Ogataea* (*Hansenula*) *polymorpha.* Tartu, 2018, 148 p.
347. **Andres Ainelo.** Physiological effects of the *Pseudomonas putida* toxin grat. Tartu, 2018, 146 p.
348. **Killu Timm**. Effects of two genes (DRD4 and SERT) on great tit (*Parus major*) behaviour and reproductive traits. Tartu, 2018, 117 p.
349. **Petr Kohout**. Ecology of ericoid mycorrhizal fungi. Tartu, 2018, 184 p.
350. **Gristin Rohula-Okunev**. Effects of endogenous and environmental factors on night-time water flux in deciduous woody tree species. Tartu, 2018, 184 p.
351. **Jane Oja.** Temporal and spatial patterns of orchid mycorrhizal fungi in forest and grassland ecosystems. Tartu, 2018, 102 p.
352. **Janek Urvik**. Multidimensionality of aging in a long-lived seabird. Tartu, 2018, 135 p.
353. **Lisanna Schmidt**. Phenotypic and genetic differentiation in the hybridizing species pair *Carex flava* and *C. viridula* in geographically different regions. Tartu, 2018, 133 p.
354. **Monika Karmin.** Perspectives from human Y chromosome – phylogeny, population dynamics and founder events. Tartu, 2018, 168 p.
355. **Maris Alver.** Value of genomics for atherosclerotic cardiovascular disease risk prediction. Tartu, 2019, 148 p.
356. **Lehti Saag**. The prehistory of Estonia from a genetic perspective: new insights from ancient DNA. Tartu, 2019, 171 p.
357. **Mari-Liis Viljur**. Local and landscape effects on butterfly assemblages in managed forests. Tartu, 2019, 115 p.